AD-753 412

Wear Resistant Coatings for Titanium Alloys

fretting fatigue of uncoated Ti-6A1-4V

General Electric Company

prepared for

Air Force Materials Laboratory

NOVEMBER 1971

AFML-TR-71-212

WEAR RESISTANT COATINGS FOR TITANIUM ALLOYS: FRETTING FATIGUE OF UNCOATED Ti-6Al-4V

R.K. Betts
General Electric Company

Technical Report AFML-TR-71-212

1971 November

Air Force Materials Laboratory
Air Force Systems Command
Wright-Patterson Air Force Base, Ohio 45433

AFML-TR-71-212

WEAR RESISTANT COATINGS FOR TITANIUM ALLOYS: FRETTING FATIGUE OF UNCOATED Ti-6Al-4V

R.K. Betts

FOREWORD

This Final Report was prepared for the United States Air Force Materials Laboratory, Contract F33615-70-C-1537, "Development and Evaluation of Coatings for Alleviating the Effect of Fretting on the Fatigue Life of Titanium Alloys," performed during the period 1970 July 1 through 1971 August 31. The report was submitted by the author on 1971 September 15.

The contract was performed by the Materials and Process Technology Laboratories, Aircraft Engine Group, General Electric Company under Air Force Materials Laboratory Project 7312, "Metal Surface Deterioration and Protection", Task No. 731201, "Metal Surface Protection". It was accomplished under the technical direction of Mr. J. Jay Crosby of the Metals Branch (LLP), Metals and Ceramics Division, Air Force Materials Laboratory, Wright-Patterson Air Force Base, Ohio.

Dr. I.I. Bessen, Manager, Coatings Technology Suboperation, General Electric, was the program manager; and, Mr. R.K. Betts was in charge of the technical effort. This technical effort has been reviewed and is approved.

I. Perlmutter
Chief, Metals Branch
Metals and Ceramics Division

ABSTRACT

Classic fretting fatigue performed in an in-situ manner between surfaces of shot-peened, forged Ti-6Al-4V was found not to affect the run-out stress capability compared to nonfretted specimens in tests at room temperature. However, at 400° F, a slight decrease in the run-out stress was observed, and at 650° F a decrease of 30% resulted from severe surface interaction.

At overstress levels of 10,000 psi above the nonfretted run-out stress, fretting reduced the cyclic life capability by two orders of magnitude at room temperature, and 2½ orders at the elevated temperatures.

At overstress conditions, a narrow threshold of inexorable fretting fatigue damage occurred between 10^4 and 5×10^4 cycles. Fluorescent penetrant inspection was capable of revealing cracks in specimens interrupted from fretting after the threshold had been exceeded, which specimens were subsequently tested to fatigue failure with no additional fretting.

Contact pressure from 5,000 to 75,000 psi in these in-situ fretting fatigue tests produced fretting damage. Very low pressure of 500 psi reduced fretting fatigue propensity at room temperature.

Common fretting wear between sliding surfaces of shot-peened Ti-6Al-4V was found not to affect the subsequent high cycle and low cycle fatigue properties of Ti below certain contact pressures and sliding displacements. Wear at a contact pressure of 10,000 psi with 0.5 mil and 2.5 mils displacement for 1000 strokes did not reduce the high cycle fatigue strength, nor did wear at 1,000 psi with as much as 10 mils displacement for 1000 strokes affect the strength. But, damage incurred at 10,000 and 50,000 psi with 5 mils displacement for 1,000 strokes did affect the high cycle and low cycle fatigue properties.

TABLE OF CONTENTS

TABLE OF CONTENTS (Concluded)

LIST OF ILLUSTRATIONS

LIST OF ILLUSTRATIONS (Continued)

LIST OF ILLUSTRATIONS (Continued)

LIST OF ILLUSTRATIONS (Continued)

LIST OF ILLUSTRATIONS (Concluded)

SECTION I

INTRODUCTION

Titanium and its alloys present one of the most critical challenges in materials engineering for modern gas turbine engines and aircraft structures. While it offers excellent strength-to-weight advantages and other favorable properties, its fatigue life is extremely sensitive to surface conditions, particularly to damage from wear.

The purpose of the work performed under this Contract was to define and establish conditions of fretting wear on uncoated, shot-peened Ti-6Al-4V under which conditions fatigue effects may be expected in aircraft gas turbine engine compressor applications. The results were expected to identify conditions of engine design under which the fatigue effects of wear may be avoided and to establish appropriate test conditions for subsequent evaluation of fretting-preventive coatings. The test techniques used were based on studies of wear and protective materials conducted by and for the Material and Process Technology Laboratories of the General Electric Company, Aircraft Engine Group. The test methods had been developed in collaboration with Metcut Research Associates, Inc., where specimen manufacture, wear, and fatigue testing were performed for this contract.

The study was divided into two tasks, each concerning a specific wear phenomenon and resulting fatigue effects. Task 1 involved classic fretting fatigue between bolted surfaces relating to aircraft compressor disc assemblies. Wear was generated by the fretting action of alternating strain at the surface of fatigue specimens to which were bolted pairs of wear shoes. Variations in shoe contact pressure were evaluated for their influence on the severity of fretting as a function of changes in fatigue life at room and elevated temperature. Task 1 also included a study of interrupted fretting, for the purpose of nondestructive inspection for early detection of fretting damage.

Task 2 involved studies of wear simulating that between surfaces of dovetails, in which contact pressure and displacement are related to dynamic loads. Tests were conducted in two steps where the fatigue specimens were first subjected to sliding wear under varied conditions of contact pressure and stroke length. Worn specimens were then tested in high cycle and low cycle fatigue to evaluate the severity of wear damage.

In both Tasks the visual appearance of worn surfaces was assessed for possible correlation with fatigue effects. Specimens were also evaluated by conventional metallography and by Scanning Electron Microscopy.

SECTION II

SUMMARY AND RESULTS

1. TASK 1 - STRAIN FRETTING FATIGUE

The purpose of this Task was to further the study of the effects of contact pressure and specimen temperature on the fretting fatigue properties of forged, shot-peened Ti-6Al-4V. The test procedure utilized flat, reduced-section specimens subjected to high cycle fatigue (HCF) in bending under a mean tensile stress. Ti wear shoes were clamped to the upper and lower gauge surfaces. The fatigue bending stresses produced minute alternating strain motion of the Ti specimen against the contacting wear shoes, under certain conditions causing in-situ fretting fatigue damage. The severity of fretting, as influenced by the varied shoe contact pressure and metal temperature, was measured by the change in fatigue life compared to nonfretted specimens.

The levels of contact pressure studied under this Task were 500, 5000, and 75,000 psi. These results were compared with previous Company-sponsored tests at 25,000 and 50,000 psi.

A series of tests was also performed with specimens heated to 400° F, under 25,000 psi shoe contact pressure. These results were compared with previous Company-sponsored tests at 650° F. Thus, data at five levels of contact pressure and three conditions of temperature were compared under constant fatigue conditions.

Figure 1 presents a summary of the results. These data indicate the following effects (at room temperature, unless noted):

1. There was no degradation of fatigue life of the specimens at the nonfretted run-out stress levels of 40,000-50,000 psi (plus 20,000 psi mean tension).

2. There was a loss in fatigue life of nearly 1½ orders of magnitude at 60,000 psi bending stress (overstress region) due to fretting at 5000 psi to 75,000 psi contact pressure, compared to nonfretted data.

3. There was a loss of about ½ order of magnitude at 500 psi contact pressure in the overstress region.

4. At 400° F fretting reduced the runout stress by 5000-10,000 psi; furthermore, the fatigue life in the overstress region was reduced by nearly 2 orders of magnitude, compared to nonfretted data.

5. At 650° F the specimen life at overstress conditions was similarly reduced; but, more importantly, the run-out stress was reduced by 20,000 psi.

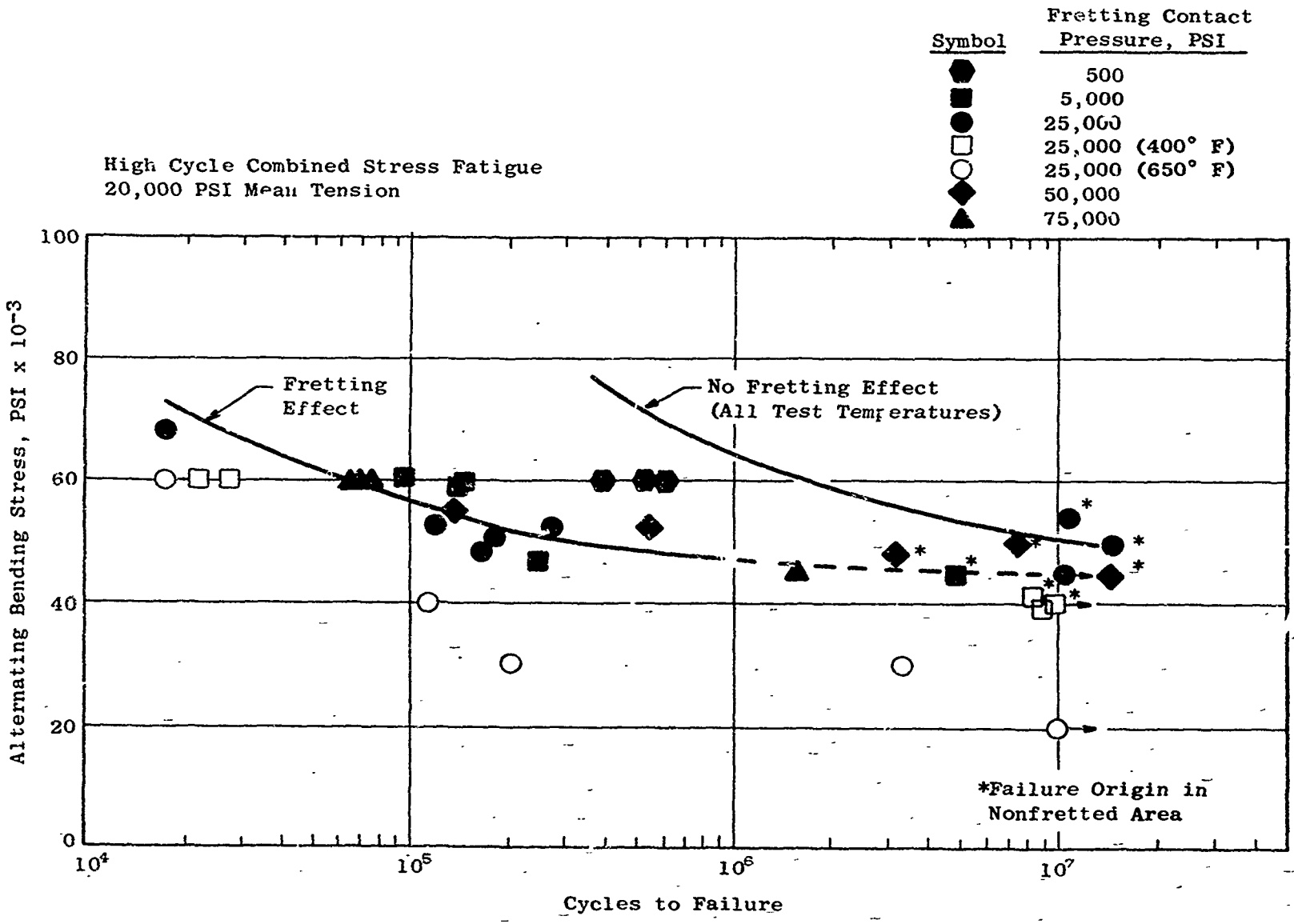

Figure 1. Effect of In-Situ Fretting During High Cycle Fatigue of Shot-Peened Ti-6Al-4V at Room Temperature, 400° F, and 650° F.

A series of interrupted fretting fatigue tests were performed at 25,000 psi shoe-contact pressure and 60,000 psi fatigue stress (overstress region). Specimens were subjected to fretting fatigue for preselected numbers of cycles prior to expected failure, inspected, then continued to failure after removal of the fretting shoes. The purpose was to determine at what cyclic life terminal fretting damage was incurred and whether the damage could be assessed by nondestructive fluorescent penetrant inspection. The fatigue results are shown in Figure 2, compared to the general data curves. They indicate a narrow threshold between 10^4 and 5×10^4 fretting fatigue cycles within which inexorable fatigue damage developed. Fluorescent penetrant revealed cracks in the short-lived specimens (none in the unaffected specimen) before each was subsequently tested to failure with no additional fretting.

2. TASK 2 - SLIDING WEAR FATIGUE

The purpose of this Task was to further the study of the effects of contact pressure and sliding wear displacement, using a two-step test in which the wear test was independent of the subsequent fatigue test. Shot-peened, forged Ti-6Al-4V fatigue specimens were first rubbed by Ti wear shoes under controlled levels of contact pressure and stroke length at a rate of one fully reversed stroke cycle per second. Worn specimens were then subjected to high cycle bending fatigue under constant mean tension or to low cycle bending fatigue at A = 1 in both series. All tests in this Task were at room temperature.

The levels of contact pressure studied were 1000 and 10,000 psi in combination with stroke lengths of 0.5-1, 2.5, 5, and 10 mils (stroke length given is one-half the stroke cycle or the displacement in one direction of travel). The number of strokes of prior wear was 1000 for all tests. These results were compared with previous Company-sponsored tests at 50,000 psi and a 5-mil stroke.

Figure 3 presents a summary of the high cycle fatigue test results against the background data curves. Under these high cycle fatigue test conditions, it had been shown previously that wear at 50,000 psi pressure with a 5-mil stroke drastically reduced the high cycle fatigue life of the Ti at the nonworn run-out stress level of 40,000 psi (plus 40,000 psi mean tension). Furthermore, it depressed the run-out stress level about 30%. It was shown in Task 2 that:

1. Reducing the contact pressure (from the 50,000 psi of background tests) to 10,000 psi with a 5-mil stroke produced scattered results from severe to no effect, relative to fatigue life at 40,000 psi alternating stress.

2. With a stroke length of 5 mils, the 10,000 psi contact pressure appeared to be a threshold level for wear damage, because at 1000 psi contact, 5 mils of stroke produced no fatigue loss.

3. Furthermore, at a contact pressure of 10,000 psi, it was shown that a 2.5-mil stroke did not cause damaging wear.

4. Finally, under a constant pressure of 1000 psi, stroke lengths up to 10 mils could be tolerated.

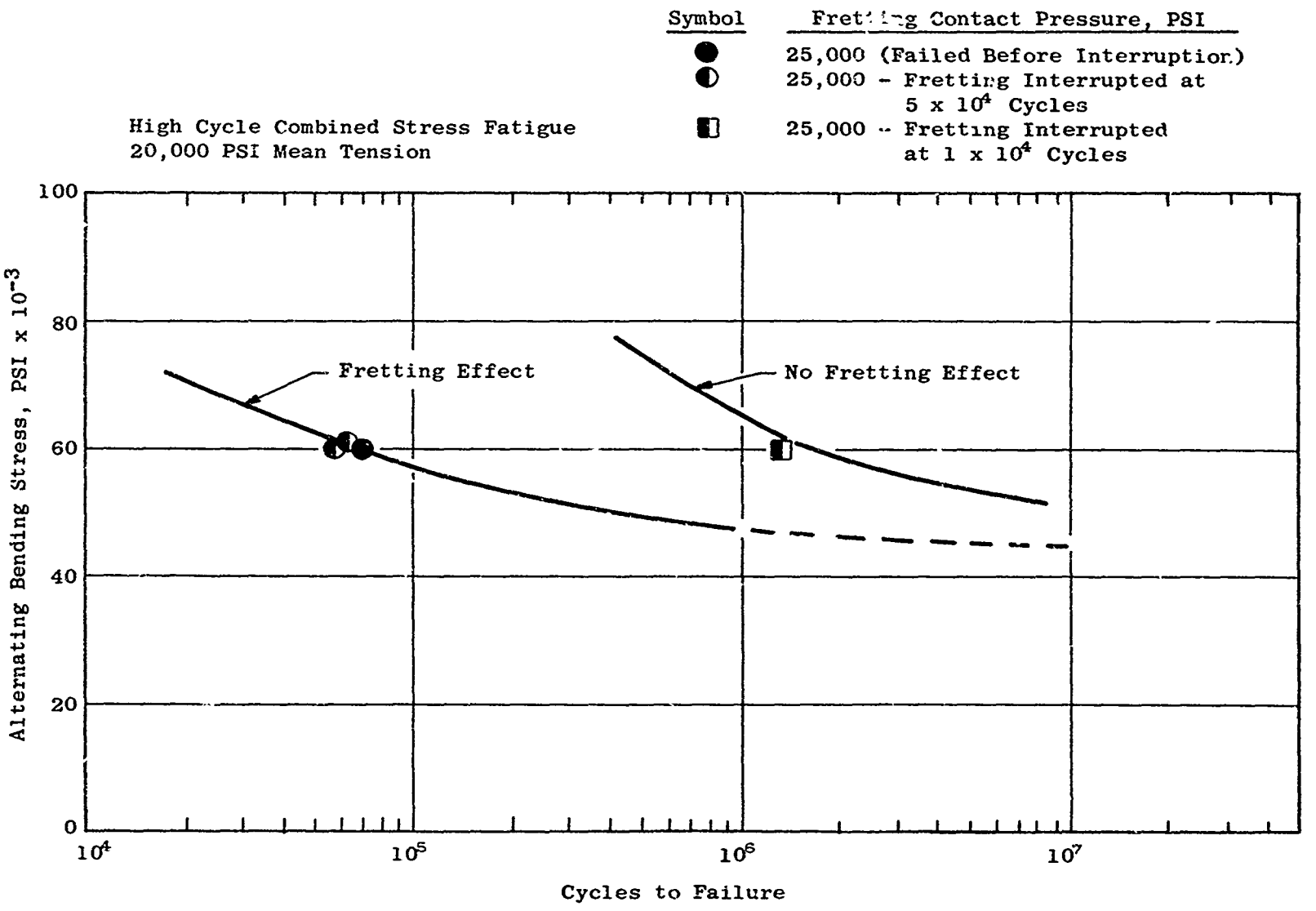

Figure 2. Effect of Interrupted In-Situ Fretting During High Cycle Fatigue of Shot-Peened Ti-6Al-4V at Room Temperature and 25,000 PSI Pressure.

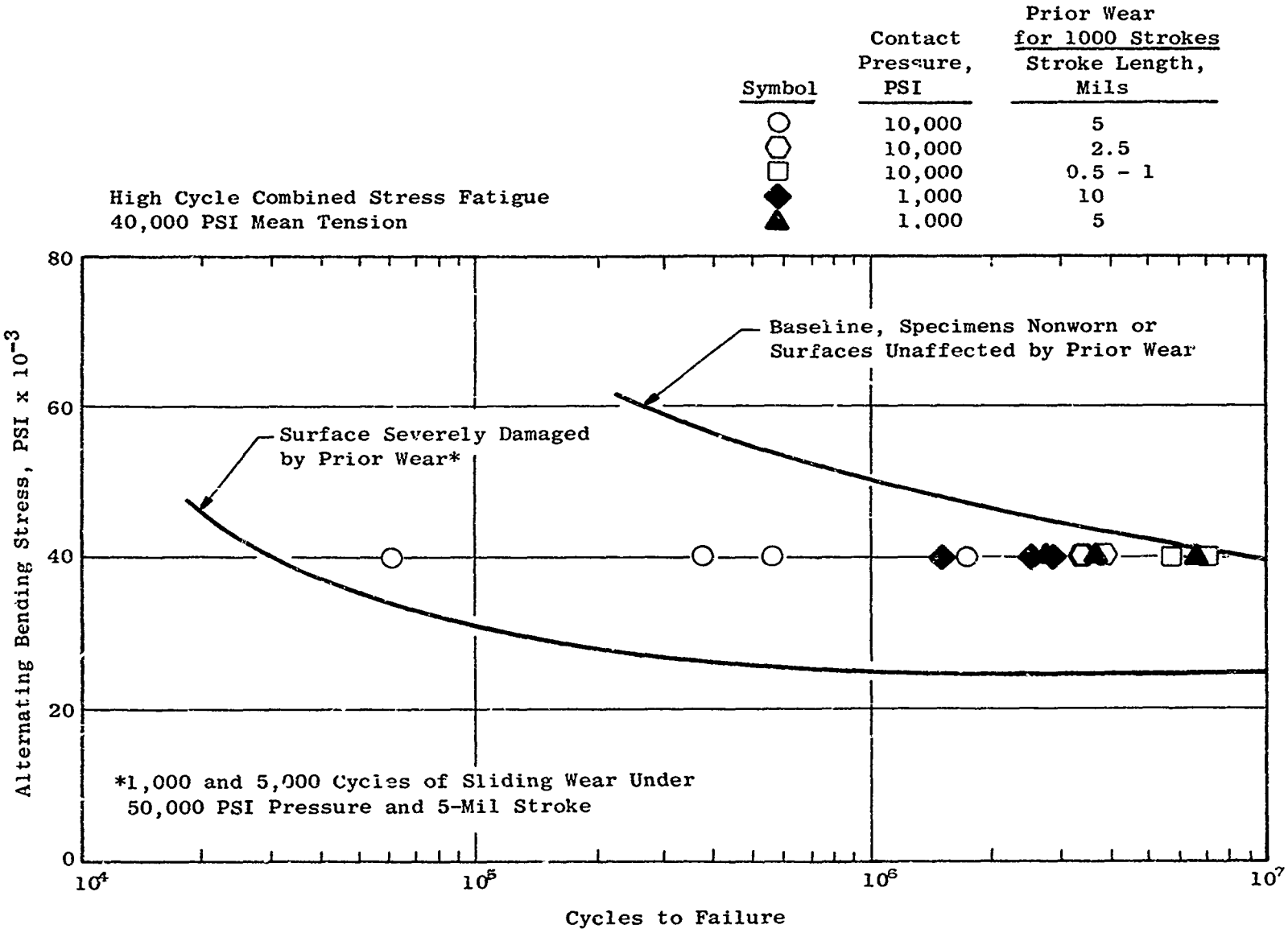

Figure 3. Effect of High Pressure Sliding Wear Damage on High Cycle Fatigue Properties of Shot-Peened Forged Ti-6Al-4V. Background Curves from Testing Reported in Reference 7. Of Data Points from Contract Tests, Only those Specimens with Fatigue Lives Less than 10^6 Cycles Failed from Wear Damage Origins.

Figure 4 summarized these results in a nomograph form. Connecting lines depict the specific test conditions of contact pressure and stroke length for which fatigue-affecting wear damage did or did not occur within 1000 wear strokes.

Low cycle fatigue tests in bending at A = 1 were performed on specimens subjected to wear under 50,000 psi and a 5-mil stroke. The results are shown in Figure 5. The imposed wear damage reduced the fatigue life by about 1 order of magnitude at the bending stress level equivalent to 10^5 cycles for nonworn specimens.

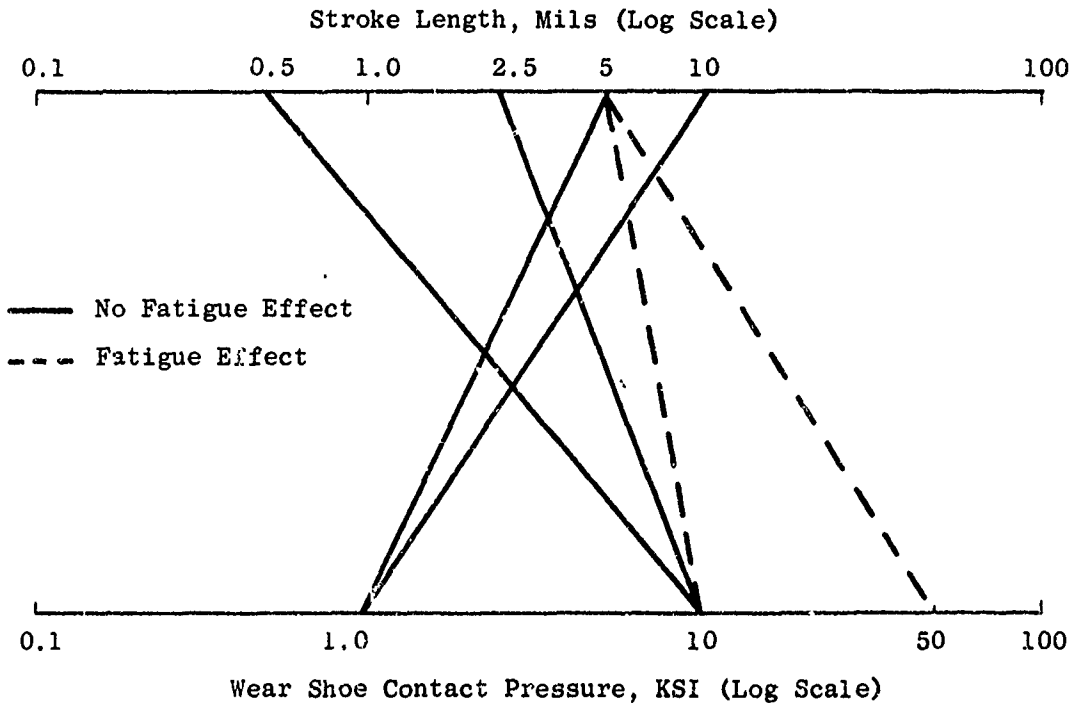

Figure 4. Summary of Wear Test Conditions for 1000 Strokes, Indicating the Effect on High Cycle Fatigue-Properties of Shot-Peened Ti-6Al-4V.

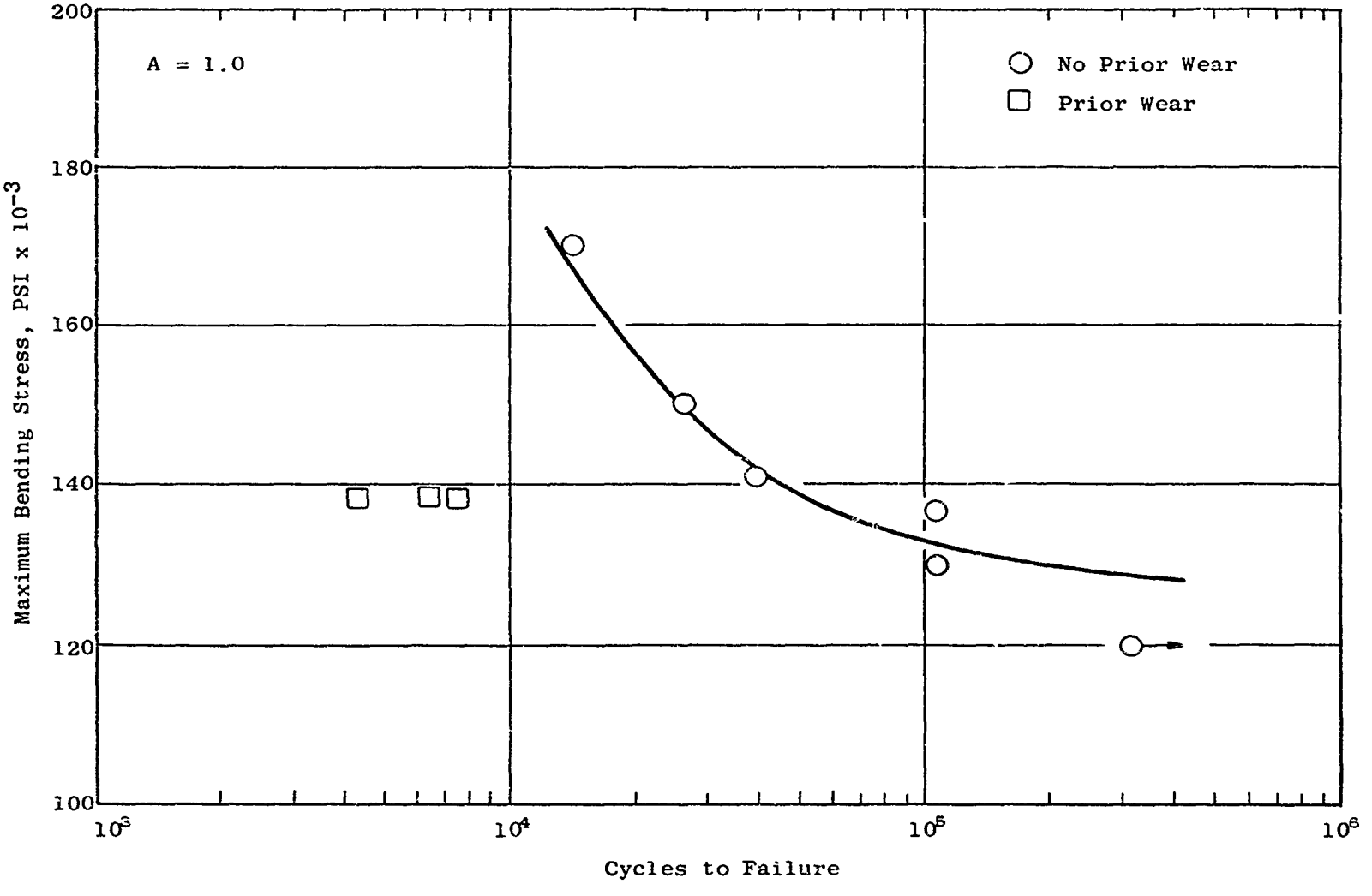

Figure 5. Low Cycle Fatigue Properties of Shot-Peened, Forged Ti-6Al-4V. Prior Wear Under 50,000 PSI Contact, 5-Mil Stroke, 1000 Cycles.

SECTION III

CONCLUSIONS

1. TASK 1 - STRAIN FRETTING FATIGUE

Shot-peened, forged Ti-6Al-4V subjected to fretting fatigue against itself should not be affected during operations at normal design stresses and below 400° F. At 400° F a slight fretting effect should be expected, and at 650° F the effect should be as much as 30% decrease in stress capability under the test conditions of this contractual study. A substantial reduction in fatigue life should be expected due to fretting during overstress conditions.

Increasing the interface contact pressure should not be expected to inhibit fretting during overstress fatigue conditions. In these cases fretting appears to persist at the edge of the contact area between the static member and the dynamic member regardless of the nominal interface contact pressure.

Decreasing the interface contact pressure to 500 psi may diminish the effect of fretting, but this pressure may be too low for normal component assembly practice.

Surface appearance of fretting damage may be misleading and should not be relied upon for assessing the severity; however, fluorescent penetrant inspection should be effective in detecting fretting fatigue cracks which preclude fatigue failure under continued overstress fatigue conditions.

2. TASK 2 SLIDING WEAR FATIGUE

Surface damage from sliding wear after 1000 strokes at contact pressure of 10,000 psi and 50,000 psi with wear displacement of at least 5 mils should be expected to degrade by 40% the high cycle fatigue strength of shot-peened, forged Ti-6Al-4V. Severe, visible surface damage should be apparent.

Sliding wear at 10,000 psi pressure with 2.5 mils or less displacement should not be expected to affect the high cycle fatigue strength. Only mild surface effect should be apparent.

At 1000 psi contact pressure, no fatigue effect should be expected with wear displacement up to 10 mils for 1000 strokes, although substantiated visible wear effects may be apparent.

The low cycle fatigue life at bending stress equivalent to 5×10^5 cycles should be expected to be reduced by one order of magnitude due to wear damage at a contact pressure of 50,000 psi with 5 mils strike.

SECTION IV

TECHNICAL PROGRAM

1. BACKGROUND

Modern aircraft gas turbine engines represent an extensive commitment to Ti alloys, whereby their effective performance depends on methods to protect the metal from wear damage. The technical program plan for this contract is based on a background of continuing studies at the General Electric Company, concerning wear phenomena and the development of protection methods for structural materials such as Ti alloys (References 1 through 8). The subject of Ti wear has been extensively treated in the scientific journals, and several comprehensive bibliographies are referenced (9 through 14). Very little of the published information deals directly with aircraft turbomachinery. However, there are basic wear processes common to all machinery. These are discussed in the following section, with particular emphasis on fretting fatigue.

2. DISCUSSION OF WEAR PHENOMENA

a. General Wear Processes

Wear has been defined as the progressive loss of material from rubbing surfaces. The rate and effect of this removal depend upon the characteristics of the materials involved and the environmental conditions. For purposes of furthering this definition, four main types of wear are commonly recognized.

- Adhesive Wear - the most common and difficult to control. It results from the welding or adhesion and subsequent rupturing of contacting asperities on a surface. It is particularly severe between sliding pairs of metals which are chemically similar and/or mutually soluble. Adhesive wear is closely related to surface friction in such a way that an increase in frictional forces generally causes a large increase in resulting wear.

- Abrasive Wear - caused by the cutting or plowing of one surface by a harder surface. The harder material may simply be a harder alloy or it may also be an oxide, carbide, work-hardened particle, or other foreign material. Erosion may be considered a form of abrasive wear.

- Fatigue Wear or Surface Fatigue Wear - commonly encountered in rolling or sliding contact, where high localized forces are cyclically imposed on a small contact area. This type of wear occurs most commonly in gears and bearings.

- Corrosive Wear - results from some type of chemical reaction with the environment. It may be due to general oxidation, chemical fumes, humidity or combustion products, and may also be inadvertently caused by ingredients in lubricants. Corrosive wear usually exists in combination with one of the types of mechanical wear noted above, encouraged by frictional heating and the continuous removal of natural protective oxide.

b. Friction and Wear

Friction is not a form of wear. Furthermore the frictional forces and calculated friction coefficients (μ) of sliding surfaces have not been shown to have a consistent relationship to wear processes or rates. In some situations high μ relates to the occurrence of adhesive wear or other interference to sliding caused by accumulation of debris. Ti is such a case. Tungsten carbide, on the other hand, slides with high μ but usually has a very low wear rate. Lubrication produces low friction generally, but this relates to wear only in the sense that the wet or dry film separates the two surfaces, thereby prohibiting wear. Friction may increase when wear is in progress, but, in general, the absolute value of μ does not relate to the wear process or its severity.

c. Forms of Wear

The forms of wear are those names given in practice to describe the appearance of a particular worn surface. There are several common forms including fretting, sliding, galling, and others. Fretting is the term most often used to characterize the form of wear observed in Ti components. It describes the cosmetic result of wear caused by and limited to the smaller amplitudes of cyclic displacement of contacting surfaces. This differentiates it from large-displacement oscillatory or undirectional sliding wear. There are two definite forms of fretting wear associated with aircraft engine components. They are:

- Classic Fretting - the form of wear limited to contacting surfaces not intended to have relative motions (e.g., bolted compressor disc flanges). The displacement therein is extremely minute, resulting mainly from alternation of mechanical strain in one or both surfaces subjected to operational vibratory stresses. Classic fretting is often termed fretting corrosion because the wear mechanism is chiefly the conversion of basis metal to an oxide. With Ti, the rutile specie of Ti oxide is produced. This reaction is fostered by the high temperatures that asperities attain when subjected to friction. Pits acting as fatigue stress raisers are formed as the result of corrosion. Adhesion is an additional factor, and abrasion from the debris trapped in the interface promotes further wear in many materials. The corrosion product may compound the stress situation due to the volume increase associated with the phase change. Classic fretting is insidious by reason of its covert existence and may produce unexpected fretting fatigue in components operating within normally safe design stress limits.

- Common Fretting - a form of wear characterized by less restricted surface motion than classic fretting, a motion that can include periodic separation. Debris and foreign matter may contribute to abrasive wear but are not necessarily entrapped. Blade dovetails and disc groove pressure faces are specific areas of occurrence. The mechanism of common fretting is usually more mechanical than chemical and may produce galling. Fatigue failures may result from the stress concentrations produced by fretting damage in applications where only moderate vibratory stresses are present. In other applications, loss of dimensional fit may be the critical result.

d. Results of Wear

While the mechanisms and forms of wear are important in understanding the phenomenon (and there are many other factors including material properties, states of stress, and environmental conditions), it is the final results of wear that are of immediate concern. The principal result of wear is loss of mechanical functionality by:

- Dimensional changes
- Fatigue failure

The gross result of fretting is normally fatigue failure brought about by surface damage in conjunction with normal or transient high stresses in a component. Visual assessment of fretting mildness or severity is at present inconclusive by itself, in that the presence of more or less fretting debris on a macroscopic examination is not necessarily relevant to the loss of surface integrity. It is the state of stress acting in conjunction with stress raisers (pits, tears, cracks) which may be microscopic, that determines the actual fatigue propensity.

This program was based on a study of the fretting wear régime where fatigue life was the absolute measure of wear severity, but where evaluations included nondestructive examination of surfaces for clues to severity other than visual assessment. Fatigue loss being the major concern, two specialized tests have been used for evaluation of fretting and the merits of surface protection methods. The methods were developed to evaluate classic fretting and common fretting as separate entities under conditions closely simulating engine service. Each is ultimately a fatigue test with the fretting produced in the classic form (in situ) or by prior fretting independent of the subsequent fatigue test.

3. WEAR AND FATIGUE TEST METHODS

a. Requirements

Utilizing meaningful test procedures is of prime importance in aircraft engine application because past experience has shown that generalized friction

and wear testing do not adequately simulate the complexities of engine operation. Furthermore, a key factor in the test technique is the means by which wear is measured. While the quantitative measurement of surface effects and material loss can be obtained by several techniques ranging from visual assessment of damage to holographic comparison of dimensional changes (and may include profilometric tracing, area and volume measurement, weight change, radioactive traces, friction changes, and others), the primary objective in wear studies must be to assess wear qualitatively by measuring its effect on tangible properties, mechanical or physical, which most seriously affect the functionality of a particular engine component. Flange and dovetail fretting both constitute fatigue-limiting situations, so that the paramount measure of wear is its effect on fatigue life.

b. High Cycle Strain-Fretting Fatigue

This test technique was developed for evaluating the fatigue of Ti-6Al-4V in the presence of fretting around the flange bolt holes of compressor discs. The state of stress existent in a bolted rotor joint consists principally of (1) a mean hoop stress, (2) high cycle bending stress, and (3) contact stress.

The test is performed in a modified four-point bending fixture, in conjunction with a mechanical fatigue shake table, as shown in Figure 6. A characteristic of the fixture is that it provides a constant bending moment across the specimen gauge section, allowing natural stress concentration to be effective. The horizontal load spring applies the mean tensile stress, while the alternating strain is induced by high cycle fatigue bending. The third stress component, from the bolted shoes, is monitored by the use of strain-gauged bolts.

In the test, the fatigue bending stresses produce minute alternating strain motion of the Ti specimen against a mating wear shoe. This causes fretting, the severity of which is measured by the change in fatigue life of the specimen.

c. Sliding Wear and Fatigue

Centrifugal forces in fan and compressor discs, combined with the contact stress on the dovetail pressure faces, produce a low cycle wear and fatigue situation related to engine power excursions. Two major changes in engine power which occur during a normal mission are takeoff and thrust reverse. With each increase in engine rotational velocity, hoop stresses cause the disc to enlarge circumferentially. The resultant spreading of the slots allows the blades to slip outward in response to centrifugal force, creating cyclic sliding wear under high contact loads in the dovetail pressure faces.

A test to simulate this condition is a two-step method involving (1) the wear of a fatigue specimen under high contact pressure, followed by (2) fatigue of the worn specimen. The wear apparatus is shown in Figures 7 and 8.

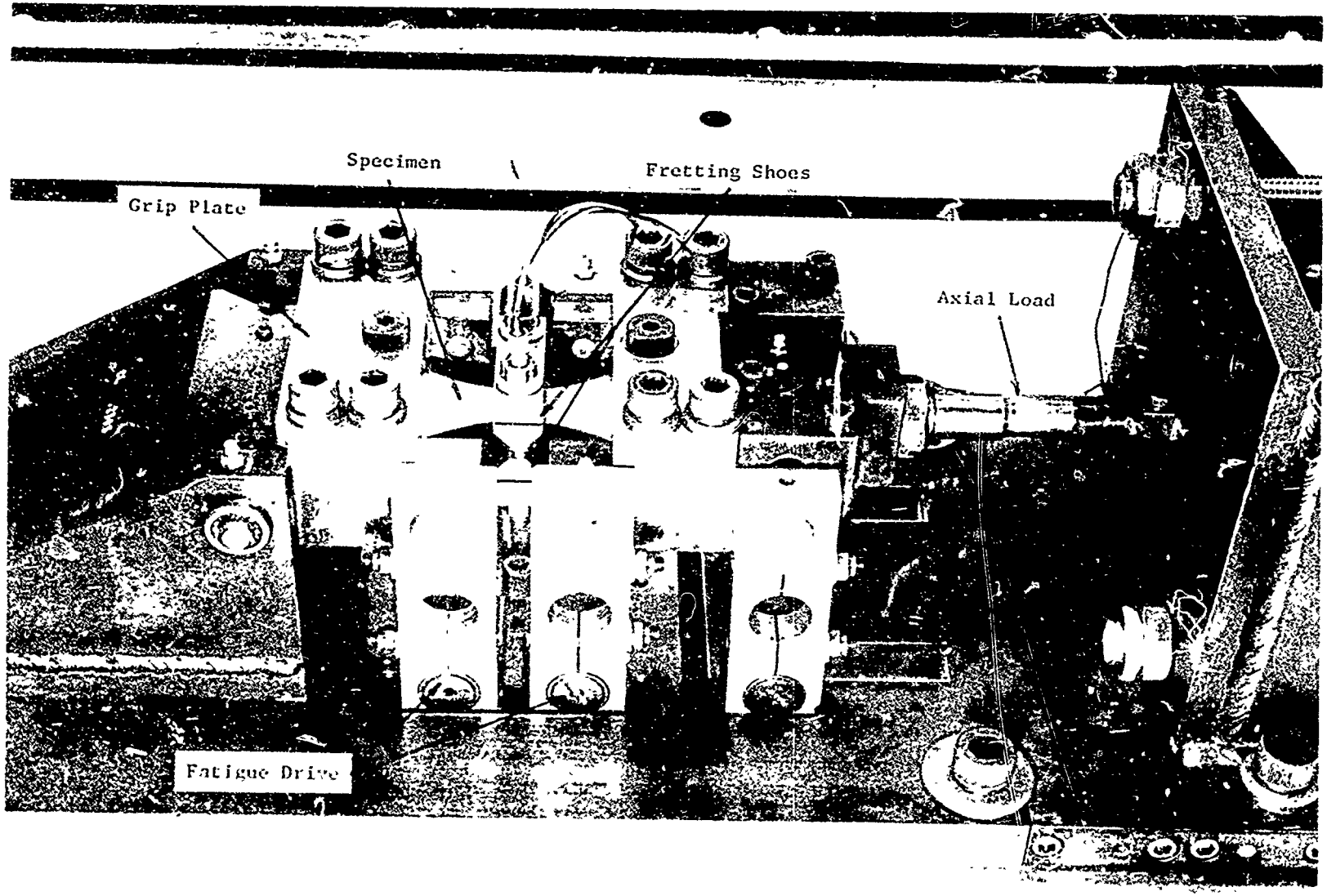

Figure 6. Overall View of Tension-Bending Fatigue Fixture Attached to Sonntag Shake Table

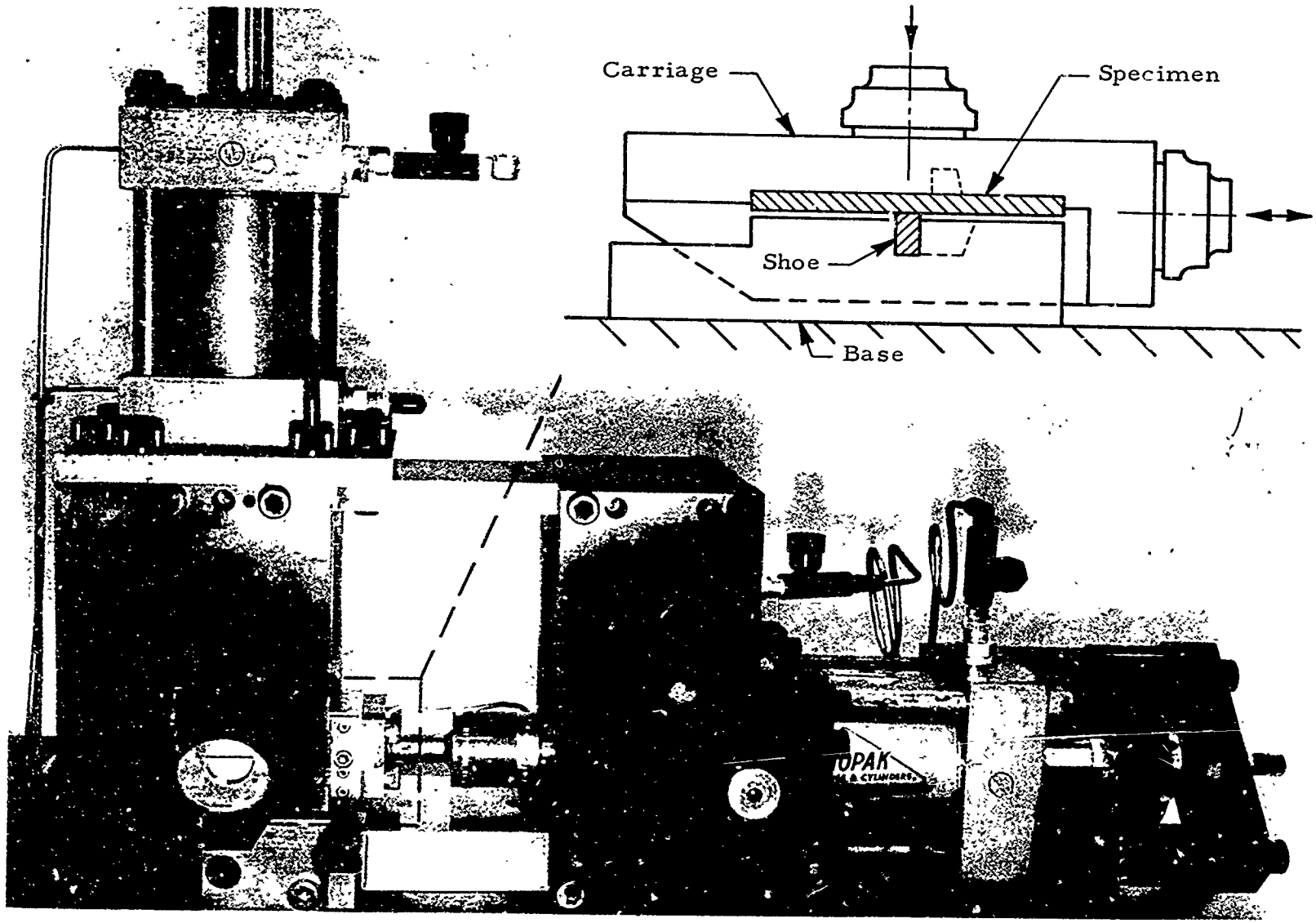

Figure 7. Apparatus for High Pressure Sliding Wear Testing. Schematic Illustrates Details of Fixture Containing Specimen and Shoe

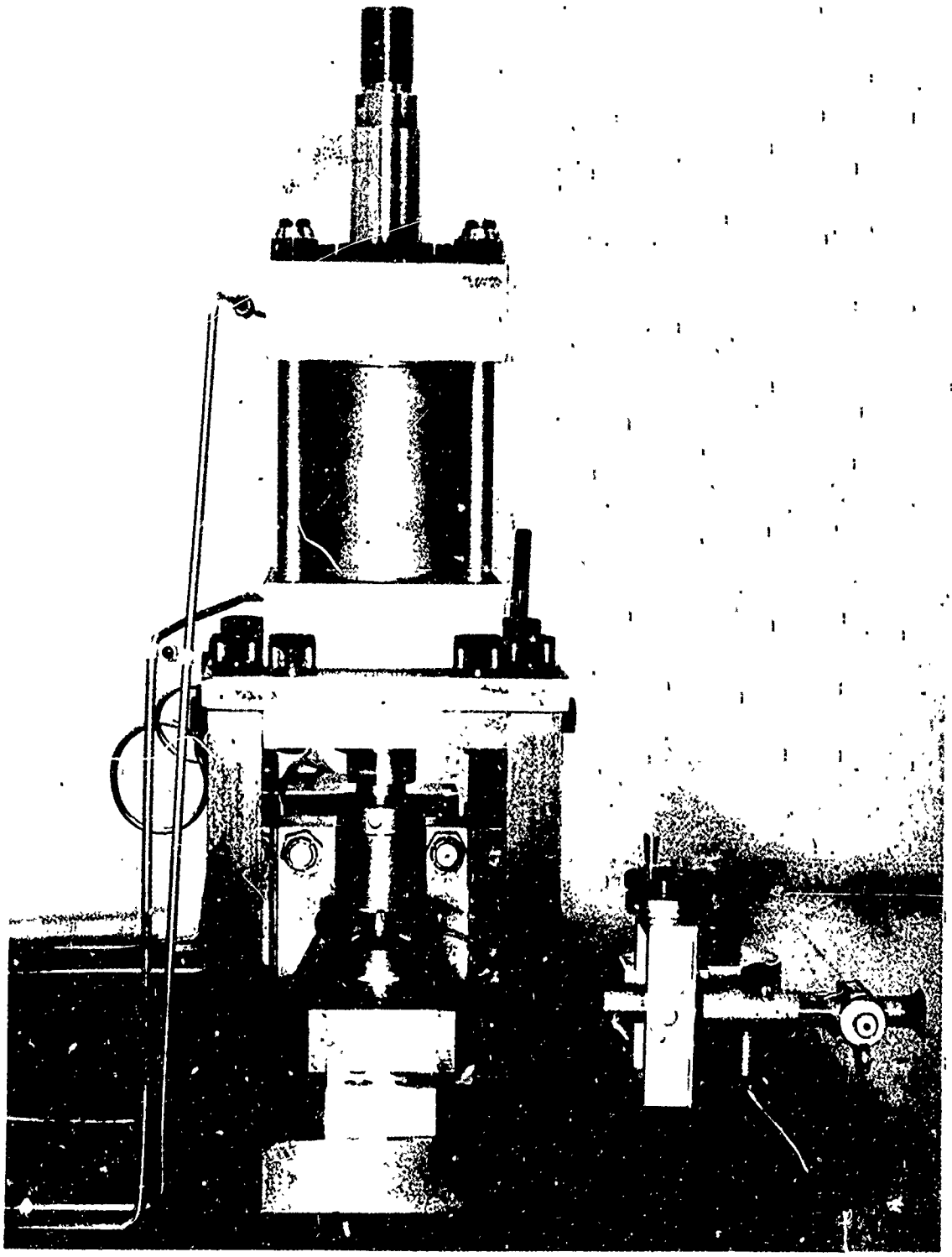

Figure 8. End View of Apparatus for High Pressure Sliding Wear Testing

The test specimen is mounted in the carriage fixture which is hydraulically actuated. The shoe is held in the fixed base block of the apparatus. Pressures to 80,000 psi on a 1/4 X 1-inch contact area are possible. The subsequent fatigue test is four-point bending in either the HCF or LCF mode.

4. CONTRACTUAL WORK STATEMENT

a. Abstract

The contractor shall establish conditions which produce fretting fatigue damage of titanium alloys in AGT engines.

b. Detailed Description

1. Purpose - The purpose of this effort is to define and establish conditions under which fretting fatigue of titanium alloys should be expected in aircraft gas turbine engine compressor applications, in order to permit establishment of appropriate test conditions for subsequent evaluation of fretting-preventive coatings for titanium.

2. Scope - The contractor shall conduct the investigation discussed below for the purpose of defining and establishing a range of environmental conditions that produce fretting-fatigue damage in titanium engine applications and define appropriate levels of the variables involved. Appropriate tests for evaluating fretting-preventive coatings shall be recommended and verified.

3. Effort - The forms of fretting associated with engine components are (1) classic fretting, limited to contact surfaces not intended to have relative motion, e.g., bolted compressor disc flanges; and (2) common fretting, generally found on less restricted surfaces that may undergo periodic separation, e.g., blade and disc dovetail pressure faces. Appropriate fretting fatigue methods for evaluating classic and common fretting are strain-fretting fatigue and sliding wear/fatigue, respectively. Therefore, the effort shall be organized into two appropriate tasks, with all tests employing uncoated, shot-peened, forged Ti-6Al-4V alloy specimens.

(1) Task 1 - Strain-Fretting Fatigue

The parameters of contact pressure, tensile load, relative motion, and metal temperature shall be evaluated in strain-fretting fatigue. The following contact pressures shall be applied, using strain-gauged shoe assembly bolts:

1. 75,000 psi shoe contact pressure at room temperature

2. 5000 psi shoe contact pressure at room temperature

3. Spring-loaded shoe contacting the specimen under a 1-pound load, at room temperature

4. 25,000 psi shoe contact pressure at 400° F

The specimens shall be subjected to tension-bending fatigue at 20,000 psi mean tensile stress and 60,000 psi alternating stress, with relative motion calculated from strain relationships.

Rating of visual and metallographic appearance shall be recorded to establish any correlation of visually observable fretting effects with absolute effect on fatigue. Radioactive Krypton methods and other techniques as appropriate may be employed to aid inspection and correlation.

The scope of these tests may be extended to include other temperatures and stress levels as appropriate, if indicated by results above and within the limits of time and funds available, upon approval by the AFML Project Engineer and AF Contracting Officer.

(2) Task 2 - Sliding Wear/Fatigue

This task shall include a two-step test method, evaluating the effects of contact pressure and relative-motion wear on subsequent bending fatigue, under the following conditions of wear:

1. First, employing a 0.005-inch stroke under 10,000 psi contact pressure for 1000 wear cycles, followed by high cycle bending fatigue tests, then:

2a. If fatigue loss is observed in 1., less severe conditions including:

(i) 0.0005-inch stroke under 10,000 psi contact pressure for 1000 wear cycles, and

(ii) 0.005-inch stroke under 1000 psi contact pressure for 1000 wear cycles, followed by high cycle fatigue tests; or

2b. If no fatigue loss occurs in 1., more severe conditions including:

(i) 0.005-inch stroke under 20,000 contact pressure for 1000 wear cycles, and

(ii) 0.0005-inch stroke under 20,000 psi contact pressure for 1000 wear cycles, followed by high cycle fatigue tests

3. In addition, the effect of a 0.005-inch stroke under 50,000 psi contact pressure for 1000 wear cycles shall be evaluated by subsequent low cycle bending fatigue. (It will be necessary to first establish a baseline of low cycle fatigue.)

Items 1 and 2 above shall be conducted in high cycle bending fatigue under 40,000 psi mean tensile stress at 40,000 psi alternating stress. Item 3 shall include baseline low cycle bending fatigue test data to be determined at A = 1.0, then evaluation of fretted specimens at an appropriately selected stress level. Surface and metallographic appearance of fretting shall be rated for comparison with fatigue results.

(3) Task 2 - Amendment

Additional tests under Task 2 shall be conducted as follows:

1. Employing a 0.002- to 0.003-inch stroke under 10,000 psi contact pressure wear cycles, followed by high cycle bending fatigue

2. Employing a 0.008- to 0.010-inch stroke under 1000 psi contact pressure for 1000 strokes, followed by high cycle bending fatigue

SECTION V

EXPERIMENTAL WORK AND RESULTS

1. SPECIMEN PREPARATION

Figures 9 and 10 illustrate respectively the specimens for high cycle and low cycle fatigue. Figures 11 and 12 show the two types of specimens with their respective wear shoes used in conjunction with the fatigue specimens. All specimens were prepared from annealed α-β processed TF39 flade forgings having mechanical property requirements of 130,000 psi minimum ultimate tensile strength and 120,000 psi yield strength. Low-stress grinding techniques were utilized for primary surface finishing; then, the fatigue specimen gauge section edges were hand radiused to 0.050 - 0.060 inch. Finally the specimens were shot peened to 0.006 - 0.008 A_2 Almen intensity using size 110 steel shot (S110) with 120% coverage. Specimens were rotated during peening for gradual, uniform buildup of stress to prevent warpage.

The fretting and wear shoes were also prepared from flade forgings. The shoes were shot peened only on the wear test surfaces.

2. TASK 1 - STRAIN-FRETTING FATIGUE TESTS

a. High Cycle Fatigue Apparatus Calibration

The HCF apparatus previously shown in Figure 6 consisted of a modified four-point constant moment bending fatigue fixture mounted on a Sonntag SF-1U Universal Fatigue Machine. The fixture performed bending fatigue combined with a mean tensile stress.

A calibration specimen was instrumented with six foil-type strain gauges as shown in Figure 13. The specimen was aligned in the fixture by monitoring strain gauge deflection under application of static axial preload. The axial force was monitored through the precalibrated pull bar load cell and with spring deflection constant. Specimen preload was applied on the basis of P/A stress desired.

Data relating specimen bending stress versus fixture displacement (amplitude) under dynamic conditions were obtained and a master calibration curve prepared. A light-beam type recording system was used to record dynamic strain. True stresses were calculated from the 90° rosette formula using 15.95×10^6 psi dynamic modulus of elasticity and 0.34 Poisson's ratio.

The specimen geometry was shown to have an edge stress concentration of zero in bending, and a concentration of $K_t = 1.1$ in tension. Therefore, under normal surface conditions, the specimens would be expected to fail at one of the four corners of the minimum cross section, unless predisposed to locations on the major surfaces of the specimen gauge section by greater K_t induced from wear damage.

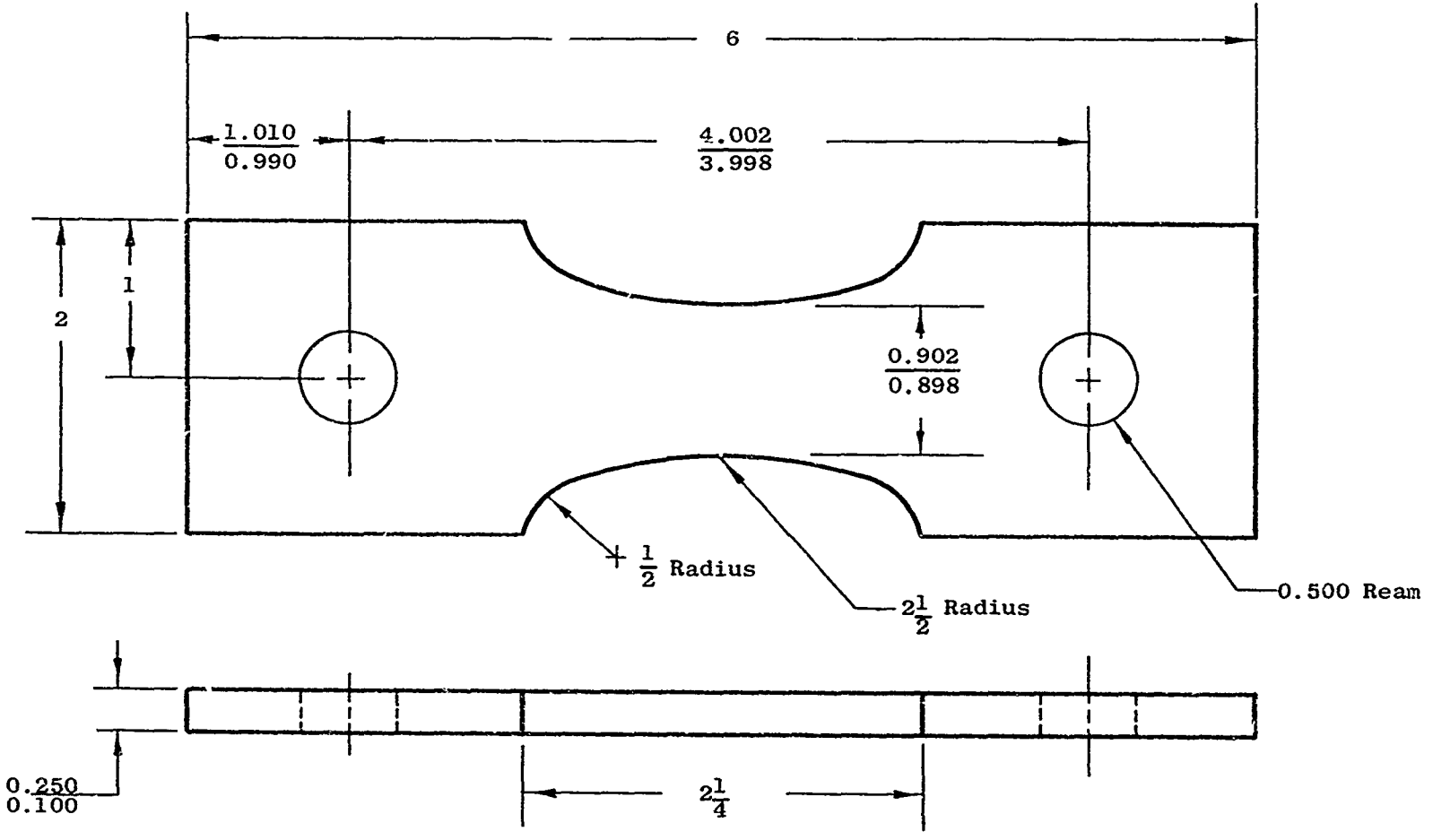

Figure 9. Configuration of High Cycle Fatigue Specimen.

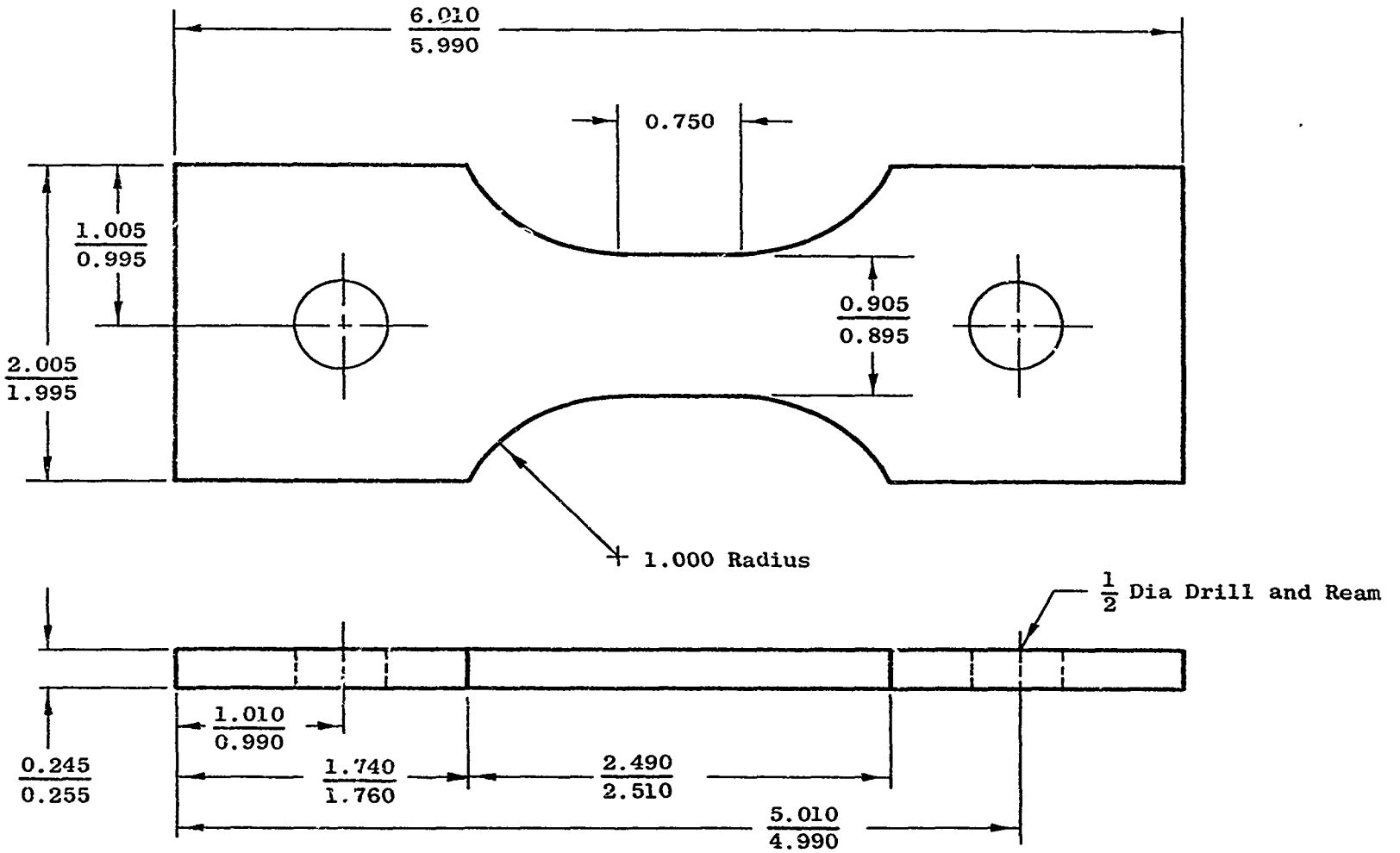

Figure 10. Configuration of Low Cycle Fatigue Specimen.

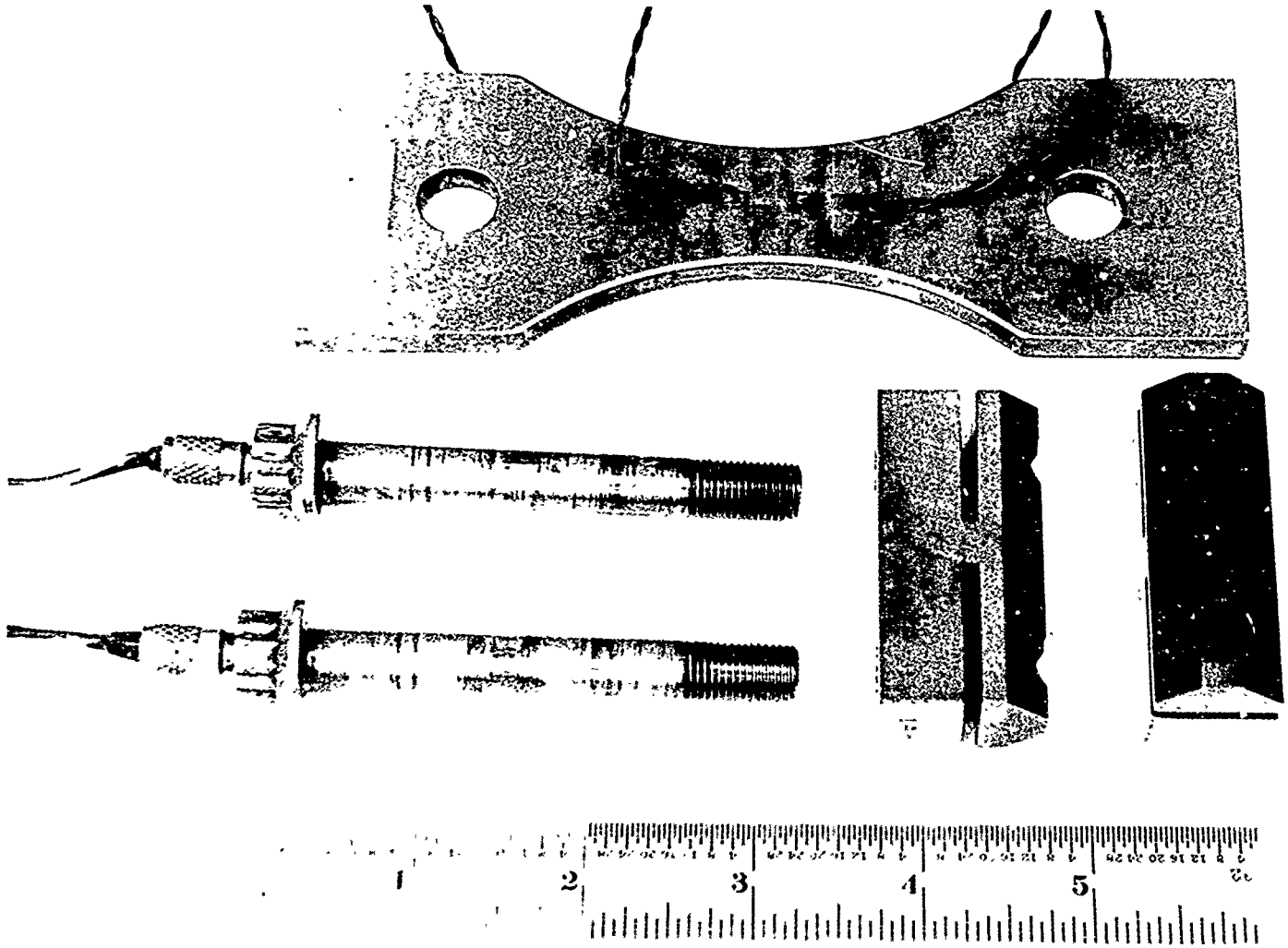

Figure 11. Fretting Fatigue Test Specimen with Pair of Wear Shoes and Internally Strain-Gaged Clamping Bolts. Strain Gages on Calibration Specimen Indicates Location where Reported Bending Stress is Monitored and Controlled.

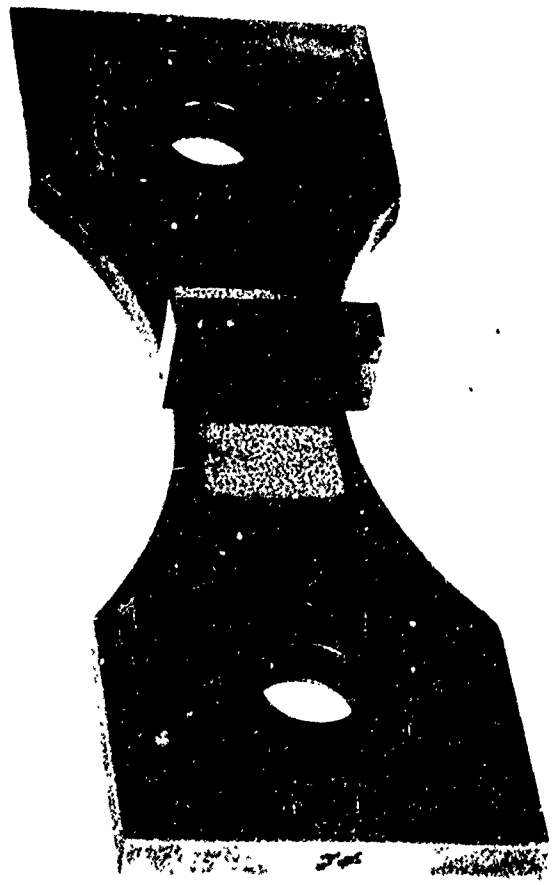

Figure 12. Specimen and Shoe Combination for High Pressure Sliding Wear Test

Figure 13. Calibration Specimen Illustrating Placement of Strain Gages on Specimen Surfaces

b. High Cycle Fatigue Test Results - Room Temperature

In this test, the fatigue bending stresses produce minute alternating strain motion of the Ti specimen surface against the mating wear shoes. This results in classic fretting, the severity of which is measured by the change in fatigue life of the specimen. The variable in this test series is the shoe contact pressure which might be expected to influence the severity of fretting under (1) very high surface contact pressure therby restricting the bending and resultant strain motion at the interface, or (2) such low surface pressure that significant fretting might not occur. Figure 11 illustrated an instrumented specimen, a set of wear shoes, and the pair of internally strain-gauged clamping bolts. Specimen strain gauges were attached within 1/32 inch of the shoe contact edge where reported bending stress was monitored. The fretting fatigue apparatus containing a specimen with bolted-on wear shoes for high contact force was shown in Figure 6. Figure 14 illustrates the specimen assembly with precalibrated springs holding the wear shoes for 500 psi contact pressure.

Tests under 75,000, 5000, and 500 psi shoe contact pressure were performed. The results are compiled in Table I and plotted in Figure 15. The S-N curves are presented in conjunction with baseline nonfretting and fretting fatigue data for 50,000 and 25,000 psi shoe pressures from background tests conducted by the General Electric Company.

Several effects are evident from these data. Specimens tested with no fretting define a 10^7 cycles run-out stress of 50,000 psi alternating (70,000 psi total including the mean tensile stress). Specimens with fretting shoes clamped at 25,000 and 50,000 psi nominal surface contact pressure, and tested at stresses in the vicinity of the baseline run-out stress, showed no loss in cyclic life capability. Fretting wear was apparent in the contact area, but failures occurred adjacent to the fretting bands. Failure always occurred outside the area of contact, and 8-15 mils subsurface, presumably below the effective shot-peened surface layer.

However, at slightly higher alternating stresses representing possible overstress conditions, a substantial loss in cyclic life capability occurred due to fretting. The effect was clearly fretting fatigue in that all specimens failed within the narrow fretting band found at the edge of the shoe contact area. All such failures originated at the surface in the area damaged by fretting.

In the original Company-sponsored studies, there was no significant difference observed as the result of varying the shoe contact pressure from 25,000 to 50,000 psi. The current tests under 5000 and 75,000 psi shoe contact pressure likewise produced no difference. The fretting fatigue loss was dependent upon the magnitude of relative strain motion at the specimen/shoe interface and independent of the nominal interface contact pressure in the range studied.

Figures 16, 17, and 18 illustrate the typical surface appearance of fretting fatigue specimens tested under 500, 5000, and 75,000 psi, respectively. Visually

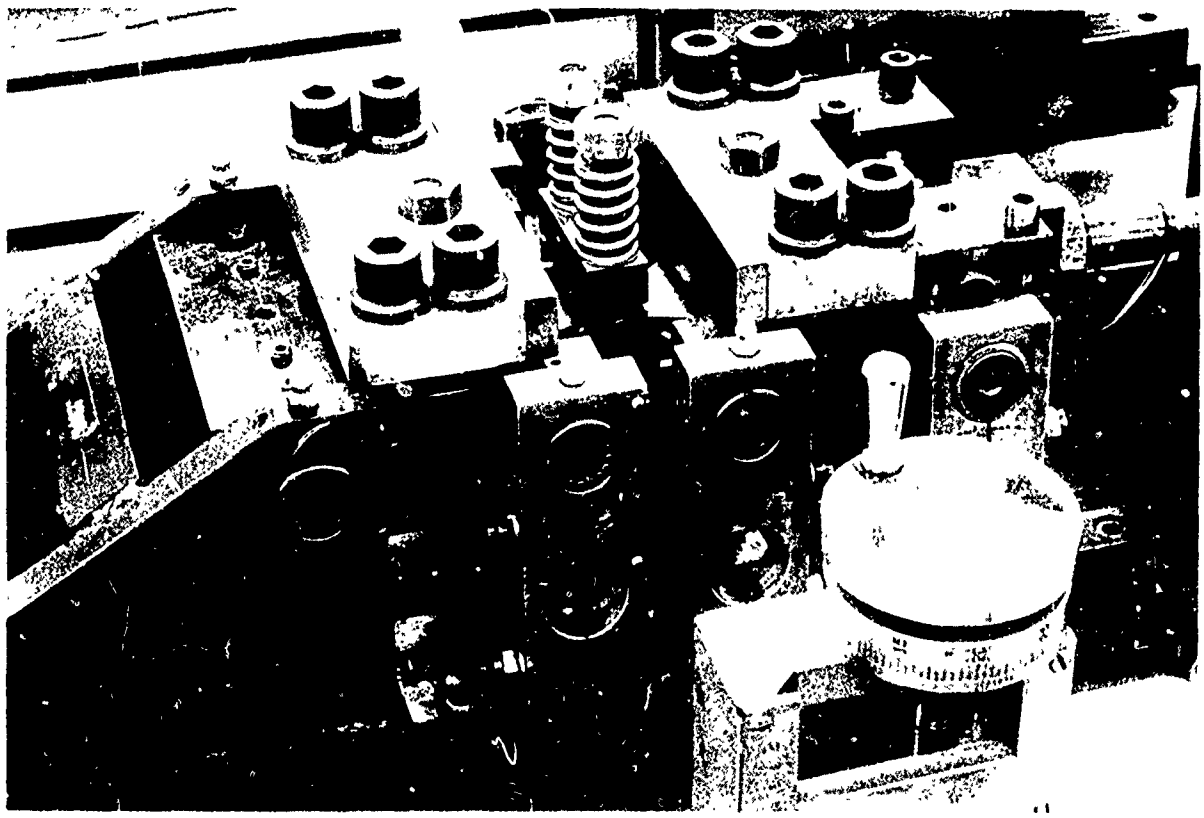

Figure 14. View of the Fretting Fatigue Test Fixture Illustrating the Method of Shoe Assembly for Low Contact Pressure (500 PSI). The Springs were Precalibrated to Provide Approximately 90 Lb of Contact Force (500 PSI).

Table I. Fretting Fatigue Test Results.

Specimen Number	Contact Pressure ksi	Mean Stress ksi	Alternating Stress ksi	Cycles to Failure X10^6	Results
Room Temperature Tests					
54	75	20	60	.078	This group generally exhibited no gross evidence of general wear or wear debris in shoe contact areas. Visible wear limited to four lines or narrow bands along the edges of shoe contact areas. Fatigue origins, single and multiple, occurred in any one band.
52	75	20	60	.070	
53	75	20	60	.069	
60	75	20	45	1.670	
49	5	20	60	.154	This group generally exhibited considerable brownish, powdery wear debris in shoe contact area, giving appearance of extensive wear. Fatigue origins, nonethless, occurred only at the edges of shoe contact, except #80 which was a corner origin.
50	5	20	60	.152	
48	5	20	60	.094	
80	5	20	45	5.113	
64	5	20	45	.242	
56	.5	20	60	.599	This group exhibited the most accumulation of debris. Wear striations indicated some shoe movement due to the light load. Wear appeared severe, but extended fatigue lives did not confirm this impression.
58	.5	20	60	.502	
57	.5	20	60	.406	
69	25(1)	20	60	1.270	Specimen wear barely discernible. Origin not in wear area.
62	25(2)	20	60	.070	Specimen exhibited edge contact fretting. No debris. Origins in fretted bands.
61	25(3)	20	60	.066	Similar to #62
63	25(3)	20	60	.056	Similar to #62
400°F Tests					
66	Non-fretted	20	65	3.03	This group with no fretting involved failed from single origins at normal stress concentration sites in one of the four radiused edges of the gauge section.
76	Non-fretted	20	65	1.30	
65	Non-fretted	20	60	2.80	
77	Non-fretted	20	50	2.36	
67	Non-fretted	20	45	12.80	Run-out
75	25	20	60	.037	This group exhibited some debris, but was characterized by the occurrence of pits and corresponding attached lumps of galled wear products on opposing specimen and shoe surfaces. Numbers 36, 79 and 42 were not affected by wear.
51	25	20	60	.026	
36	25	20	40	10.245	
79	25	20	40	8.92	
42	25	20	40	6.86	

(1) Interrupt at 10^4 cycles
(2) Interrupt at 10^5 cycles
(3) Interrupt at $5X10^4$ cycles

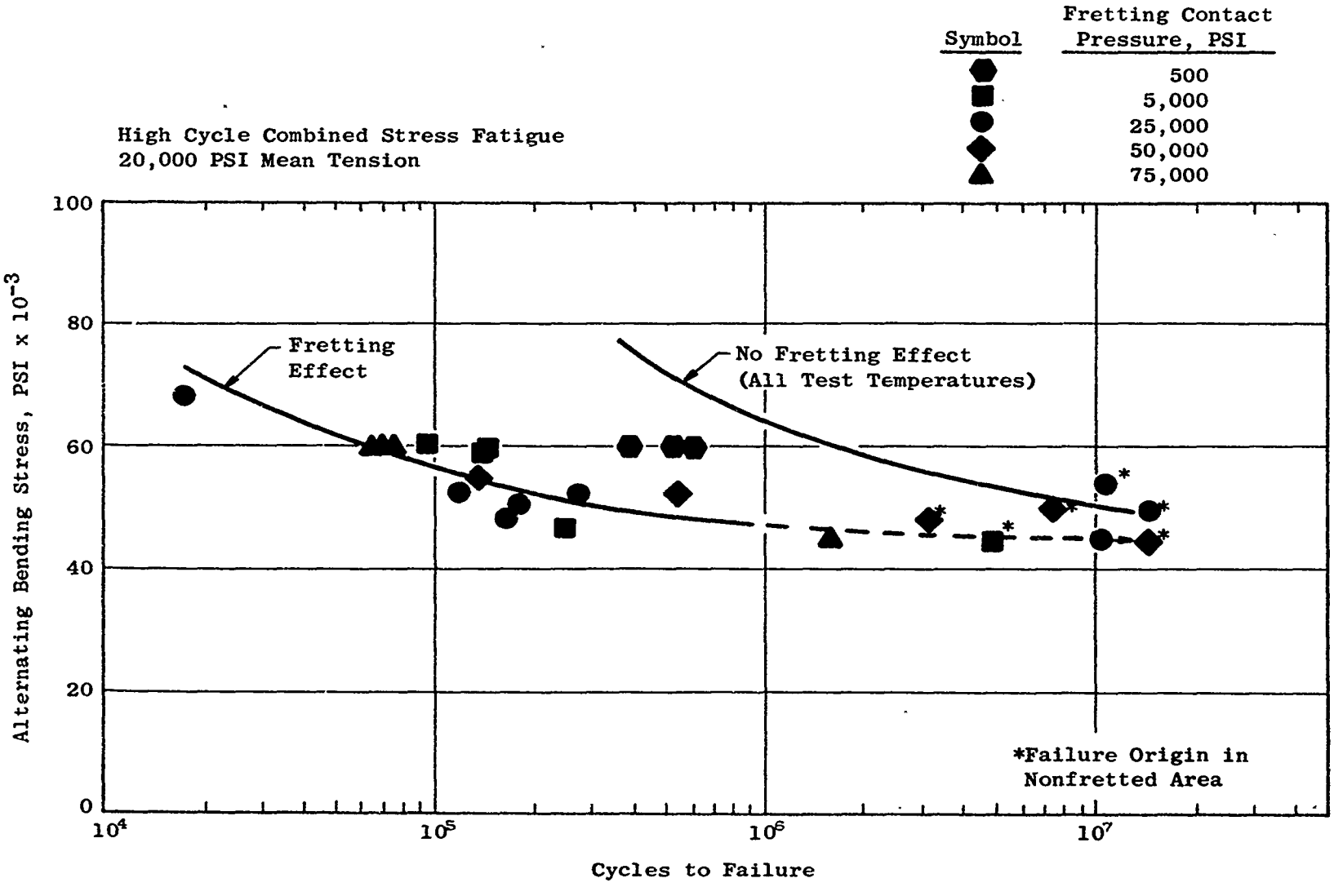

Figure 15. Effect of In-Situ Fretting During High Cycle Fatigue of Shot-Peened Ti-6Al-4V at Room Temperature.

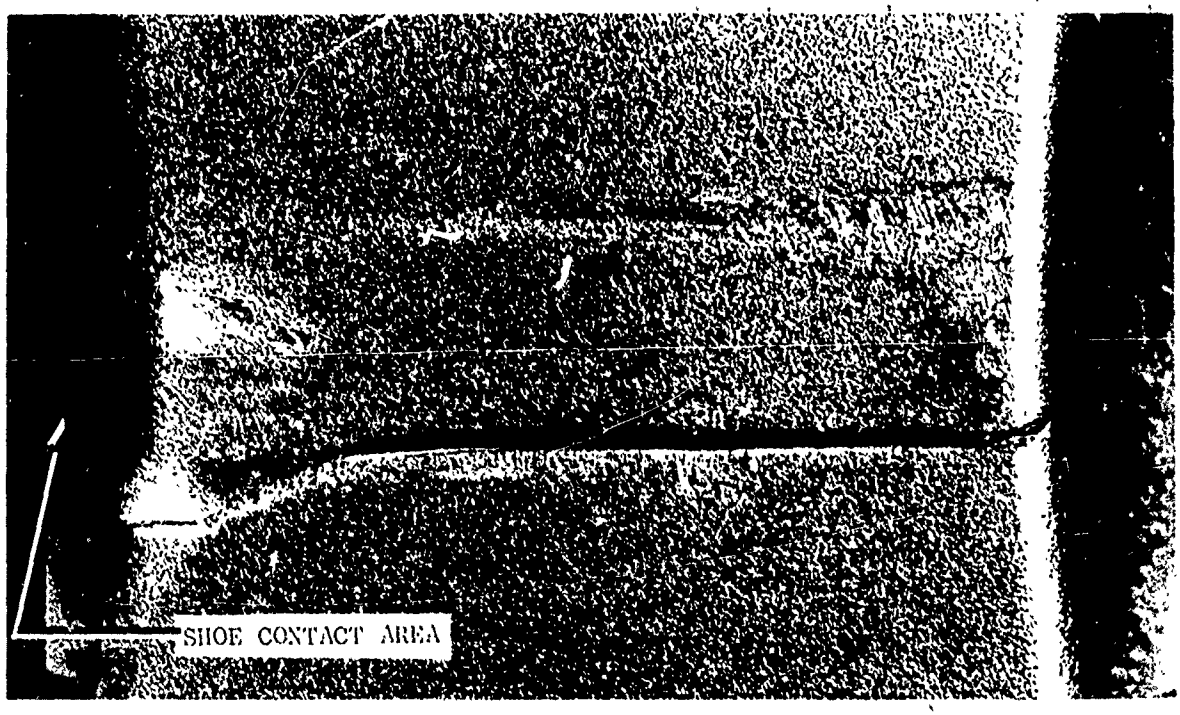

Neg 4787

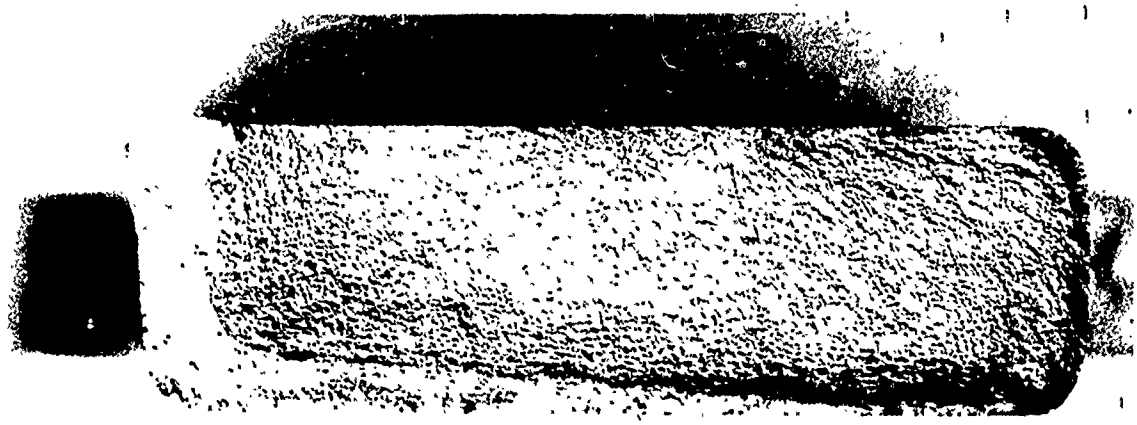

Neg 4788

Figure 16. Fretting Fatigue Specimen 56 Tested Under 500 PSI Shoe Contact Pressure at 20,000 PSI Mean Tension and 60,000 PSI Alternating Bending Stress to 6 x 10^5 Cycles. The Shoe Contact Area Shows Fretting Debris Along the Edges and Pits at the Ends. The Failure Initiated from a Single Origin Visible on the Fracture Face, Corresponding to Fretting Damage Along the Edge of the Shoe Contact Area. (6X)

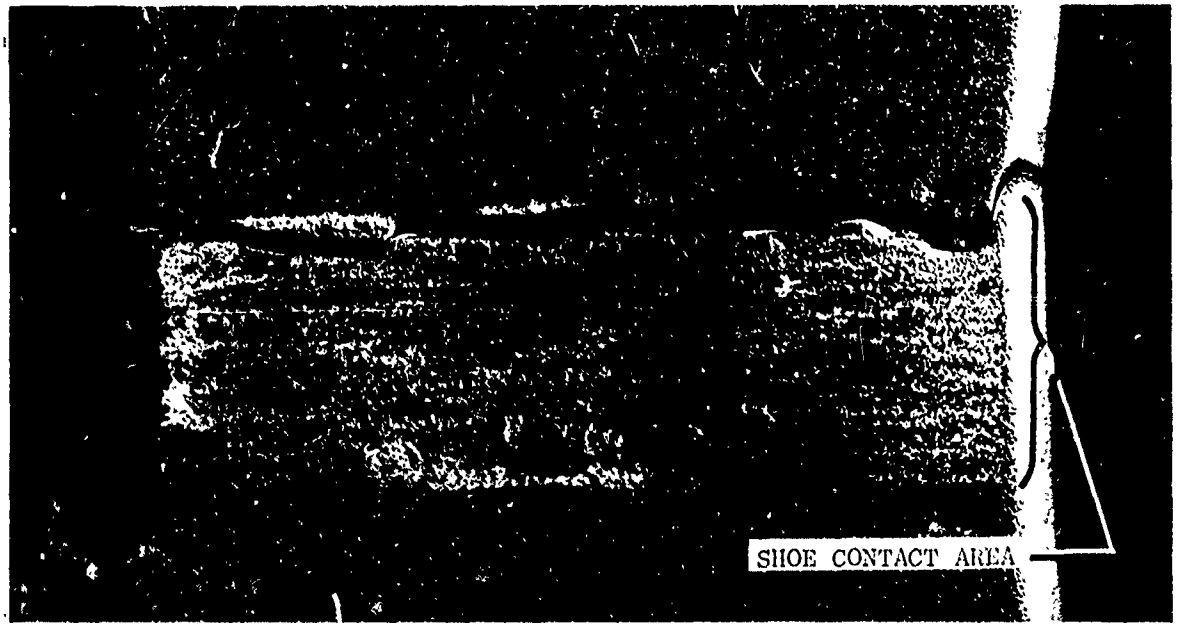

Neg 4783

Neg 4784

Figure 17. Fretting Fatigue Specimen 48 Tested Under 5,000 PSI Shoe Contact Pressure at 20,000 PSI Mean Tension and 60,000 PSI Alternating Bending Stress to 9.4×10^4 Cycles. Upper Photograph Illustrates the Fretted Area where the Shoe was in Contact. Origins Visible in the Lower Photograph Show the Initiation of Failure from Surface Damage at the Edge of the Shoe Contact Area. (6X)

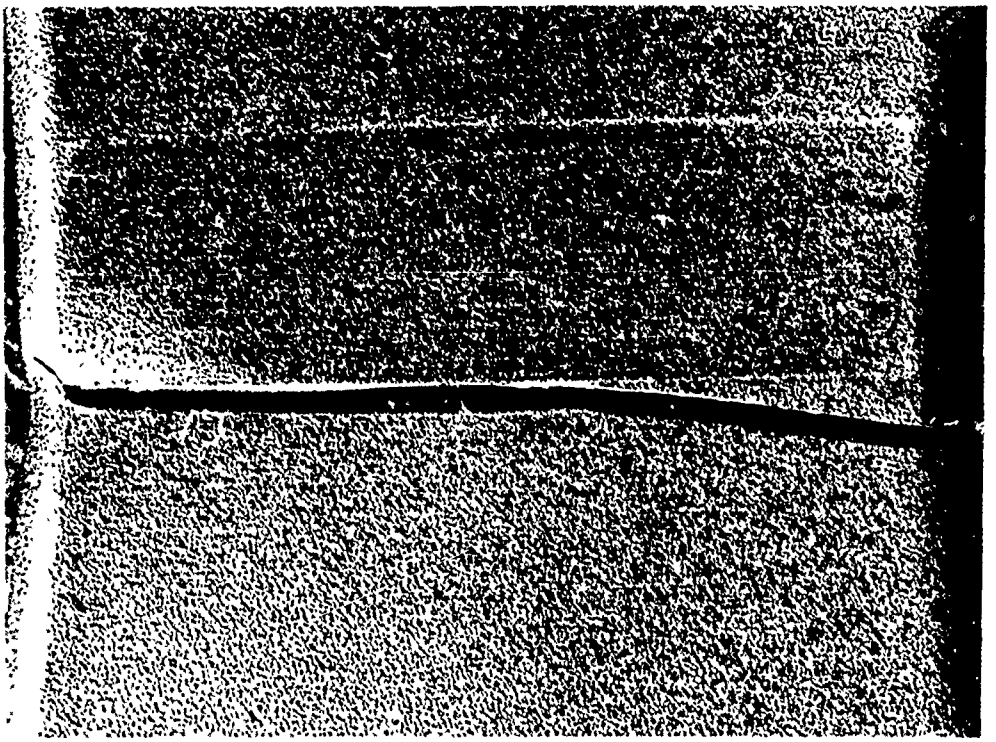

Neg 4789

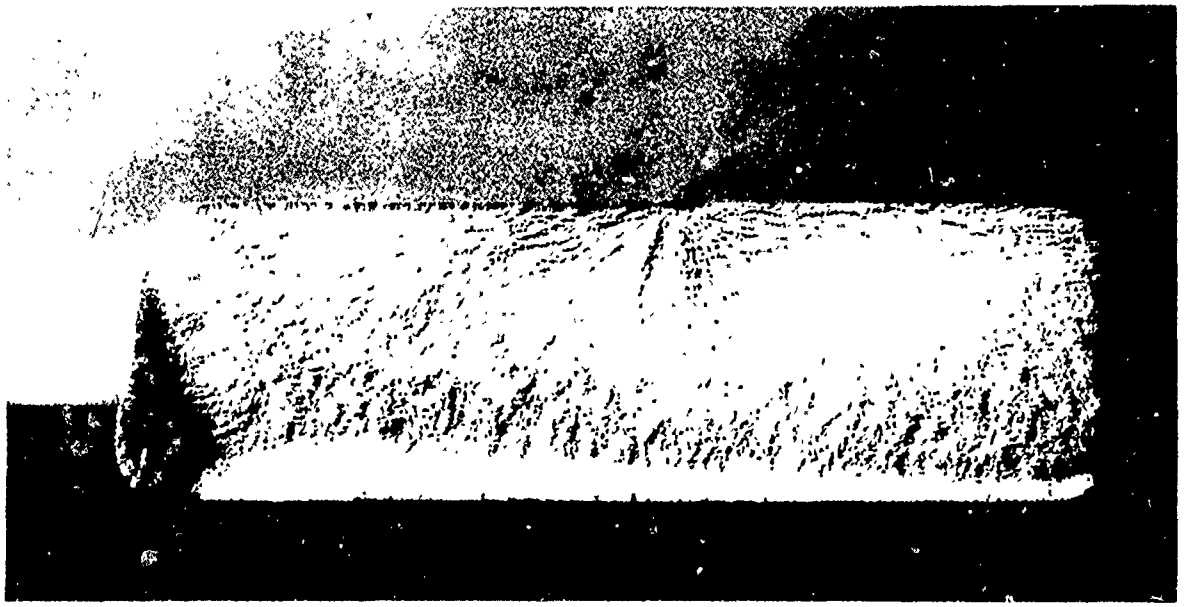

Neg 4790

Figure 18. Specimen 60 Tested Under 75,000 PSI Shoe Contact Pressure. Upper Photograph Illustrates the Mild Appearing Fretted Area where the Shoe was in Contact. Origins Visible in the Fracture Face Show the Initiation of Failure from Surface Damage. Detail of the Wear Damage is Shown in Figure 20. (6X)

the fretting was more evident on the lower-pressure specimens, and it extended over more area under the shoes. Lesser restraint of specimen bending under the lower-pressure shoes apparently permitted more relative motion from bending strain and Poisson effect throughout the interface. But at 75,000 psi contact pressure, bending restraint prohibited large strain motion except in a finite band along the edge of each shoe contact area. It is this fretted band at the edge of contact where fretting-related failures always occur on test specimens. No specimen failed under a shoe between the fretted bands, and no fatigue crack propagated into the contact area.

Except for a moderate increase in the life of the specimens fretted under 500 psi contact pressure (and regardless of the appearance of more apparent fretting at 500 and 5000 psi), the combination of strain motion, fatigue stress, and mean stress produced fretting damage of significant magnitude in terms of fatigue life reduction under the five levels of contact pressure which have been investigated.

Figure 19 (Specimen 52) illustrates what was found to be the typical metallographic appearance of the fretted specimens. Figure 19A shows the mild-appearing fretting wear surface. Figure 19D shows the lip of the fracture face and a fretted depression on the adjacent wear surface. At the end of the fretted depression there is a shear crack. The depression contains wear debris. Figure 19C is a section through the fretted area at the other edge of the contact area. Fretting debris prevented good adherence of the Ni-plate applied for metallographic preparation, but the fretted depression is evident. Surface shear cracks are visible as is an incipient fatigue crack, characterized by its nearly vertical direction. Note the fatigue crack propagated from a more oblique shear crack. In the metallography of fretted specimens, the oblique shear cracks from which fatigue fracture initiates were only observed in the locations shown, i.e., corresponding to the fretted bands described previously. None occurred any farther under the shoes.

Note that the direction of the shear cracks is toward the contact area and away from the applied bending stress. This pattern has also been consistent in the fretted areas observed. The cracks allude to the shear stresses resulting from relative sliding motion of the surfaces. The cracks develop in tension, i.e., when the specimen is bending away from the shoe. The benefit of shot peening as a deterrent to fretting, relates to the formation of a compressive surface layer which tends to offset a portion of the tensile shear stress. Lubricants would also act to deter fretting by reducing the friction coefficient, thus lowering the shear stress.

Figure 20 is a series of SEM photographs of Specimen 60 illustrated previously in Figure 18. Figure 20A shows a macrophoto of the single major origin. Figure 20B shows the origin in perspective with the fracture edge and the dimpled peened texture of the specimen surface (part of the shoe contact area during test). Successively detailed views of the origin in Figures 20C and 20D reveal no readily discernable primary site of failure. Nonetheless, they show the fretted band from shoe contact along the fracture edge. In the center view it

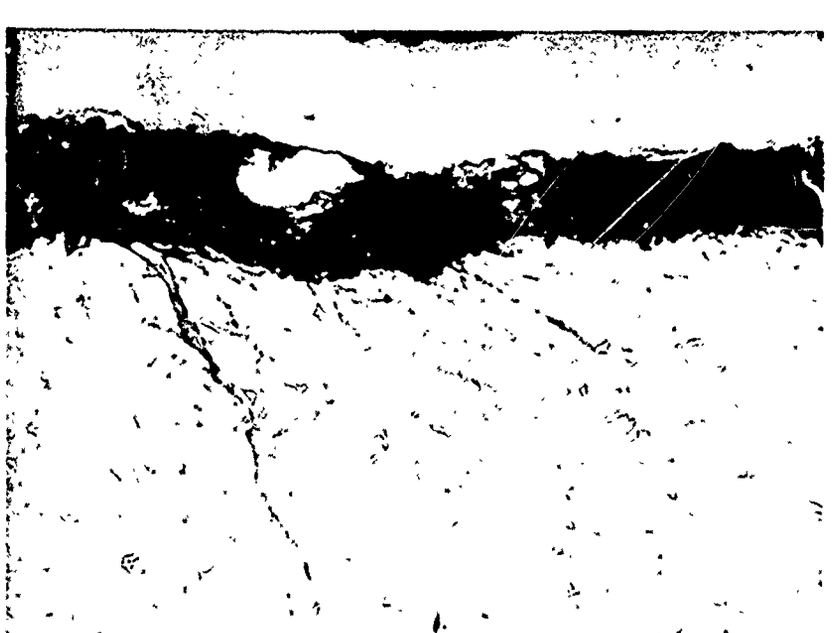

Mount 6901, Neg G 6300 1000X
C

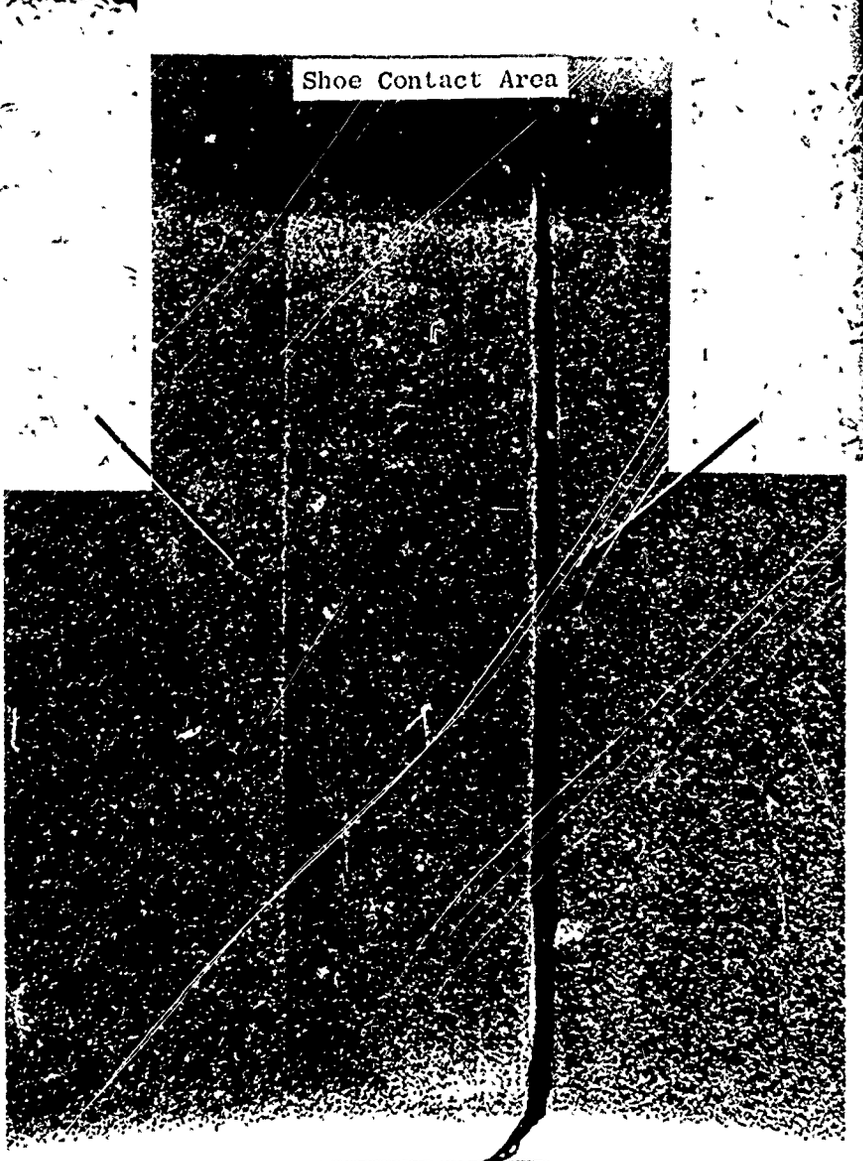

4785, 6X

A

Figure 19. Composite Macro- and Microphotographs of Specimen 52 After Fretti
The Metallographic Sections Reveal Oblique Shear Cracks and Wear
Shoe Edges. An Incipient Fatigue Crack is Visible in View C. T
from Multiple Origins. SEM Photographs of Such a Wear Surface a

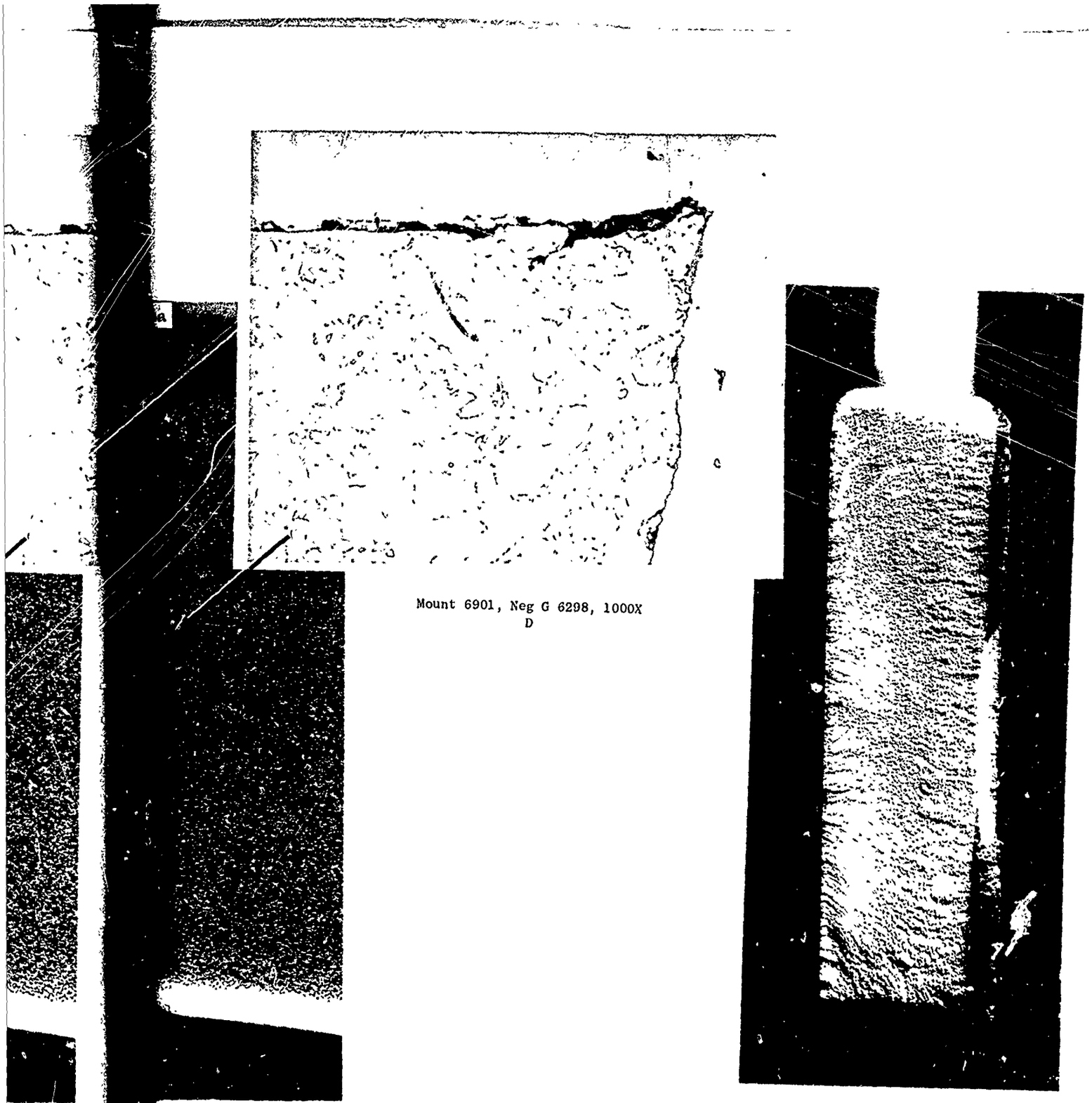

Mount 6901, Neg G 6298, 1000X
D

4785, 6X

4785, 6X

4796, 6X

B

fter Fretti
s and Wear
View C. T
Surface a

pecimen 52 After Fretting Fatigue Under 75,000 PSI Shoe Contact.
Shear Cracks and Wear Pits in the Bands of Contact of the Fretting
Visible in View C. The Fracture Surface Reveals Fatigue Failure
Such a Wear Surface are Shown in Figure 20.

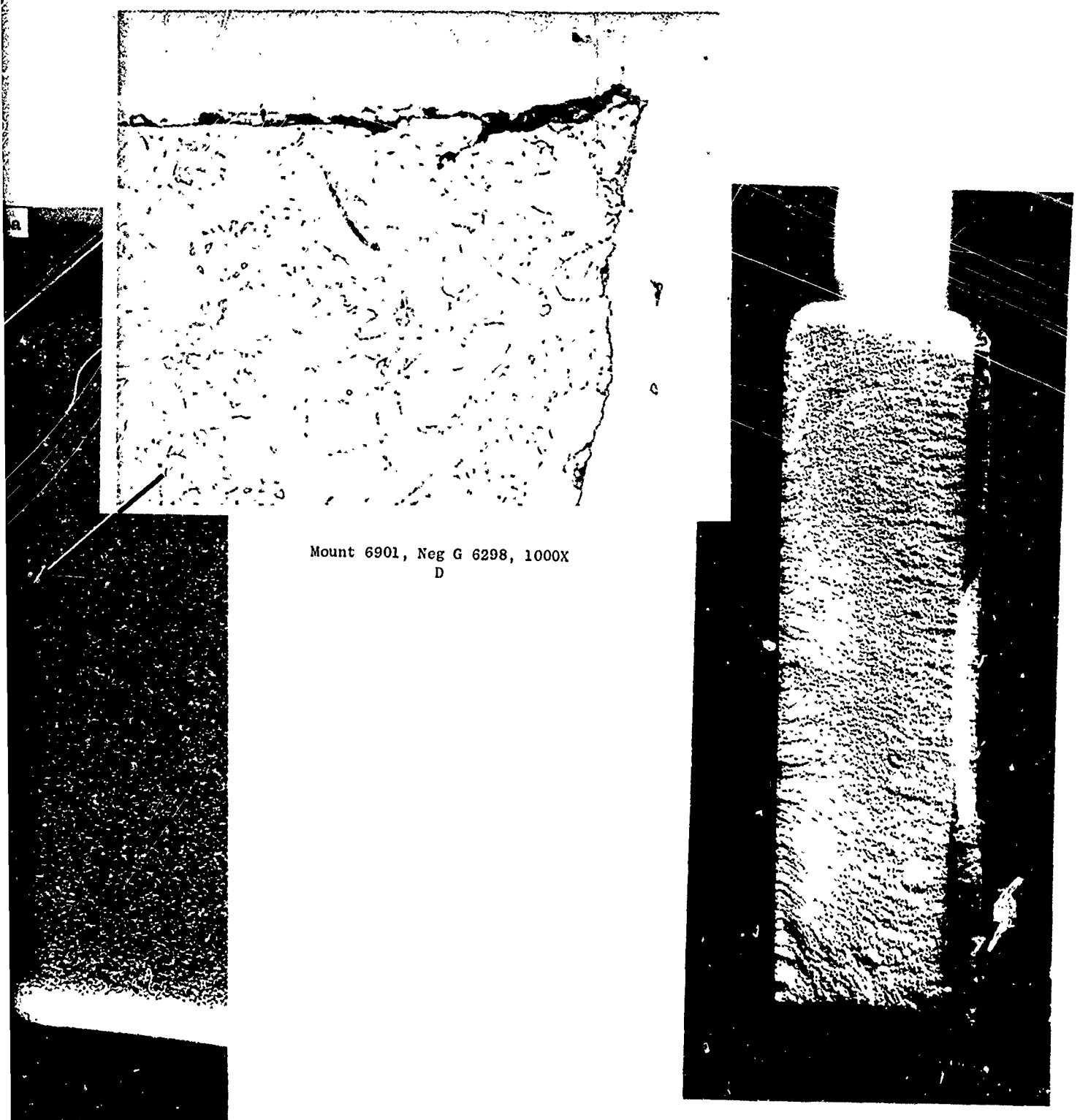

Mount 6901, Neg G 6298, 1000X
D

4785, 6X

4796, 6X

B

pecimen 52 After Fretting Fatigue Under 75,000 PSI Shoe Contact.
Shear Cracks and Wear Pits in the Bands of Contact of the Fretting
Visible in View C. The Fracture Surface Reveals Fatigue Failure
Such a Wear Surface are Shown in Figure 20.

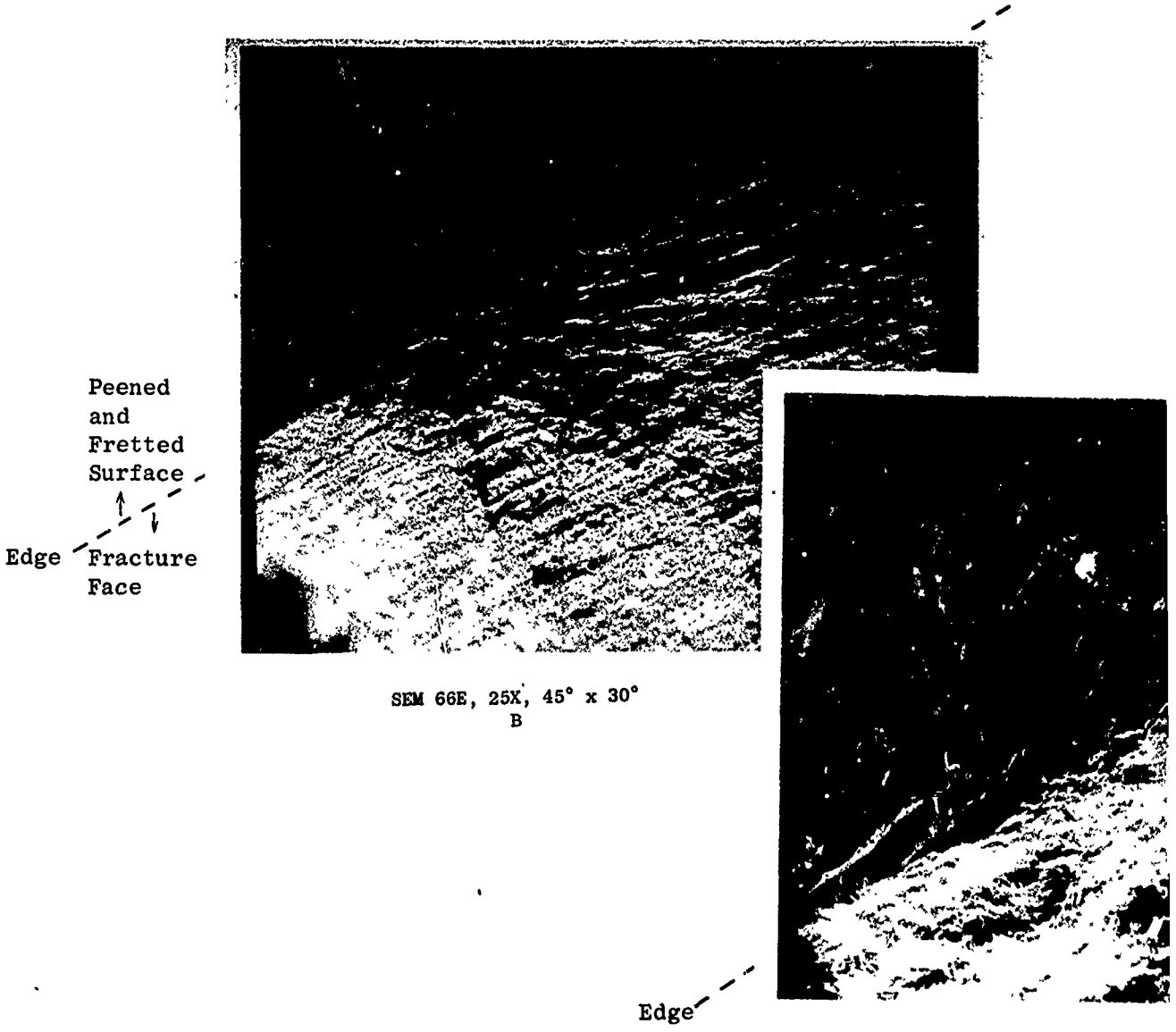

Figure 20. Composite SEM and Macrophotographs of Specim
Specimen Surface was Illustrated Previously
Fracture Face in the Origin Reveal the Surfa
Figure 19 Previously Illustrated Typical Met
Typical Shot-Peened Surface in a Nonfretted

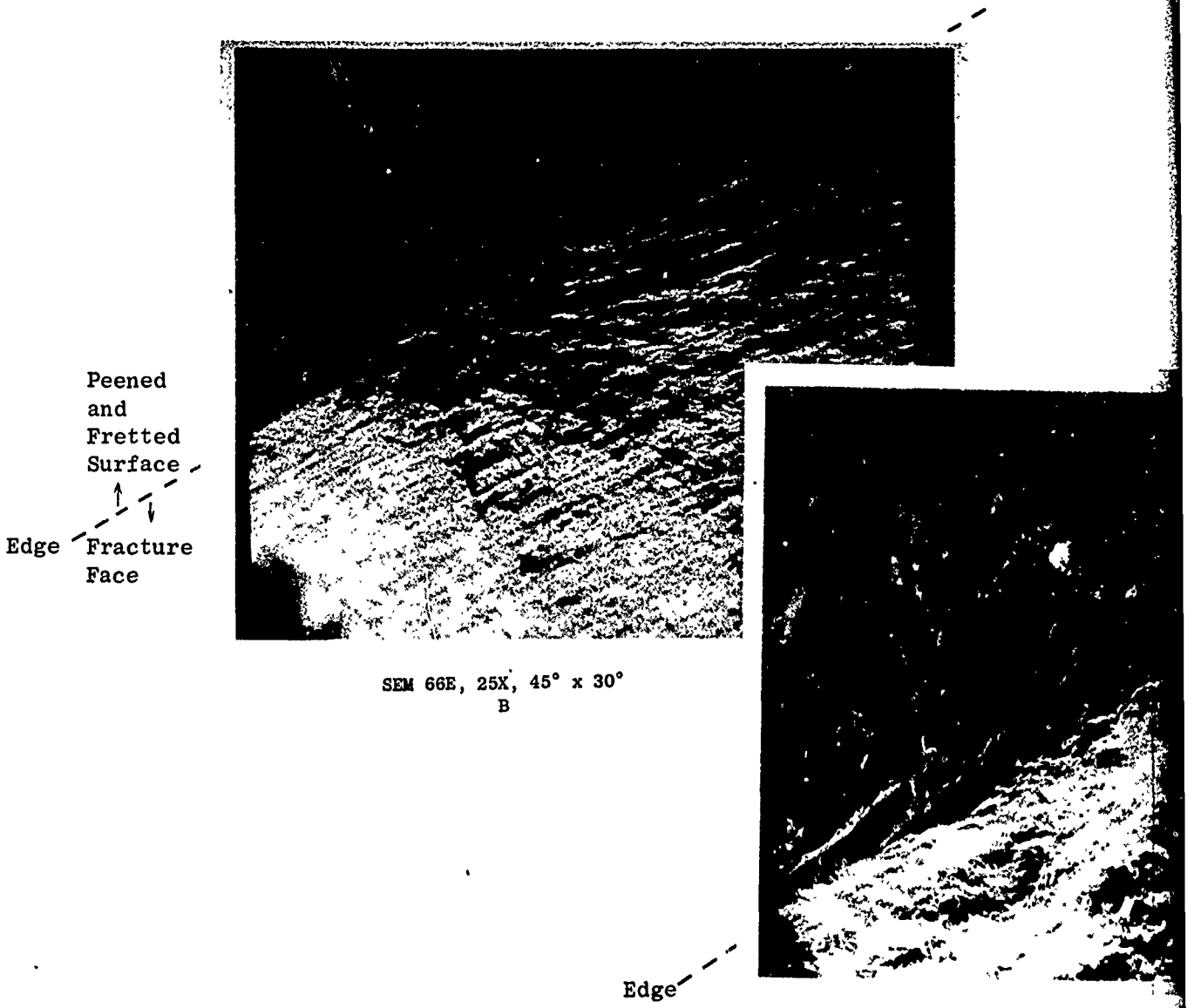

SEM 66E, 25X, 45° x 30°
B

C

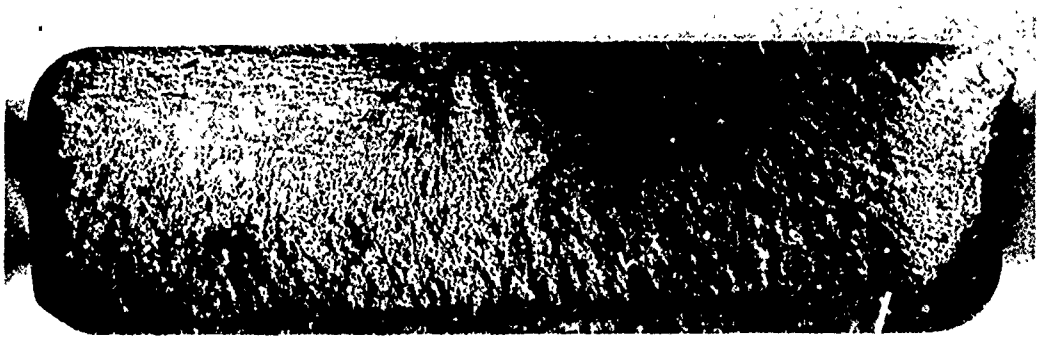

Neg 4790, 6X
A

Figure 20. Composite SEM and Macrophotographs of Specimen
Specimen Surface was Illustrated Previously in
Fracture Face in the Origin Reveal the Surface
Figure 19 Previously Illustrated Typical Metall
Typical Shot-Peened Surface in a Nonfretted Are

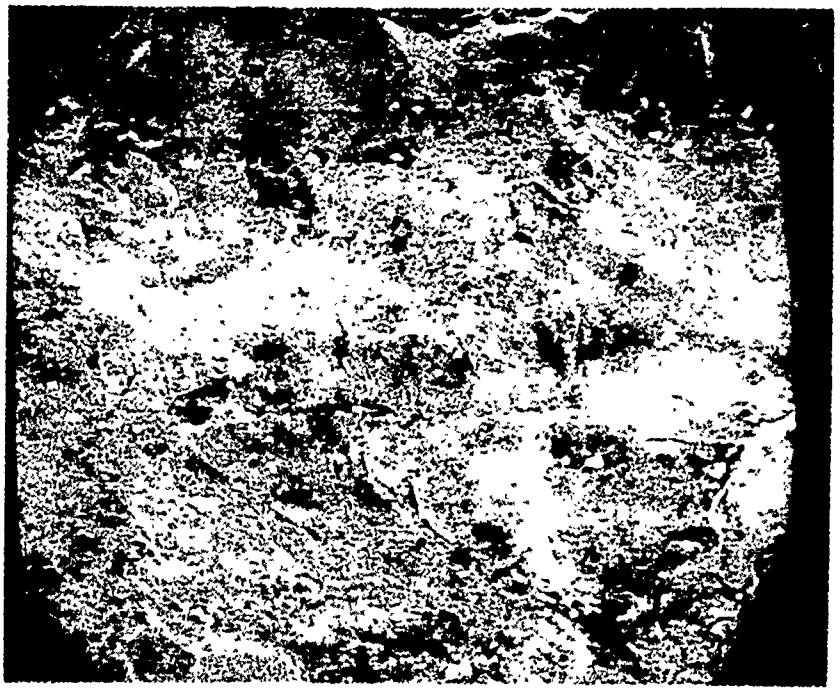

625X, 5° x 0°
E

C 250X

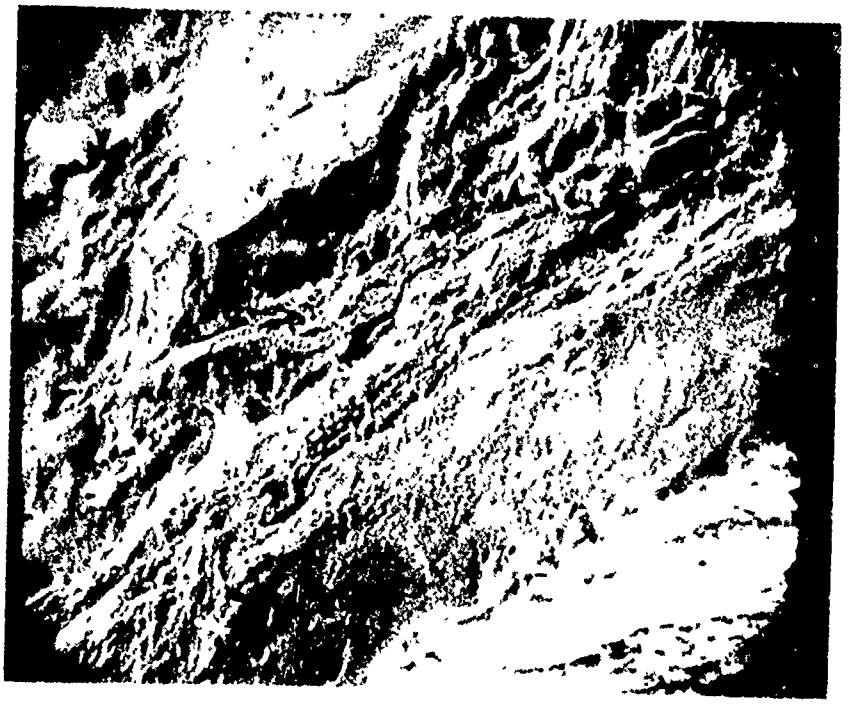

Edge

, 6X

1250X

D

hs of Specimen 60 After Fretting Fatigue Under 75,000 PSI Shoe Contact. The
Previously in Figure 18. Successive SEM Views of the Fretted Surface and
al the Surface Damage and Shear Cracks Along the Band of Shoe Edge Contact.
Typical Metallographic Cross Sections of a Fretted Band. View E is a
Nonfretted Area.

is seen that severe fretting is confined to a narrow surface area along the edge. The undulating shot-peened surface is visible in the background.

The detail at 1250X (Figure 20D) shows several basic features typical of the fretted specimens examined during this program. In the upper field of view is a plateau of original peened surface. The escarpment was formed by the shearing away of metal flakes such as seen at the nose or promontory of the plateau. On each side are flakes of fretted metal scraped back from the fretting band area in the foreground. The wear mechanism of adhesion and abrasion may be clearly imagined from this view. The plateau was protected from wear by perhaps being lower than the general original topography or having been kept separated by accumulated debris in the shoe interface.

The fretted band appears to be free of debris but exhibits a pattern of interconnecting cracks and shear lips. A metallurgical cross section would appear like that for Specimen 52 shown previously in Figure 19. Similar failure mechanisms have been reported in fretting studies for brass and aluminum[18]. No single site of failure origination was discernable. It is apparent that the many cracks in the damaged surface combined to form the visible macro-origin.

Figure 20E is an SEM view of the shot-peened surface of Specimen 60 in an area beyond the shoe contact zone. Metallographic sections of many specimens examined showed that peened surfaces were not faultless, but included occasional flaky overlays of surface metal amid the general undulations from peening. The reason is evident in the SEM view, where it is seen that the surface does indeed contain many overlaps and seams. As surface integrity features, they are minutely shallow and their detriment, if any, is unknown. However, they are suspected as possible sites for the initiation of fretting fatigue cracks.

c. Interrupted Fretting Fatigue

The object of this study was twofold: (1) to determine a threshold fatigue life for specimens at one set of fretting pressure and stress conditions, and (2) to determine the effectiveness of fluorescent inspection to preempt specimen failure by early detection of cracks. Radioactive Krypton was shown in background studies to delineate effectively the fretted areas of fatigued specimens, as shown in Figure 21. The more common fluorescent penetrant method was shown to be very effective in detecting cracks.

The fretting fatigue test method consisted of subjecting the specimens to the usual fretting exposure for a preselected number of fatigue cycles. Then the test was stopped, the shoes removed, and the specimen inspected by hot fluorescent penetrant technique. Specimens were then continued in fatigue without the fretting shoes. Fretting was to be interrupted as close to impending failure as possible. Under the conditions of 25,000 psi shoe pressure and 60,000 psi alternating stress, failure was expected to occur in the vicinity of 10^5 cycles. Describing the tests chronologically, the first specimen tested in the group failed short of the intended interruption goal of 10^5 cycles, as was shown in Figure 2. An end point of 5×10^4 cycles was then selected to terminate fretting and inspect the specimens.

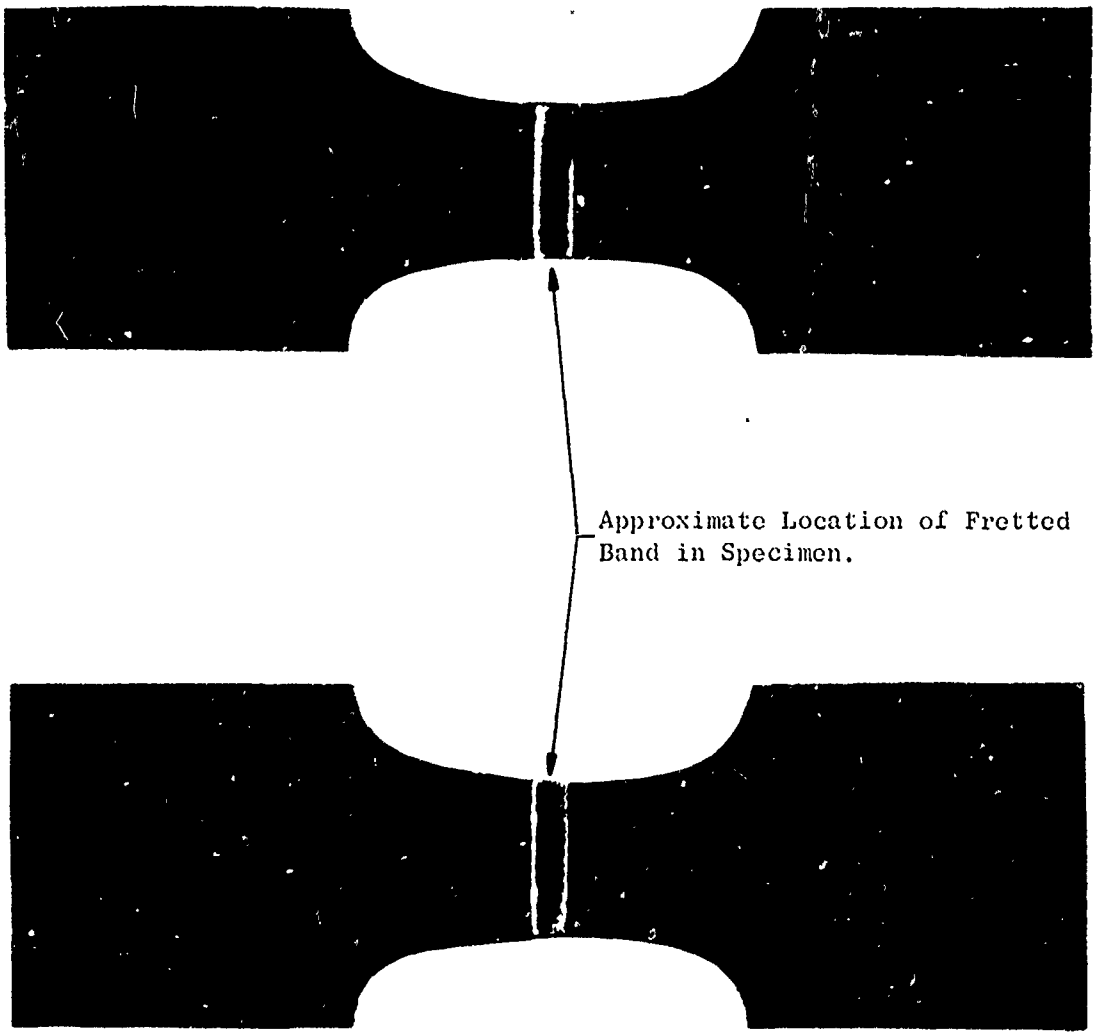

Figure 21. Autoradiograph Exposures of Kryptonized Fretted Specimens. The Fretted Bands were Effectively Outlined by the Method, but Crack Detection was Difficult. (Industrial Nucleonics)

The next test was interrupted at 5×10^4 cycles, and fatigue testing continued to failure without the fretting shoes. This specimen was not removed from the fixture (no axial load cycle) nor was it given the penetrant inspection, to be certain that such operations did not affect the remaining fatigue life. The specimen failed after an additional 6000 fatigue cycles in the absence of continued fretting.

The next specimen was removed from the fixture after 5×10^4 fretting fatigue cycles and processed through a hot penetrant inspection. The treatment included first a mild etching in dilute HNO_3-HF and then immersion while heated to 180° F into the penetrant solution. Fluorescent inspection distinctly revealed the fretting pattern along the edges of shoe contact on the top and bottom surfaces, as illustrated by the "black light" photograph in Figure 22. In addition, cracks were in evidence along the center one-third of each of the four fretting lines. (These cracks were also clearly visible at 10X stereomagnification without the penetrant inspection.) The specimen, returned to fatigue testing without shoes, failed in 16,000 additional cycles. Figure 23 illustrates the specimen after failure, photographed under normal lighting, showing the origins to have been present on both fretted surfaces.

Because the previous specimens were terminally damaged by fretting before they had accumulated 5×10^4 cycles, the final specimen of the series was interrupted at 1×10^4 cycles. Neither visual nor fluorescent penetrant inspection revealed any cracking, although a slight fretting condition was visible along the edges of the shoe-contact areas. This specimen was then tested without shoes to a total endurance of 1.27×10^6 cycles. The specimen life was equal to nonfretted baseline conditions; and, confirming this, it failed outside the fretting bands.

Figure 24 shows an SEM view of Specimen 61, interrupted from fretting, then fatigued to early failure. Both photographs illustrate fretting fatigue cracks which were enlarged and blunted by the HNO_3-HF chemical cleaning prior to penetrant inspection. Figure 24 also shows a metallographic cross section of such a crack. Acid pitting of the general surface is also evident in the SEM photographs. The upper photograph illustrates the fretted band at the edge of fracture.

The results of these tests showed that under the conditions where fretting failure can be expected there was a narrow threshold between 10^4 and 5×10^4 cycles where irrevocable fretting damage was done. Those specimens fretted for 5×10^4 cycles failed in a few thousand additional fatigue cycles after fretting shoes were removed. Furthermore, under the test conditions used the incipient failure was clearly evidenced by cracks, highlighted by fluorescent penetrant, but visible at 10 - 15X unaided by the treatment. Similar tests were reported in[18] for brass having such a short crack propagation time that cracks could not be detected, whereas they were easily seen in an Al alloy.

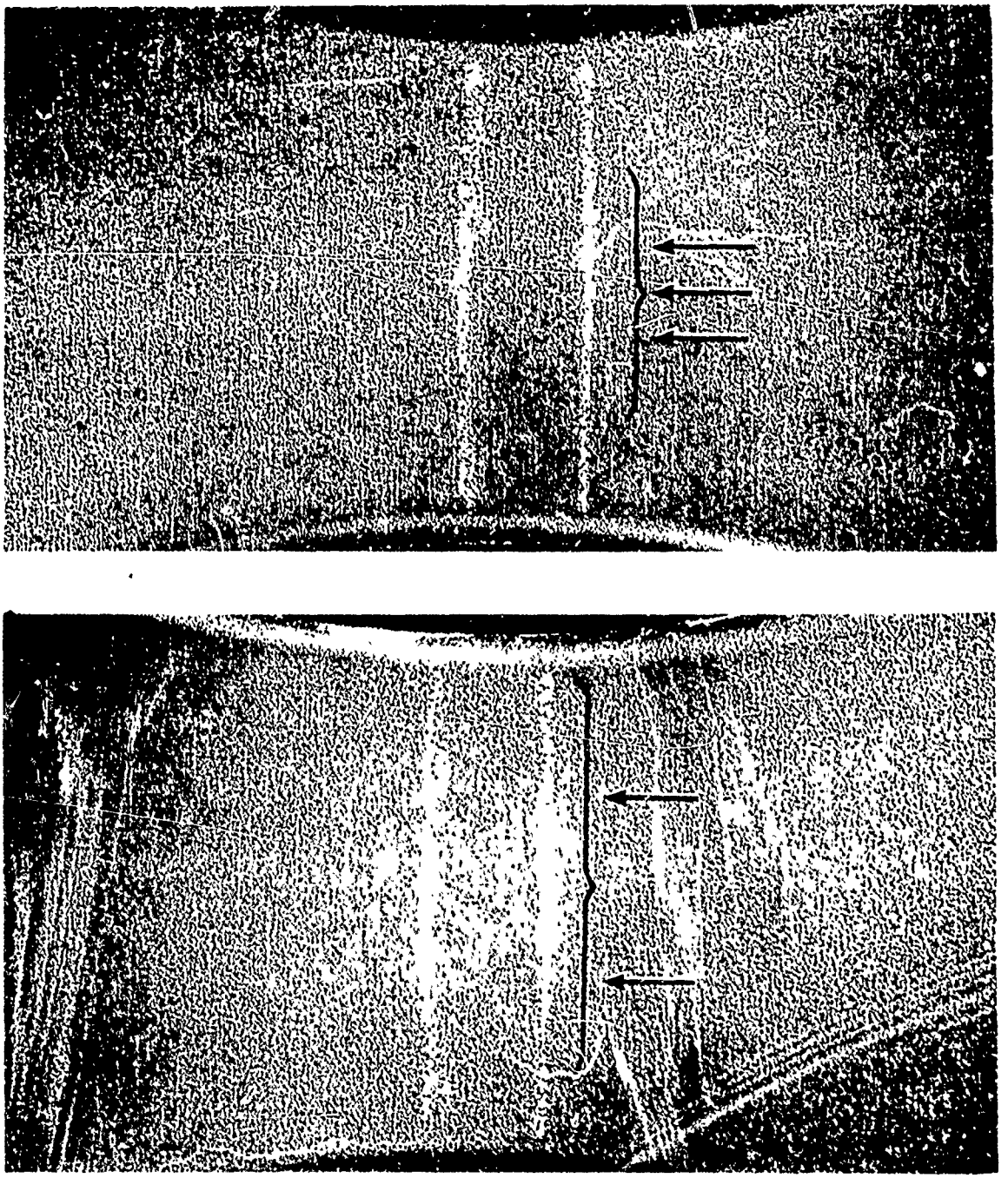

Figure 22. Fretting Fatigue Specimen 61 Photographed Under Ultraviolet Light, Revealing Fluorescent Penetrant in the Fretted Bands of the Shoe Contact Areas. The Specimen was Fretted Under 25,000 PSI Shoe Contact Pressure at 20,000 PSI Mean Tension and 60,000 PSI Alternating Bending Stress, Interrupted After 5 x 10^5 Cycles for Inspection. The Right-Hand Band in Each View Shows Bright Fluorescence Corresponding to Cracks where the Specimen Eventually Failed (See Figure 23). (Neg 4771, 72, 3.5X)

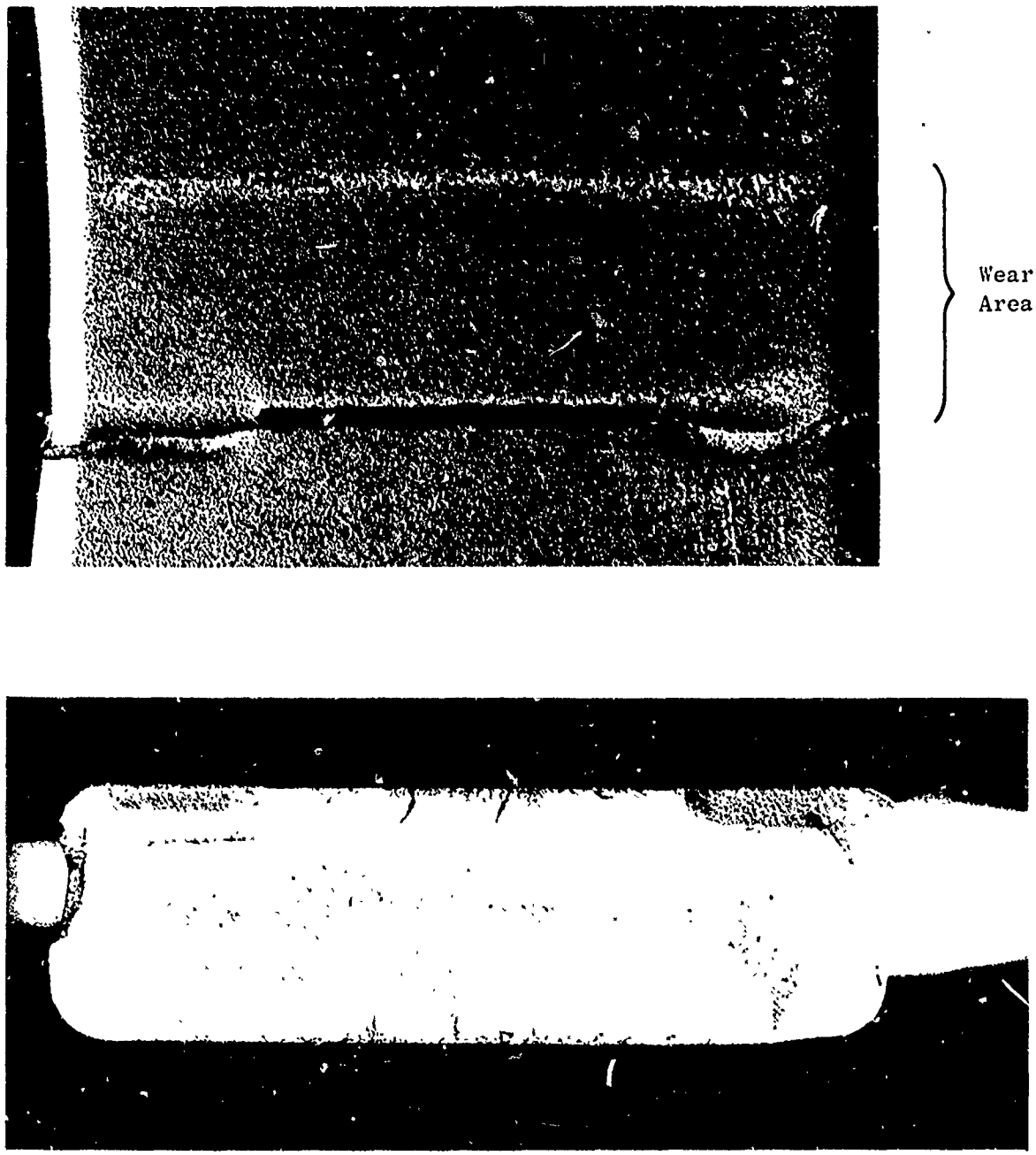

Figure 23. Fretting Fatigue Specimen 61 Tested Under 25,000 PSI Shoe Contact Pressure at 20,000 PSI Mean Tension and 60,000 PSI Alternating Bending Stress. Fretting was Interrupted at 5×10^4 Cycles for Fluorescent Penetrant Inspection Shown in Figure 22. Fatigue was Continued, Without Fretting, to Failure at 6.6×10^4 Cycles. Fracture Originated from Both Surfaces where Cracks were Disclosed at Inspection.

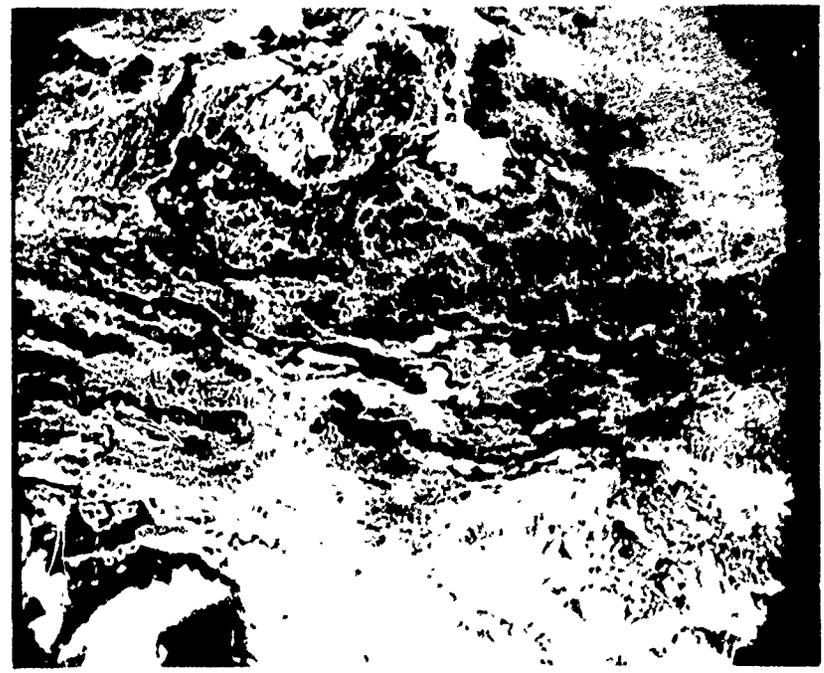

SEM 66G, 615X, 45° x 0°

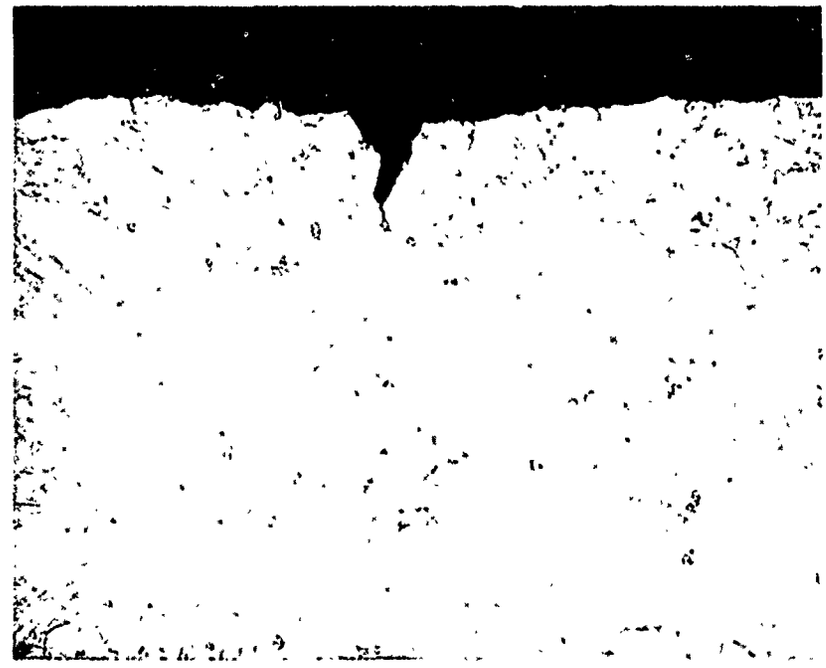

Mount 2012, Neg G 6311, 1000X

Figure 24. SEM and Metallographic View of Specimen 61 Showing Fretting Fatigue Cracks Enlarged by Etching for Fluorescent Penetrant Inspection The Metallographic Sections Show Apparent Propagation During Subsequent Fatigue Without Fretting.

The test also revealed that if fretting were interrupted before the threshold, no cracks were detected in the fretted bands, nor was the specimen life shortened. Relative to this, it has been observed in previous tests and in this program that "run-out" specimens have not exhibited cracks in metallographic sections of the fretted bands. This not only is further evidence of a narrow threshold to failure, but also may indicate a futility in attempts toward preventive inspection for cracks to forestall problems under suspected severe fretting conditions.

d. Elevated Temperature Tests

The same test fixture and specimen design used for room temperature high cycle fatigue was modified for 400° F combined stress testing. Dynamic stress calibration was performed at 400° F using the same procedure used for room temperature calibration. A new calibration specimen was instrumented with high-temperature strain gauges and a stress-versus-amplitude curve developed at 400 ° F.

Figure 25 illustrates the test fixture fitted with a heat chamber that was purged with preheated air as a heat source. Hot air was chosen because of the limited space around the specimen in the fixture and the better temperature uniformity provided by a dynamic heat source versus radiation heat. This is especially beneficial when heating the irregular masses that are encountered with the large fretting shoes clamped to the flat fatigue specimens. In Figure 25, the temperature calibration specimen is visible with thermocouples attached to the sides of the gauge section along the neutral axis. Temperature calibration was performed with four 28-gauge chromel-alumel thermocouples welded to a dummy test specimen. Temperature distribution around the test section was ± 5° F. The fatigue test specimens were instrumented with two thermocouples welded on the neutral bending axis on both sides of the specimen. One thermocouple was for control, the other for continuous recording during test. The specimen was allowed to stabilize at temperature for a minimum of 1/2 hour prior to testing.

The results of tests conducted at 400° F are compiled in Table I. Fretting fatigue test results at 400° F are shown in Figure 26. The specimens tested at 40 ksi included one run-out and two long-lived results. The two failed specimens had corner origins indicating no fretting effect. However specimens tested at 60 ksi failed in short times and exhibited fretting-related fatigue origins.

The results are compared in Figure 27 with General Electric Company test results at 650° F. The tests at 650° F at the higher stress levels resulted in the same substantial reduction in fatigue life as occurred at 400° F and at room temperature. However, there was a significant difference in the effect of temperature in tests at lower stresses. Figure 27 shows that at 650° F there was greater loss of fatigue life due to fretting at the run-out stress level. This effect appeared to be related to more severe damage incurred by the specimens, damage as severe as that occasioned by galling during sliding wear tests to be discussed in Task 2.

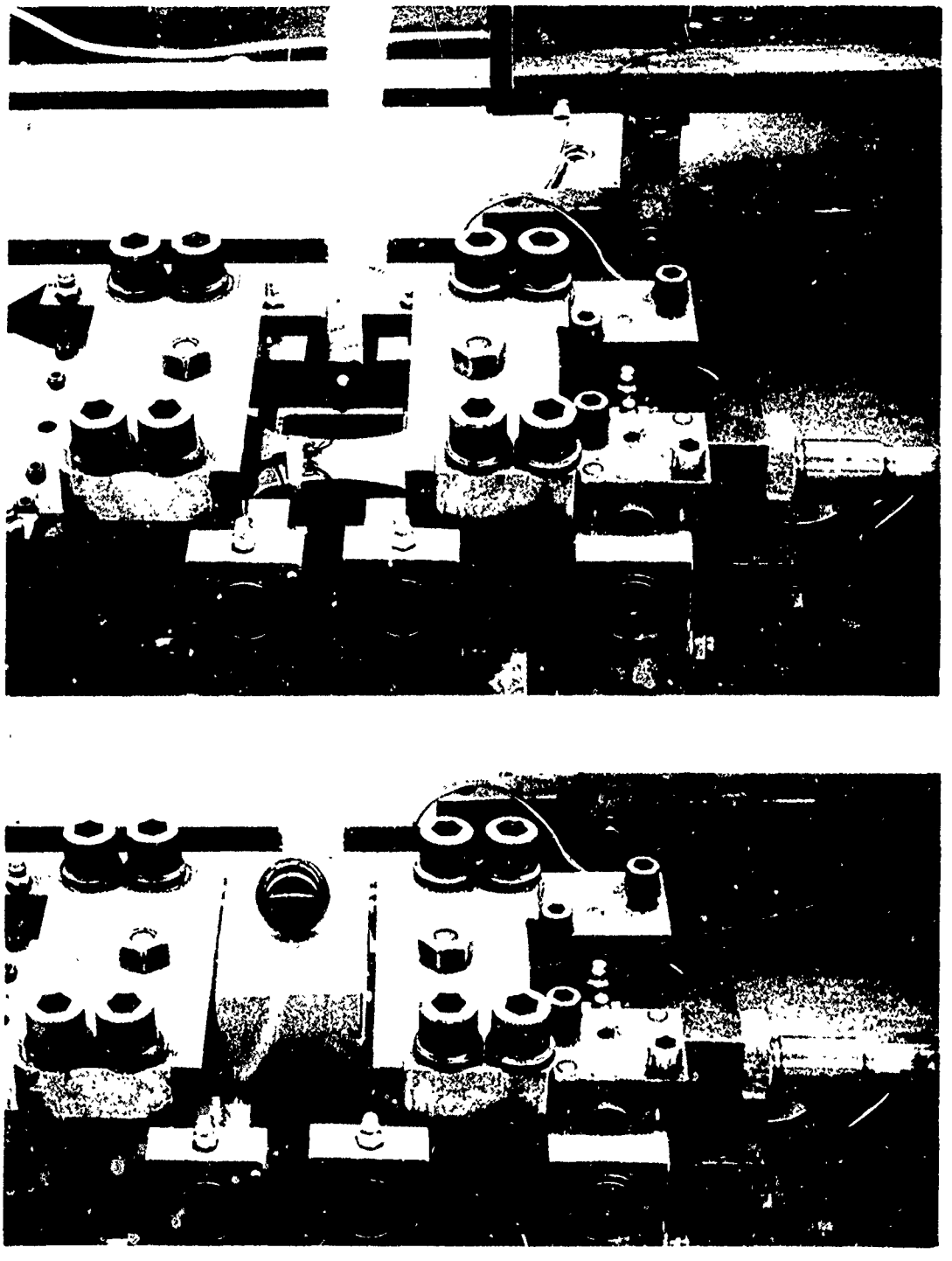

Figure 25. View of the Fretting Fatigue Fixture Showing the Assembly for 400° F Testing. Heated Air from a Tube Furnace is Blown into the Chamber (Lower Photograph) which Contains the Instrumented Specimen, Exposed in the Upper Photograph.

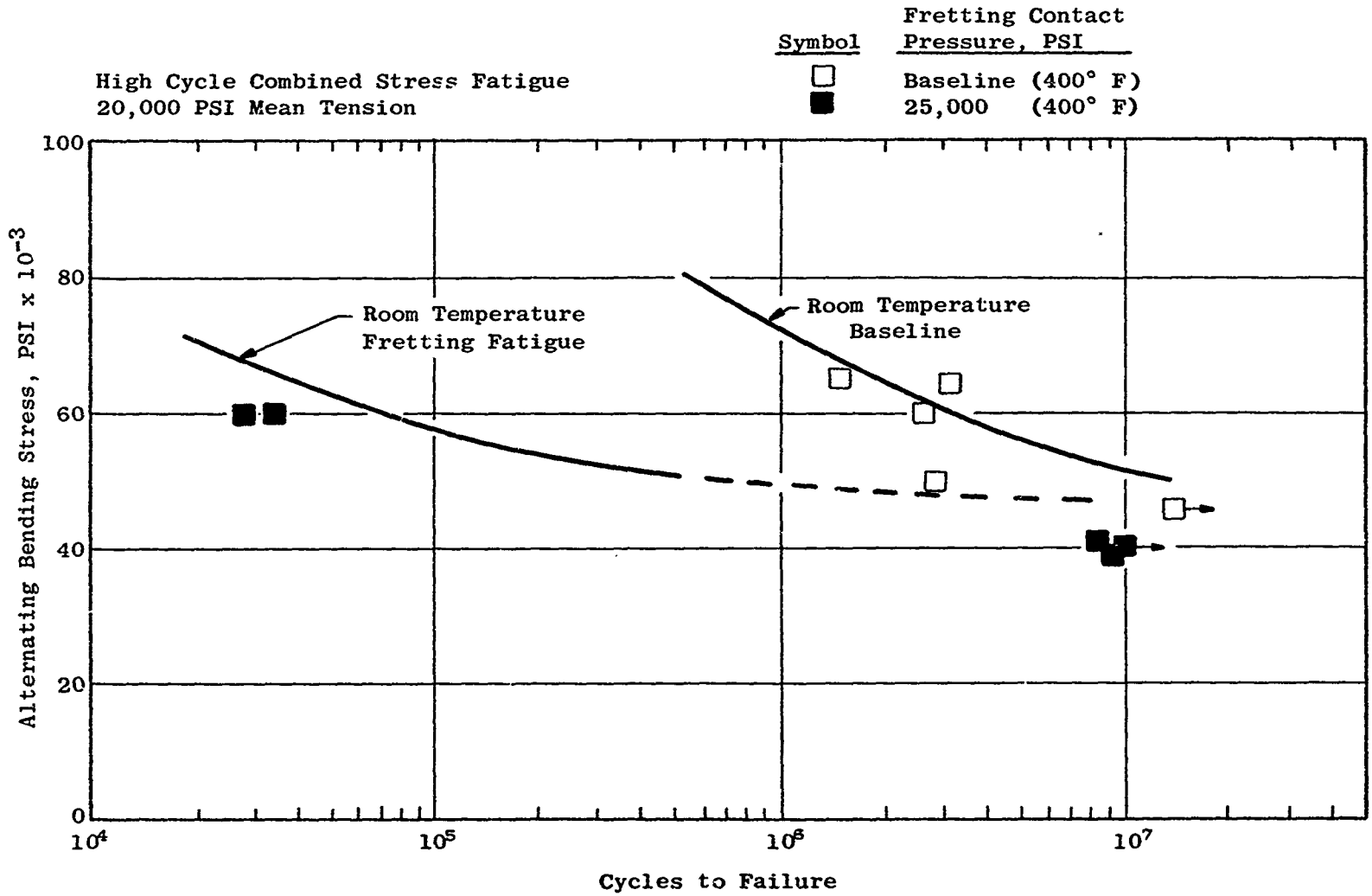

Figure 26. Bending Fatigue Strength of Shot-Peened Ti-6Al-4V at 400° F Compared to Room Temperature Baseline and Fretting Curve.

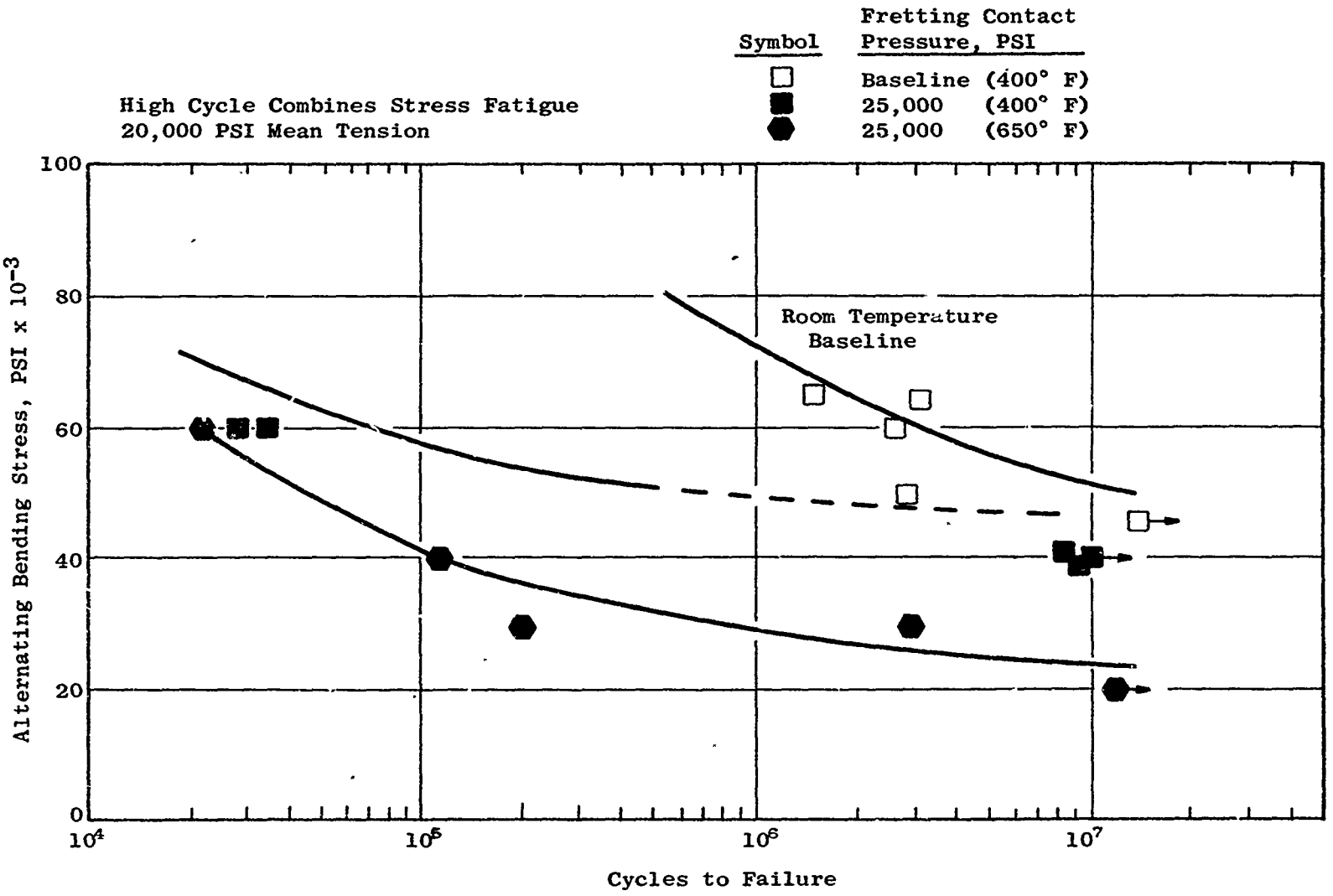

Figure 27. Effect of Elevated Temperature of 400° and 650° F on the Fretting Fatigue Strength of Shot-Peened Ti-6Al-4V.

Figure 28A is a macrophotograph of 400° F Specimen 75 prepared for SEM viewing. Note the presence of deeply scoured wear pits and of raised, attached debris. This gross pitting and adhesive buildup of debris was characteristic of the elevated temperature tests and was more severe at 650° F. Figures 28B and C are SEM views of Specimen 75, respectively, illustrating areas of galled Ti buildup and scoured pits in a portion of the wear band.

Pits corresponding to specimen lumps, and vice versa were present on the wear shoe surfaces. This is clearly illustrated in Figure 29. There the center photograph is a portion of the specimen surface at one end of the shoe contact area. The fracture surface extends along the lower edge of the photograph, having originated in that fretted band. The corresponding photograph of the gauge section of the fretting shoe has been cut in half and the halves placed adjacent to the corresponding fretted band of the specimen as mirror images. Surface illumination was from below and slightly left for each view. Study of the surface relief shows the matching patterns of pits and attached lumps of debris.

Figure 30 illustrates a lump of debris on Specimen 75. Like the room temperature tests the debris is largely titanium oxide with bits of unoxidized metal. Other investigations have identified the debris as rutile, the tetragonal form of TiO_2. The wear mechanism of fretting corrosion which produces oxide debris even at room temperature testing is no doubt favored by higher local specimen temperature as evidenced by the greater accumulations noted.

Figure 30 also illustrates the oxidation of a shear crack in Specimen 75. The fretted band adjacent to the fracture lip displays the same oblique shear cracks as at room temperature, but they were extensively oxidized. The fretting corrosion pits observed did not exhibit cracks, being located generally farther into the shoe contact area where bending fatigue stresses are minimal.

Figure 31 is a SEM photograph of two pits and a detail of the larger showing the scoured metal and some debris. Note that around these pits there is only slight indication of wear striations. This is evidence that the conversion of metal to lower-density oxide creates debris which is more voluminous than the metal particles which it replaces. Accumulation of this wear product causes the metal surfaces to separate. Wear then intensifies at the remaining areas of contact forming the observed pits and contributes to locally severe surface damage.

3. TASK 2 - SLIDING WEAR/FATIGUE

a. High Cycle Fatigue Effects from Sliding Wear

Task 2 studies were conducted under a two-step test method with specimens first subjected to high pressure sliding wear and then tested in high or low cycle fatigue. The wear test apparatus was shown previously in Figures 2 and 3 and the specimen in Figure 7. As for Task 1, all specimens and shoes were

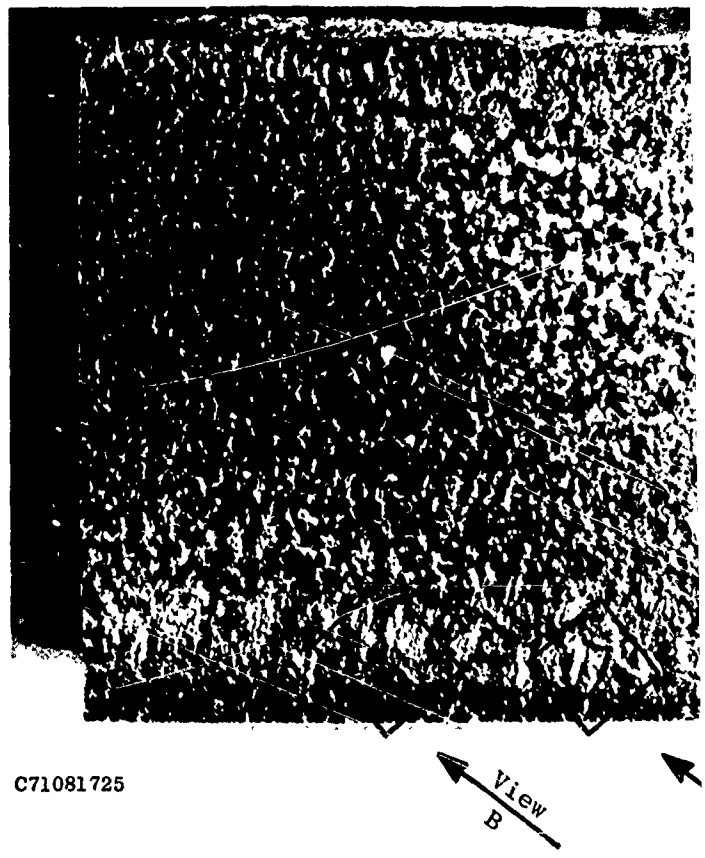

A

C71081725

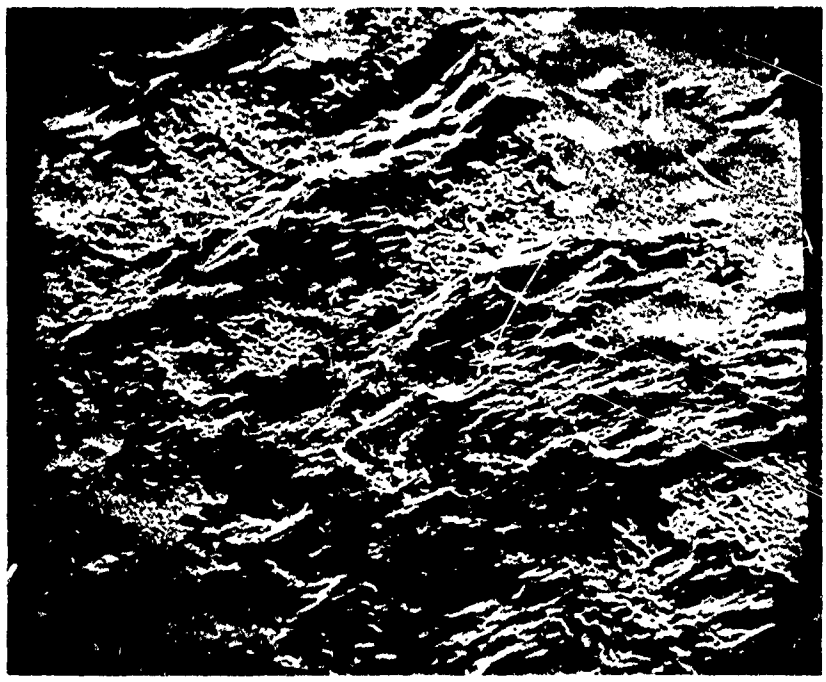

B

C

151B, 120X, 45° x 45°

Figure 28. Specimen 75 Tested in Fretting Fatigue at 400° F. The Macrophotogra
Pattern. The SEM Views Show Details of the Gross Wear Features, Inc
Raised Lumps of Adhered Debris.

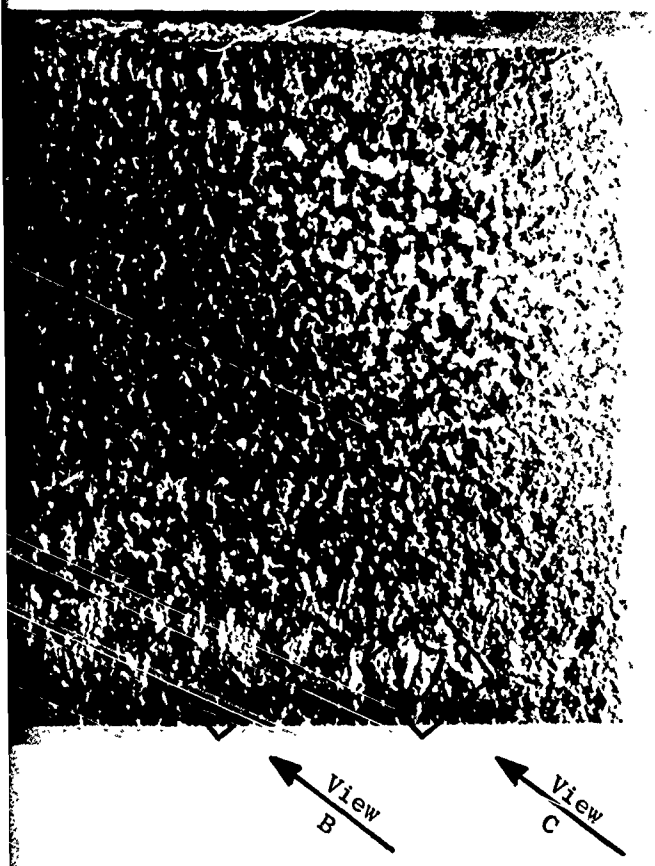

C

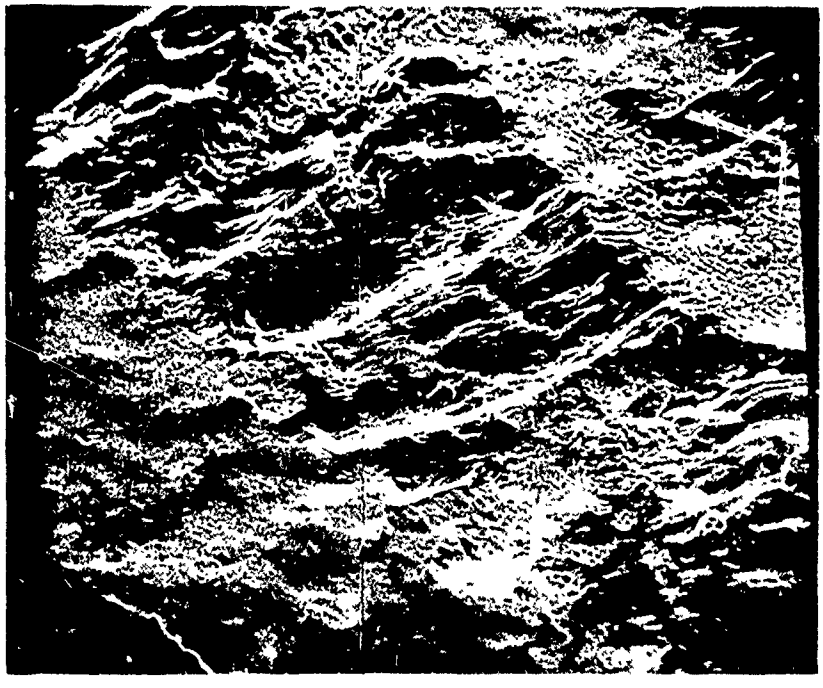

151B, 130X, 45° x 45°

tigue at 400° F. The Macrophotograph Shows the Generally Extensive Galling
ls of the Gross Wear Features, Including Scoured-Out Pits and Adjacent

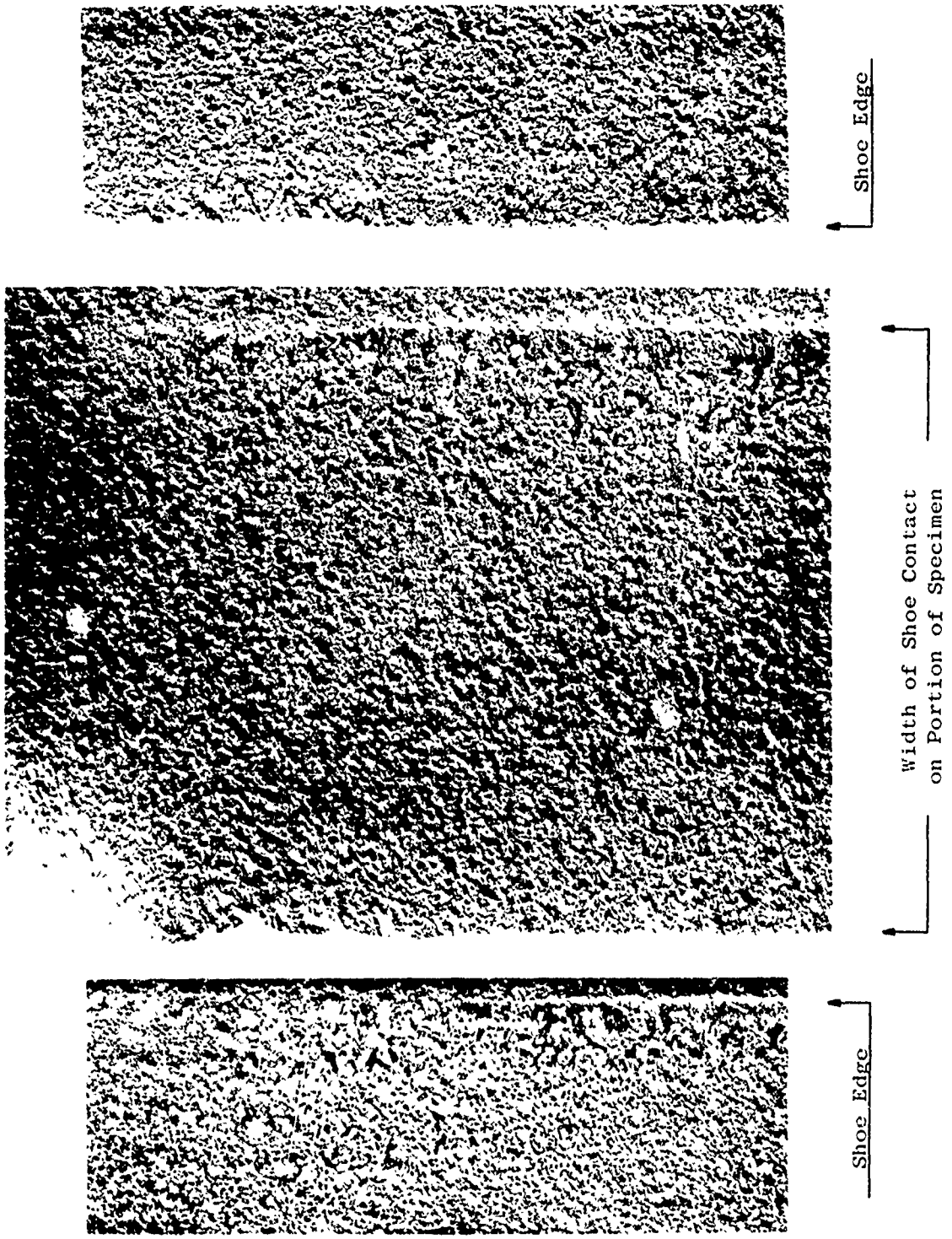

Figure 29. Portion of Specimen from Fretting Fatigue Tests at 650° F Illustrating a Specimen and Split View of Mated Shoe. Each Half of Shoe Photograph is Positioned Adjacent to the Wear Area to Show the Mirror Image of Pits and Debris Lumps. (Metcut 450304, 18X)

Mount 6903, Neg 6301

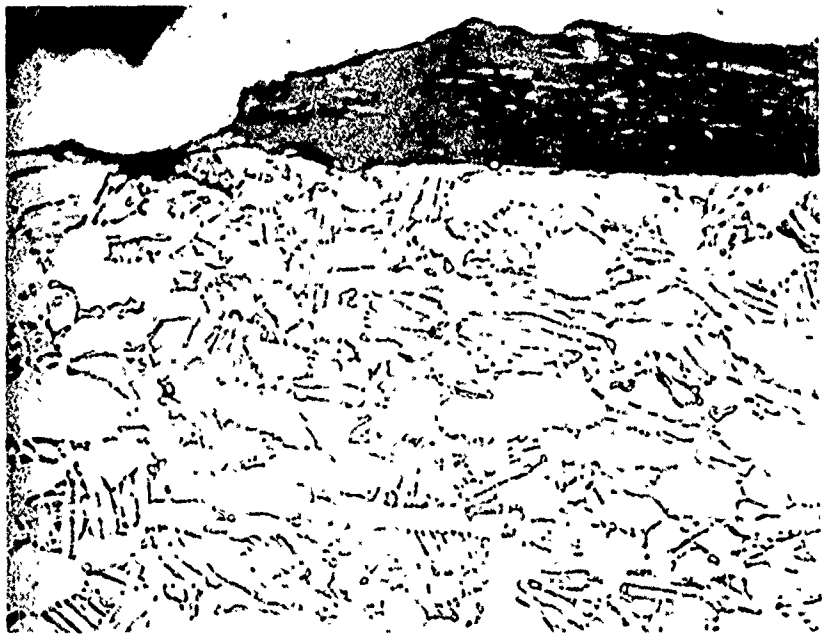

Mount 6903, Neg 6304

Figure 30. Cross Sections of Specimen 75 After 400° F Fretting Fatigue Showing Fretting Oxide Debris in Area of Fatigue Fracture Origin. Lower Photograph Illustrates a Lump of Fretting Oxide Debris Such as Shown in the Macrophotographs in Figures 28 and 29. (HNO_3-Hf etchant, 1000X)

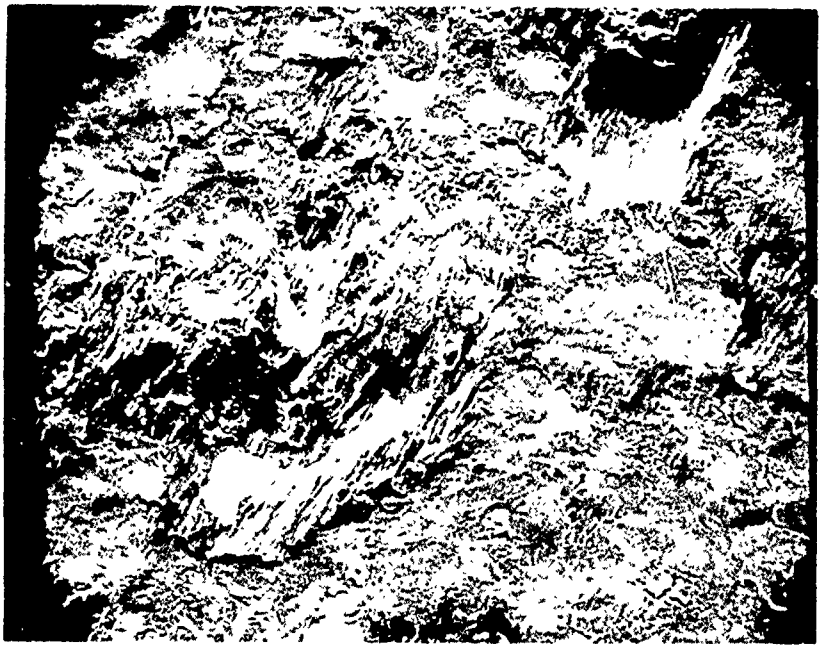

SEM 151C-1, 135X, 20° x 35°

SEM 151C-2, 675X, 20° x 35°

Figure 31. Specimen 36 Showing a Wear Pit and Detail of Galled Metal Inside. Absence of Extensive Wear Striations on Surface Around Pit is an Example of Surface Separation Due to Formation of Voluminous Oxide Debris in Isolated Contact Areas Such as the Pit.

prepared from α-β processed Ti-6Al-4V airfoil forgings and shot peened to 6-8 A_2 intensity as described in Section V, paragraph 1.

During background studies sliding wear was performed under 50,000 psi contact pressure with a 5-mil stroke. Severe surface damage resulted in as few as 1000 wear strokes and the fatigue life was substantially degraded. These test results are shown in Figure 32. Whereas nonworn (or coating-protected) specimens exhibited a baseline strength of 40,000 psi alternating stress under 40,000 psi mean tension, the effect of wear damage was nearly a 40% decrease in the run-out stress. Furthermore, the life capability at 40,000 psi alternating stress was reduced by $2\frac{1}{2}$ orders of magnitude.

In Task 2 other levels of contact pressure and stroke lengths were investigated for their relative effect. Data are compiled in Table II and plotted as S-N curves in Figure 3. The overall results are summarized in Figure 4 as a nomograph for a constant 1000 wear strokes.

In Task 2 other levels of contact pressure and stroke lengths were investigated for their relative effect. Data are compiled in Table II and plotted as S-N curves in Figure 3. The overall results are summarized in Figure 4 as a nomograph for a constant 1000 wear strokes.

Selecting a 5-mil stroke for reference, it is seen that wear damage from contact pressures of 50,000 psi and 10,000 psi produce fatigue loss, whereas 1000 psi did not. At 1000 psi contact pressure, a stroke of 10 mils could be tolerated. At 10,000 psi, the maximum stroke length was at least 2.5 but less than 5 mils. These results are for high cycle bending fatigue with a constant mean tensile stress of 40,000 psi and A = 1.

(1) 10,000 PSI Contact Pressure, 5-Mil Stroke

The effect of wear under 10,000 psi contact pressure and a 5-mil stroke produced a large scatter in fatigue results, although visually there was no discernible difference among the specimen wear patterns. Each appeared severely worn, with extensive galling and debris visible on specimen and shoe surfaces. However, the high cycle fatigue tests produced varied results, indicating an apparent threshold situation of wear damage incurred under these particular conditions. For example, with Specimen 35 of this series, the reductions in fatigue life was as much as for the background specimens tested under 50,000 psi pressure. But, for Specimen 43, there was no reduction in fatigue life. This specimen failed from a corner origin opposite the worn surface. The other two specimens of the series exhibited intermediate fatigue lives, but failed from sites in the wear areas.

Figure 33 illustrates Specimen 38, its wear shoe and fracture face. It was tested in the 10,000 psi contact pressure series with a 5-mil stroke. The shoe exhibits many scoured-out pits while the specimen wear surface shows an accumulation of debris. A detail of Specimen 39 in Figure 34 shows that it consists mainly of pits, smeared debris, and isolated areas of original peened

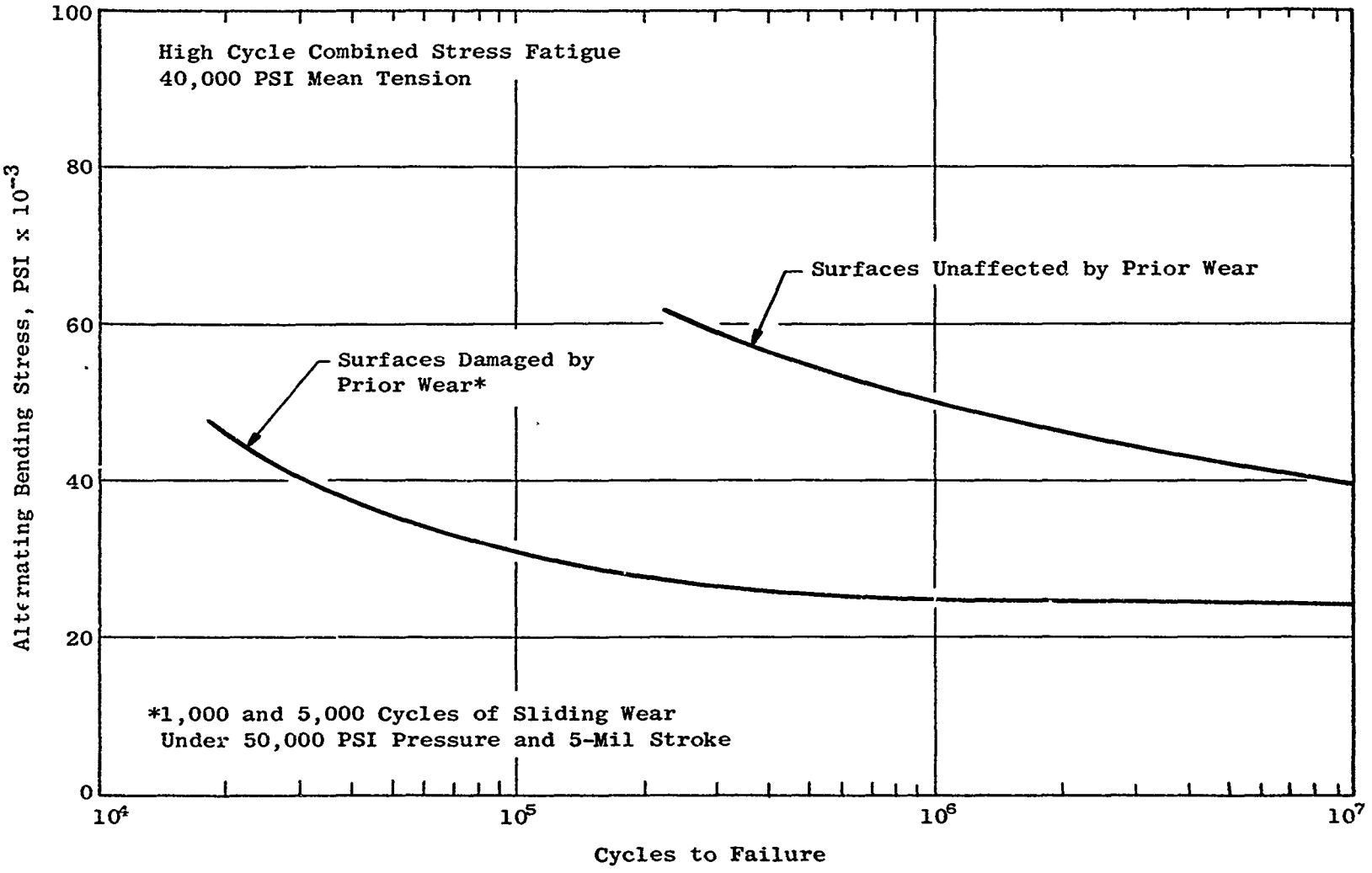

Figure 32. Effect of High Pressure Sliding Wear Damage on High Cycle Fatigue Properties of Shot-Peened, Forged Ti-6Al-4V.

Table II. Sliding Wear and Fatigue Test Results.

Specimen Number	Wear Conditions for 1000 Strokes: Contact Pressure (Ksi)	Stroke Length (Mils)	Friction Coefficient	High Cycle Fatigue(1): Alternating Stress (Ksi)	Cycles to Failure (x10^6)	Results
43	10	5	.83 - .94	40	1.70	This group exhibited extensively galled wear surfaces
39	10	5	.80 - .99	40	.574	with metal transfer from surface to surface. All but
38	10	5	.82 - .88	40	.381	#43 failed from origins at galled streaks.
35	10	5	.80 - .85	40	.062	
82	10	2.5	.39 - .48	40	3.85	Brownish debris and striations prevalent on the wear
84	10	2.5	.70 - .72	40	3.32	area but no evidence of galling. Failures were base-
83	10	2.5	.63 - .85	40	3.30	metal origins at the corners of the gauge section.
41	10	.5-1	.58 - .59	40	7.15	Wear was barely discernible except for slight stria-
40	10	.5-1	.46 - .48	40	5.80	tions at high stero-magnification. Failures orginated
42	10	.5-1	.34 - .41	(Retested at 400F)		in gauge section corners.
85	1	10	.69 - .79	40	2.74	This group exhibited extensive brownish debris and
86	1	10	.66 - .76	40	1.625	striations but no galling was evident. Failures were
87	1	10	.66 - .77	40	3.107	basemetal origins at the corners of the gauge section.
45	1	5	.64 - .64	40	6.66	Brownish debris prevalent with significant-appearing
70	1	5	.71 - .71	40	3.67	galled striations, but failures were in the corners,
44	1	5	.66 -1.07	40	2.83	not associated with apparent wear effects.
				Low Cycle Fatigue (x10^3)		
22	No wear exposure		--	170	14.7	Specimen failed from multiple sites across max-stress
21	No wear exposure		--	150	27.5	surface. Same for specimen #21
25	No wear exposure		--	136	105.5	Failed in corner origin
24	No wear exposure		--	130	106.0	Same as #25
23	No wear exposure		--	120	317.7	Run-out
19	50	5	.05 - .55	138	7.82	Specimens exhibited extensive wear striations and gal-
27	50	5	.63 - .66	138	6.39	ling. Debris accumulated at edges of shoe contact
26	50	5	.52 - .67	138	4.30	area. Failure originated in wear areas.

(1) 40 ksi mean tension

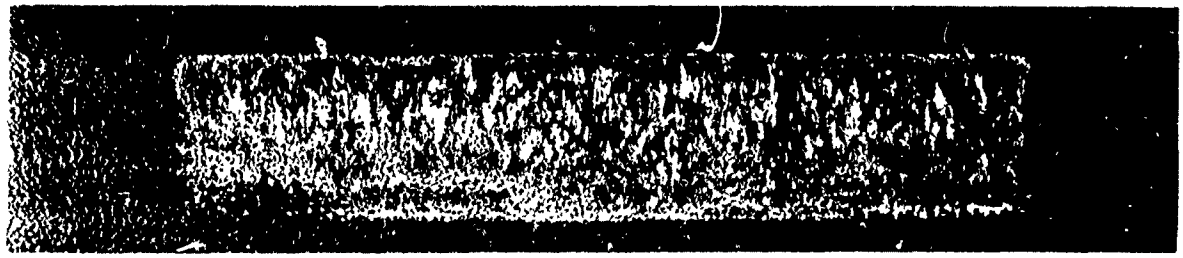

Neg 4781

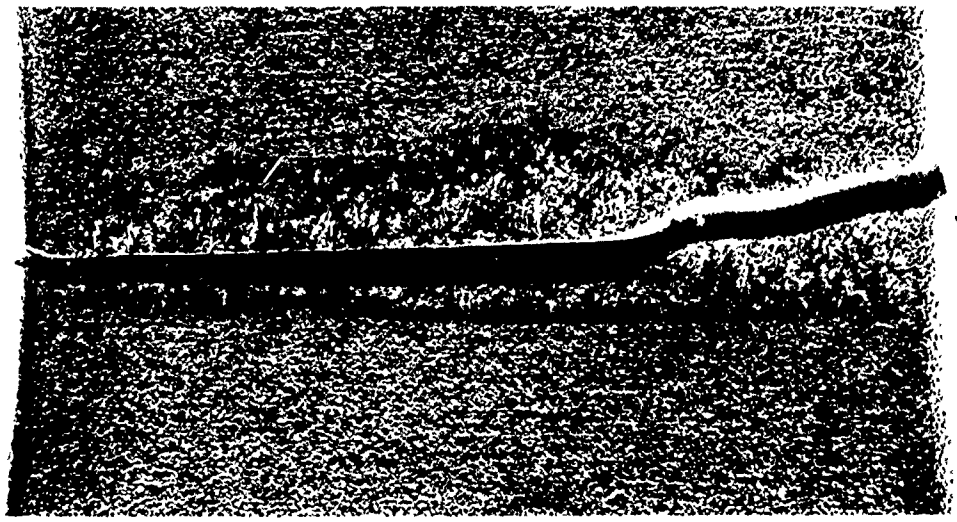

Neg 4780

Neg 4782

Figure 33. Specimen 38 Illustrating the Galling Wear and Fatigue Fracture Pattern After Testing Under 10,000 PSI Contact Pressure and 5-Mil Stroke.

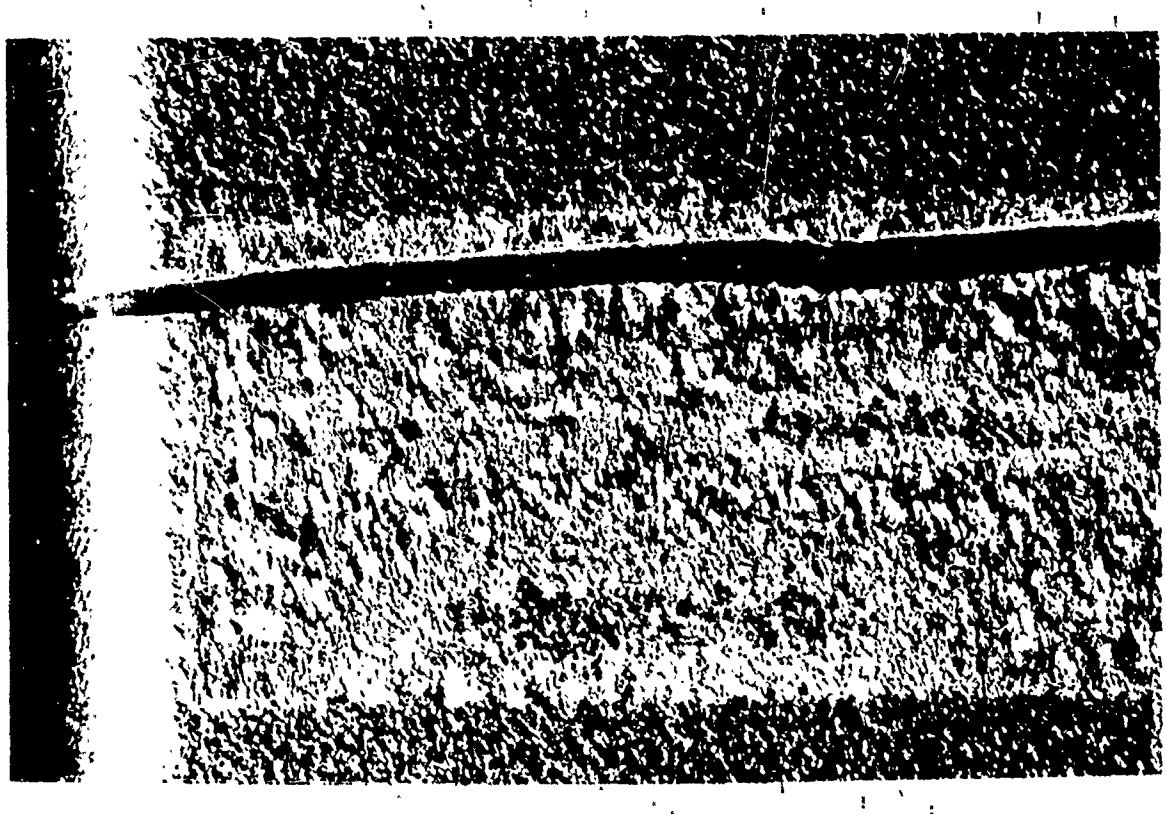

Figure 34. Specimen 39 Showing Detail of Galled Surface After Wear Under 10,000 PSI Contact Pressure and 5-Mil Stroke. (C71081728, 13X)

surface. SEM views of the surface of Specimen 38 in Figure 35 illustrate the wear striations in fresh metal adjacent to a peened area. In the lower photograph a detail is shown of the smeared layer of wear debris. Figure 36 is a metallographic section of the debris layer. It consists of a churned and stratified mixture of oxides and metallic particles. The upper flat surface is the wear interface. Beneath the debris the scoured metal forms a pit about 0.002 inch deep. The right-hand portion of the debris/metal interface reveals fresh debris fractured and ready to be dislodged. To the left there is evidence of distortion in the interface metal grain structure.

Shown previously in Figure 33, the fracture face of Specimen 38 displayed a single major origin. Like the Task I fretting fatigue tests previously discussed, Task 2 specimens tested in fatigue after sliding wear displayed multiple origins as well as single sites. Unlike the fretted fatigue specimens in Task I, where failures were confined to the edges of shoe contact, the prior-worn specimens in Task 2 exhibit failures anywhere in worn areas that sufficient damage develops. Multiple origins sometimes lined up to form a single fracture plane; in other instances, they were in such random locations on the wear surface that a stepped fracture face resulted. Specimen 48 in Figure 12 is an example of the latter. No trend toward greater or lesser fatigue life was determined for the occurrence of single or multiple origins.

(2) 10,000 PSI Contact Pressure, 0.5-1 Mil Stroke

Because of the strength loss which occurred under the initial conditions selected in Task 2 (10,000 psi, 5-mil stroke), the contractural options of lower pressure and stroke rate were investigated. It was found that decreasing the stroke to 0.5-1 mil under 10,000 psi pressure did not produce damaging wear. In fact, visually, the effect of sliding was barely discernible, and no fatigue loss resulted as shown in Figure 3. The specimens failed in corner sites at cyclic lives comparable to nonworn baseline specimens. Figure 37 illustrates the very mild wear pattern on Specimen 41.

(3) 1000 PSI Contact Pressure, 5-Mil Stroke

In the second option to bracket the fatigue-affecting wear parameters, decreasing the contact pressure to 1000 psi and retaining the 5-mil stroke resulted in no loss of fatigue properties. Although considerably more visible wear debris (oxide powder) occurred in the low-stroke variation, the surfaces did not exhibit the extensive galling that the high-pressure, high-stroke test parameters produced. The high cycle fatigue results are shown in Figure 3. Each specimen failed from a corner origin, in each case opposite the worn surface. Figure 38 illustrates Specimen 45 of this series. These results indicate that the conditions of 10,000 psi pressure and a 5-mil stroke comprise an apparent lower limit of fatigue-affecting parameters for 1000 cycles of wear.

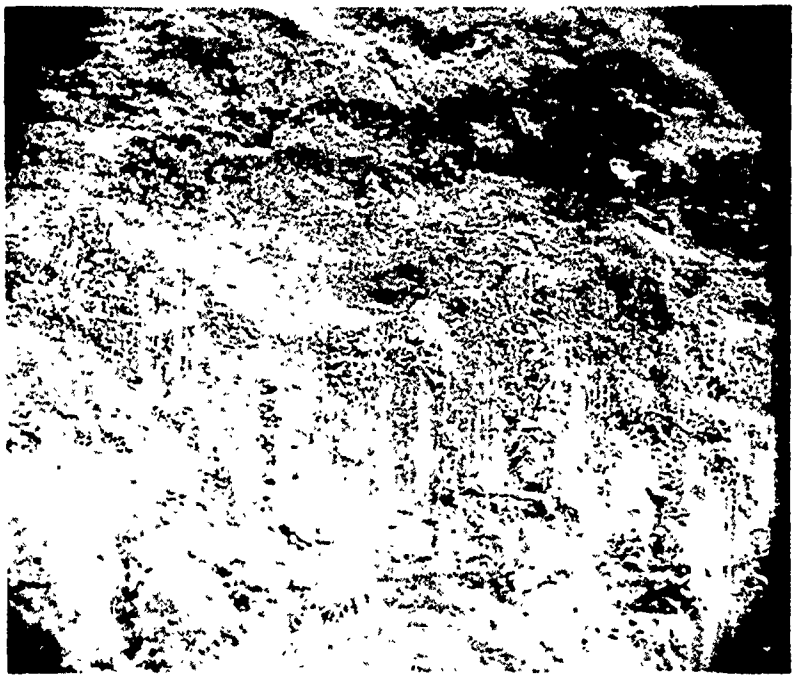

SEM 66B-1, 265X, 45° x 0°

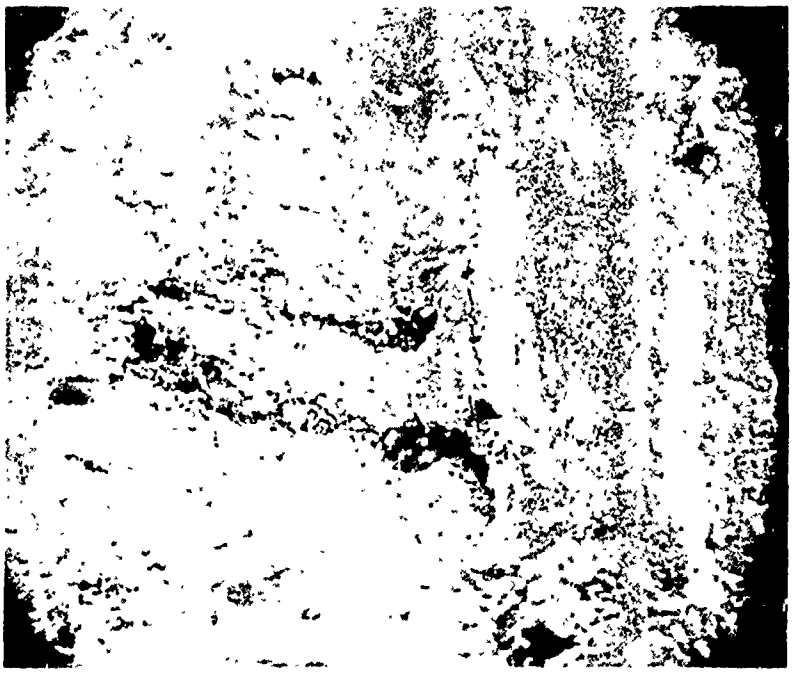

SEM 66B-3, 1380X, 45° x 0°

Figure 35. Specimen 38 Showing Wear Striations and Detail of Debris Layer After Galling Wear Under 10,000 PSI Contact Pressure and 5-Mil Stroke.

Figure 36. Metallographic Section of Specimen 38 Showing Wear Debris Layer in Substrate Pit. (Mount 1917, Neg G6305, 1000X)

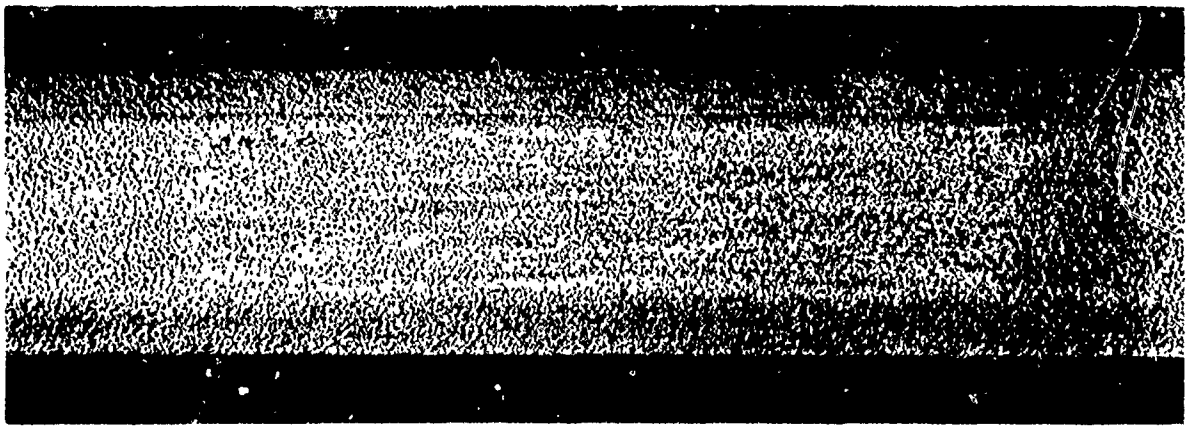

Shoe 41, 4774

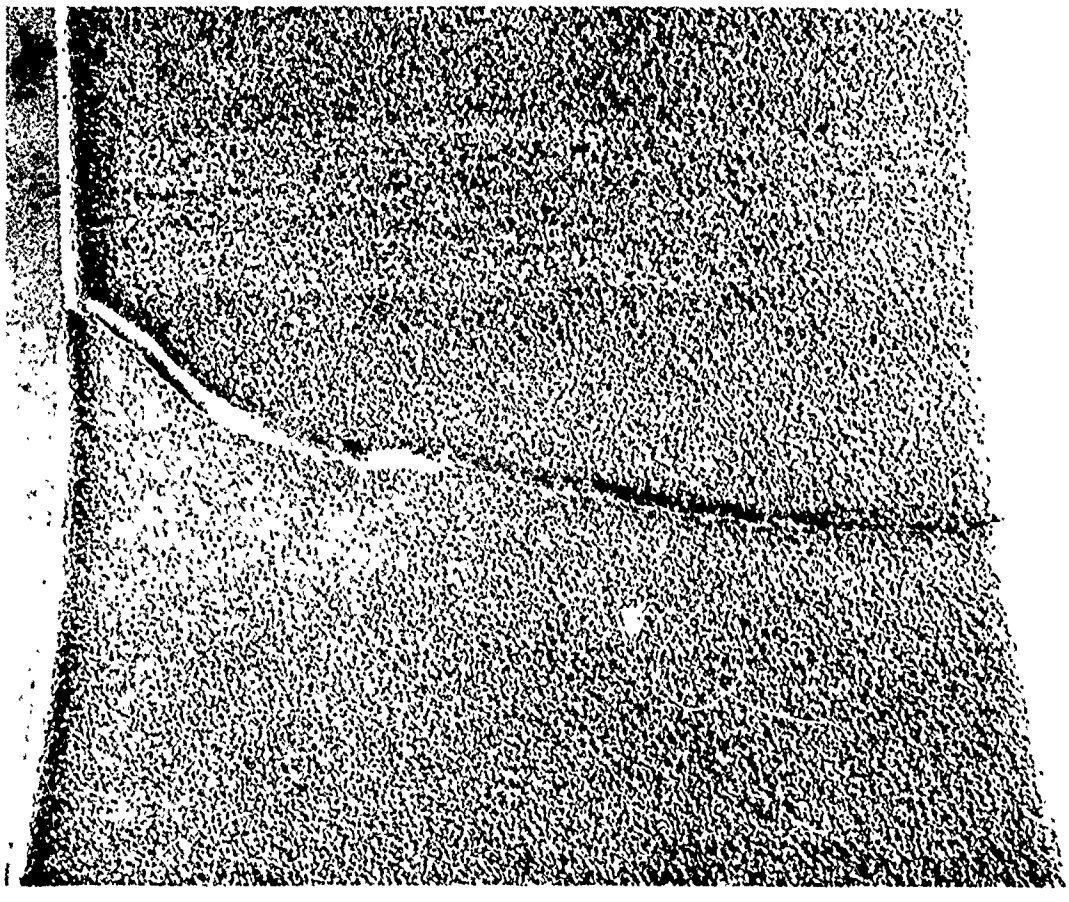

Wear Area

Specimen 41, 4773

Figure 37. Specimen 11 Illustrating Very Mild Wear Pattern on Shoe and Specimen After Wear Test Under 10,000 PSI Contact Pressure and 0.5- to 1-Mil Stroke. (Metcut, 6X)

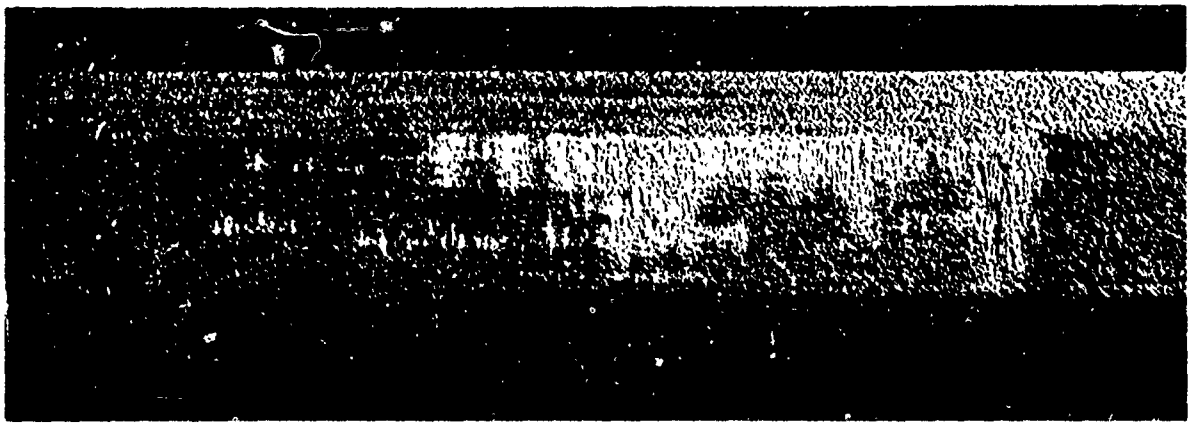

Shoe 45, 4776

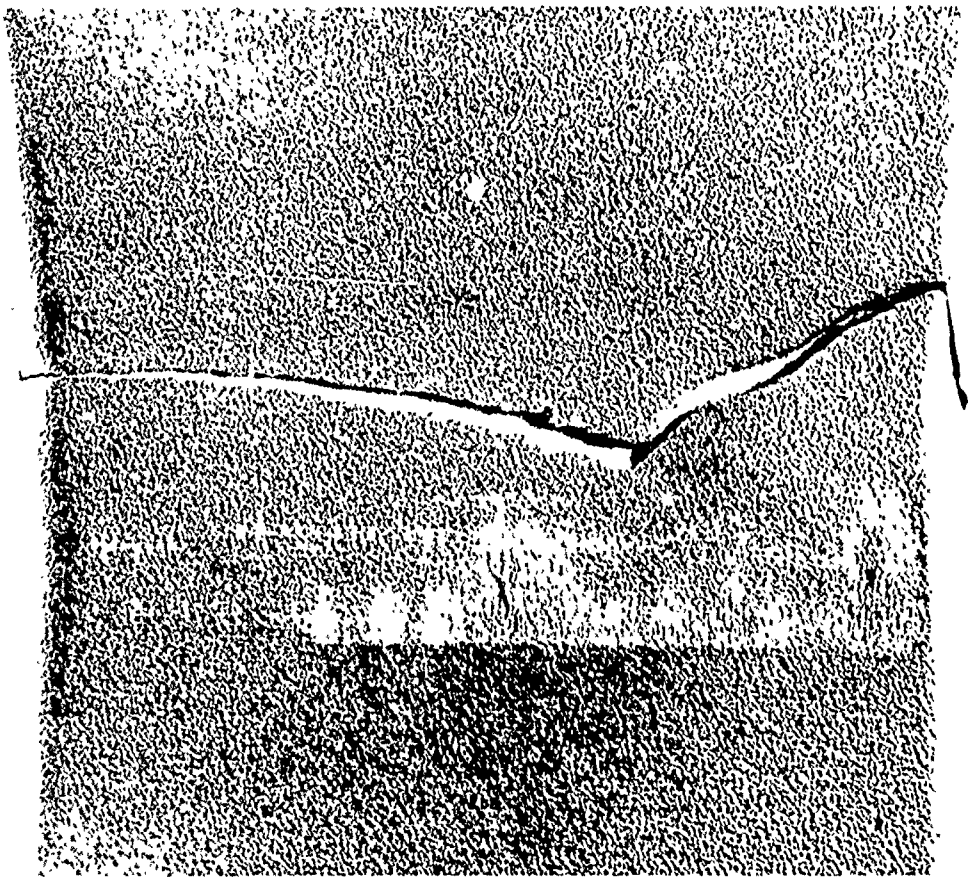

Specimen 45, 4775

Figure 38. Specimen 45 Illustrating Wear Pattern on Shoe and Specimen After Testing Under 1000 PSI Pressure and 5-Mil Stroke. (Metcut, 6X)

(4) 10,000 PSI Contact Pressure, 2.5-Mil Stroke

As part of the amended contract, an intermediate level of 2.5 mils stroke was evaluated under 10,000 psi contact pressure. The specimens exhibited only very slight visual wear effect. No fatigue strength loss was encountered.

(5) 1000 PSI Contact Pressure, 10-Mil Stroke

The amended contract included a further evaluation of 1000 psi contact pressure at a stroke length extended to 10 mils. The longer stroke produced the most extensive visible surface debris of any of the wear conditions; however, there was no effect on the fatigue properties of the substrate.

b. Low Cycle Fatigue Effects from Sliding Wear

Specimens were subjected to the baseline wear condition of 50,000 psi pressure and a 5-mil stroke for 1000 wear cycles. Extensive, visually-severe wear damage occurred. As was shown in Figure 5, all specimens failed with an order of magnitude loss of low cycle fatigue life under 138,000 psi bending stress at A = 1.0.

Figure 39 illustrates the surface appearance of Specimen 27 and its fracture face. SEM observations of the specimen and its shoe shown in Figure 40 reveal the typical presence of galled metallic-appearing flakes on the specimen and the accumulation of debris on the shoe. Metallographic sections of the specimen and wear shoe are shown in Figure 41. The shoe is seen to have not only an accumulation of debris, but also a shear crack indicating the mode of surface breakdown which has been described for the specimens themselves. Shown below the shoe is the fracture edge of Specimen 27, showing the characteristic shear cracks, debris-filled pockets, and disturbed metal at the surface.

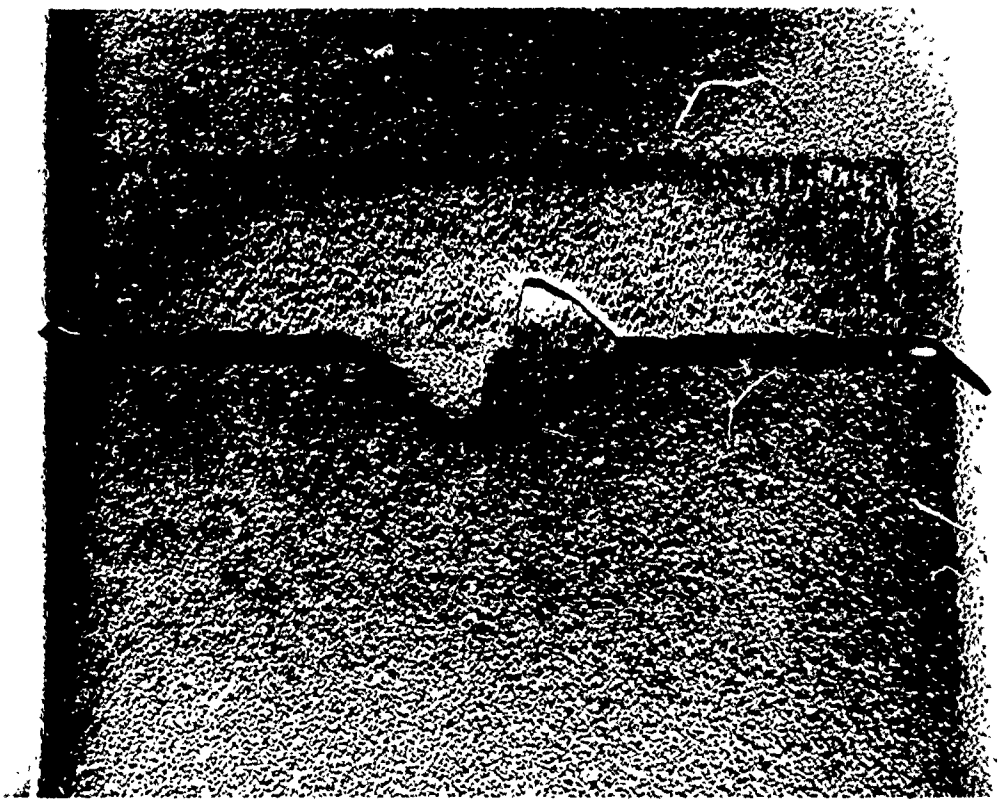

Neg 4777

Neg 4779

Figure 39. Specimen 27 Showing Wear and Fracture Pattern After Low-Cycle Fatigue Wear Testing Under 50,000 PSI Contact Pressure and 5-Mil Stroke. (Metcut, 6X)

SEM 66A, 590X, 45° x 0°

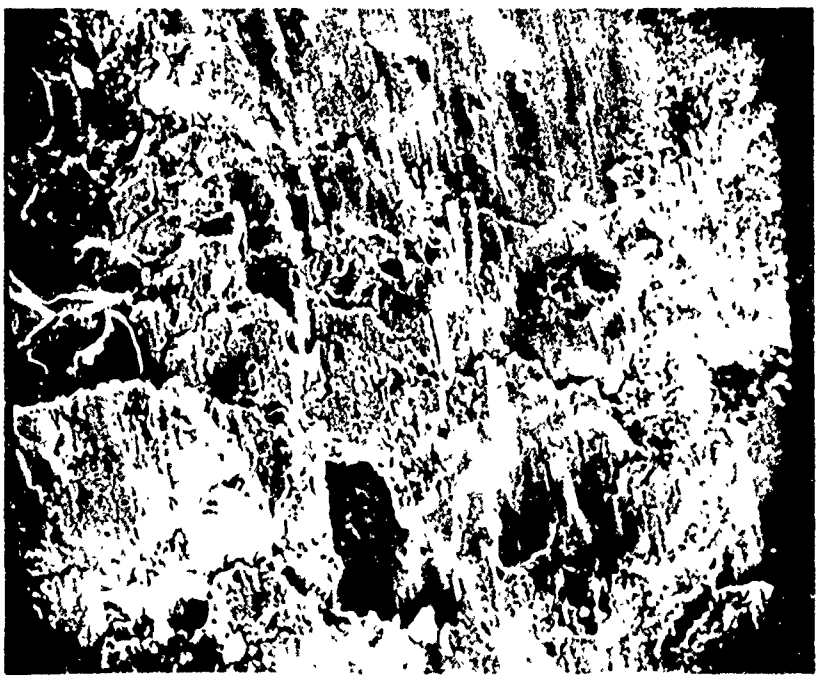

SEM 66F, 900X, 45° x 0°

Figure 40. Specimen 27 Showing Wear Debris of Shoe (Upper Photograph) and Galled Metal Flakes on Specimen (Lower Photograph) After Testing Under 50,000 PSI Contact Pressure and 5-Mil Stroke.

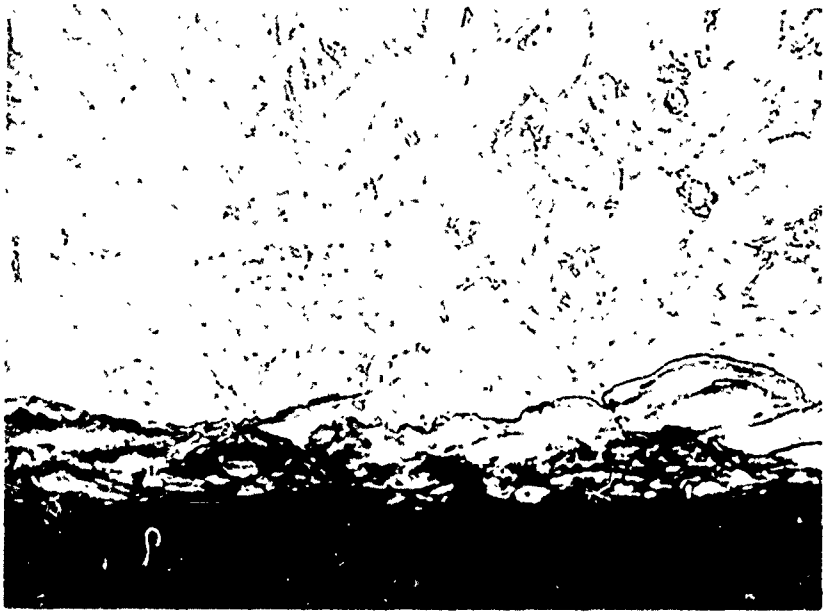

Mount 2013, Neg G 6310

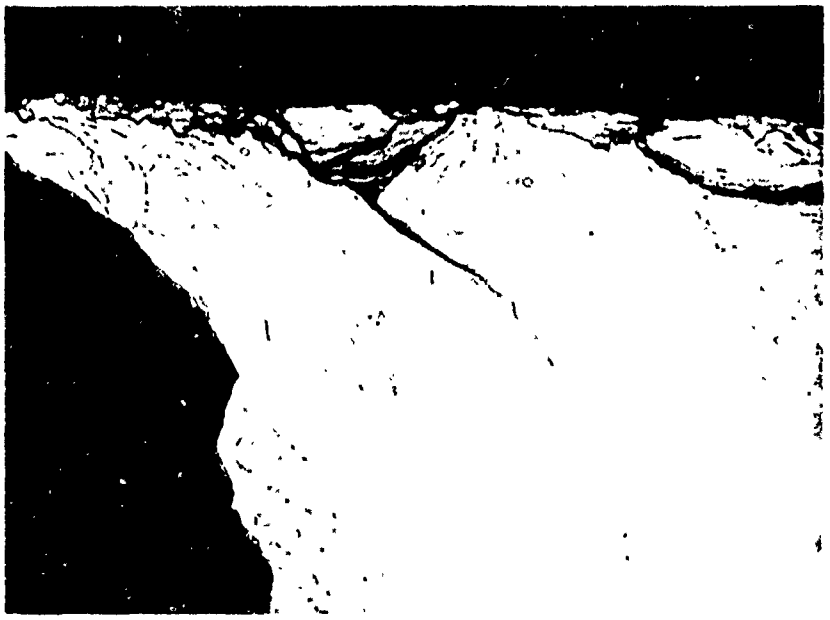

Mount 2011, Neg G 6307

Figure 41. Specimen 27 Showing Metallographic Section of Wear Shoe and of Specimen Fracture Edge in the Vicinity of a Failure Origin. (1000X)

SECTION VI

REFERENCES

1. B.L. Koff, Titanium Fatigue Investigation, GE Technical Report, R67FPD252 (1967).

2. R.K. Betts, W.P. Koster and W.J. Stross, Fretting Fatigue of Forged Ti-6Al-4V Related to J-79 Compressor Disc Application, G.E. Technical Report No. TM67-773, (1967).

3. R.K. Betts, W.L. Starkey, R.T. Hagon, Final Report - Investigation of Fretting - Fatigue Damage of Titanium Alloy Ti-6Al-4V in Fretting Contact with 4340 Steel and Ti-6Al-4V Collars, General Electric Company, TM68-388, June, 1968.

4. R.K. Betts, W.P. Koster, W.J. Stross, Fretting Fatigue of Forged Inconel 718 Relative to J-97 Compressor Disc Application, General Electric Company TM68-404, June, 1968.

5. R.K. Betts, AEG Wear Programs, Status Report No. 1, General Electric Company, TM68-319, May, 1968.

6. V.J. Erdeman, R.D. Radcliffe, Effects of Shot Peening on the Cyclic Life of Thermally Exposed and Non-Exposed Ti-6Al-4V and Ti-6Al-2Sn-4Zr-2Mo, General Electric Company, R69AEG166, April, 1969.

7. R.K. Betts, High Cycle Fatigue Effect of Sliding Wear and Prevention by CuNiIn/MoS_2 Coating on Ti-6Al-4V, General Electric Company, TM70-82, March, 1970.

8. R.K. Betts, Titanium Dovetail Wear Coatings - Wear/Fatigue Comparison of CuNiIn, CuNi and NiAl, also MoS_2 and Graphite Lubrication, General Electric Company, TM70-633, August, 1970.

9. E. Rabinowicz, Friction and Wear of Materials, Wiley & Sons, (1965).

10. F.P. Bowden and D. Tabor, The Friction and Lubrication of Solids, Part II, Oxford Press (1964).

11. R.A. Wood, Surfact Treatment of Titanium, DMIC Technical Note, Battelle Memorial Institute, March, 1965.

12. N.J. Finch, J.E. Bowers, Surface Treatment of Titanium Alloys: A Review of Published Information, British Non-Ferrous Metals Research Association, Report No. A 1536 (DDC AD439954) May, 1965.

REFERENCES (concluded)

13. M.W. Mallett, Surface Treatments for Titanium Alloys, NASA Technical Memorandum X-53429, October, 1965.

14. R.C. Bowers and C.M. Murphy, Status of Research on Lubricants, Friction, and Wear, Naval Research Laboratory, NRL Report 6466 (1967).

15. R.K. Betts, Effect of Edge Radius and WC-Co Coating on the High Cycle Bending Fatigue Strength of Ti-6Al-4V Relative to Blade Interlock Geometry, General Electric Company, TM71-214, May, 1971.

16. R.K. Betts, Low Cycle Fatigue Effects of Wear, General Electric Company, TM71-215, August, 1971.

17. R.K. Betts, Dovetail Wear Coating Evaluation, General Electric Company, TM71-216, April, 1971.

18. R.B. Waterhouse, The Effect of Clamping Stress Distribution on the Fretting Fatigue of Alpha Brass and Al-Mg-Zn Alloy, American Society of Lubrication Engineers Transactions 11, 1-5, 1968.

19. M. Cocks, Interaction of Sliding Metal Surfaces, Journal of Applied Physics, Volume 33, No. 7, July 1962.

20. Eugene F. Finkin, What Happens When Parts Wear, Machine Design, March 19, 1970.